

Modeling Water Use at Thermoelectric Power Plants

by

Michael J. Rutberg

B.S. Engineering
Swarthmore College, 2003

SUBMITTED TO THE DEPARTMENT OF MECHANICAL ENGINEERING IN PARTIAL
FULFILLMENT OF THE REQUIREMENTS FOR THE DEGREE OF

MASTER OF SCIENCE IN MECHANICAL ENGINEERING
AT THE
MASSACHUSETTS INSTITUTE OF TECHNOLOGY

JUNE 2012

© 2012 Massachusetts Institute of Technology. All rights reserved.

Signature of Author: _____
Department of Mechanical Engineering
May 11, 2012

Certified by: _____
Ahmed F. Ghoniem
Ronald C. Crane (1972) Professor of Mechanical Engineering
Thesis Supervisor

Accepted by: _____
David E. Hardt
Chairman, Committee on Graduate Students

Modeling Water Use at Thermoelectric Power Plants

by

Michael J. Rutberg

Submitted to the Department of Mechanical Engineering on May 11, 2012 in Partial Fulfillment of the Requirements for the Degree of Master of Science in Mechanical Engineering

ABSTRACT

The withdrawal and consumption of water at thermoelectric power plants affects regional ecology and supply security of both water and electricity. The existing field data on US power plant water use, however, is of limited granularity and poor quality, hampering efforts to track industry trends and project future scenarios. Furthermore, there is a need for a common quantitative framework on which to evaluate the effects of various technologies on water use at power plants.

To address these deficiencies, Part 1 of this thesis develops an analytical system-level generic model (S-GEM) of water use at power plants. The S-GEM applies to fossil, nuclear, geothermal and solar thermal plants, using either steam or combined cycles, and outputs water withdrawal and consumption intensity, in liters per megawatt-hour. Two validations of the S-GEM are presented, one against data from the literature for a variety of generation types, the other against field data from coal plants in South Africa.

Part 2 of the thesis then focuses on cooling systems, by far the largest consumers of water in most power plants. The water consumption of different cooling systems is placed on a common quantitative basis, enabling direct comparison of water consumption between cooling system types, and examination of the factors that affect water consumption within each cooling system type. The various cost, performance, and environmental impact tradeoffs associated with once-through, pond, wet tower, dry, and hybrid cooling technologies are qualitatively reviewed.

Part 3 examines cooling of concentrating solar power (CSP) plants, which presents particular problems: the plants generate high waste heat loads, are usually located in water-scarce areas, and are typically on the margin of economic viability. A case study is conducted to explore the use of indirect dry cooling with cold-side thermal energy storage, in which cooling water is chilled and stored at night, when ambient temperatures are lower and the plant is inactive, and then used the following day. This approach is shown to hold promise for reducing the capital, operational, and performance costs of dry cooling for CSP.

Thesis Supervisor:
Ahmed F. Ghoniem
Ronald C. Crane (1972) Professor of Mechanical Engineering

ACKNOWLEDGEMENTS

Many people made possible the work described herein. The author gratefully acknowledges all of them, particularly the following individuals:

- Prof. Ahmed Ghoniem (MIT), for his stalwart supervision;
- Frank O’Sullivan and Howard Herzog (MIT), for their invaluable input;
- Anna Delgado and Rand Hidayah (MIT), for their collegial contributions;
- Eric Adams and Randy Field (MIT), for their astute advice;
- John Maulbetsch (Maulbetsch Consulting), for his sage suggestions;
- Ned Spang (UC Davis), for his prudent pointers;
- Tim Diehl (USGS), for his relevant research;
- Petro Hendriks et al. (Eskom), for their meticulous measurements;
- Silvia Boschetto, Ellen Williams et al. (BP), for their sustaining support;
- and Pooja, the superlative spouse.

TABLE OF CONTENTS

Introduction and Motivation.....	7
Key Concepts, Definitions and Tradeoffs	7
Water as a Factor in Cost of Electricity	14
Available Data Sources	15
Part 1 – A System-Level Generic Model of Power Plant Water Use.....	17
Introduction	17
The System-level Generic Model (S-GEM).....	19
S-GEM Validation: U.S. Wet Tower Cooled Plants	24
S-GEM Validation: Eskom Coal Plants	29
Discussion	33
Part 2 – Water Consumption in Power Plant Cooling Systems: A Review	35
Introduction	35
Once-Through and Pond Cooling.....	36
Wet Tower Cooling	44
Dry and Hybrid Cooling.....	53
Discussion	60
Part 3 – Cold-Side Thermal Energy Storage for Dry-Cooled Concentrating Solar Power Plants.....	61
Introduction	61
Case Study Design Basis.....	64
Case Study Results and Discussion.....	67
Details of Case Study Analysis	70
Nomenclature	72
References	74

Introduction and Motivation

In many regions of the world, water use at thermoelectric power plants, predominantly for cooling, has a significant effect on the overall water supply and on the ecological health of surface water bodies. In some instances, permits for proposed plants have been denied because of water availability concerns or potentially adverse effects on aquatic life. In other cases, plants have been constructed with cooling systems that use less water but cost more and result in lower plant efficiency, or existing plants have been retrofitted with such systems. Power plants have even shut down during droughts to comply with water use regulations. Water withdrawal and consumption at power plants is thus an issue that affects regional ecology and security of supply of both water and electricity.

The existing field data on US power plant water use, however, is of limited granularity and poor quality, hampering efforts to track industry trends and project future scenarios. Furthermore, there is a need for a common quantitative framework on which to evaluate the effects of various technologies on water use at power plants. A broadly-applicable model of power plant water use, which does not exist in the current literature, is needed.

This issue is here addressed in three parts. Part 1 develops and validates an analytical system-level generic model (S-GEM) of water use at thermoelectric power plants. Part 2 then focuses on cooling systems, by far the most largest consumers of water in most power plants. The water consumption of different cooling systems is placed on a common quantitative basis, and the cost, performance, and environmental impact tradeoffs associated with various cooling technologies are qualitatively reviewed. Part 3 examines cooling of concentrating solar power plants, which presents particular problems, investigating the potential of a new cooling system architecture to reduce water consumption while minimizing capital, operating and performance costs.

First, however, a high-level introduction to the primary issues involved is presented.

Key Concepts, Definitions and Tradeoffs

In discussing water use at power plants, it is first of all important to distinguish between water withdrawal and consumption. “Withdrawal” refers to water taken from a watershed or aquifer. “Discharge” refers to water withdrawn that is then returned to the watershed. “Consumption” refers to water withdrawn that is specifically not discharged back to the watershed. In this thesis the term “water use” refers generically to both withdrawal and consumption.

In many cases water use in power plants is dominated by cooling. Thermoelectric generation processes (see Figure 1) inherently produce large quantities of “waste” heat, which must be rejected to the

environment using a cooling system. In a steam cycle, a bigger temperature difference between the hot “thermal reservoir” (which generates the steam) and the cold thermal reservoir (which condenses the steam) generally means a higher plant efficiency. Higher efficiency means more electricity and less waste heat, and less waste heat means less water used in the cooling system. So, for a given cooling system, higher efficiency means lower water use per MWh.

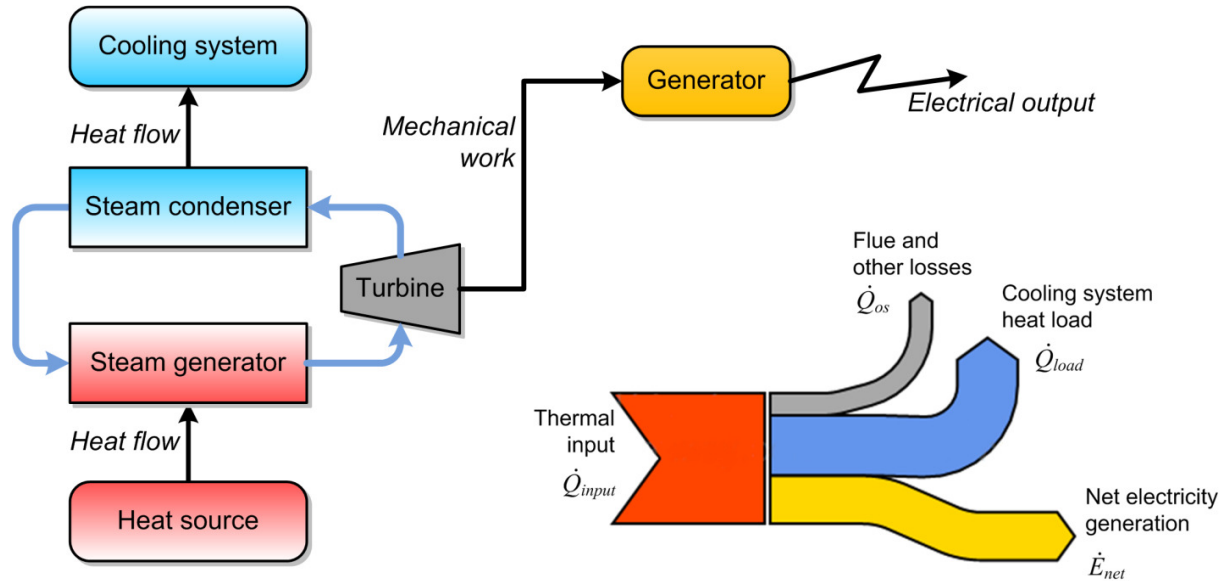


Figure 1: a) Block diagram of a generic thermal power plant; b) Energy flow through a generic thermal power plant

Solar thermal, geothermal, and nuclear heat sources have a much lower carbon footprint than fossil fuel combustion, but they also produce steam at lower temperatures, and thus have lower efficiencies. For a given type of cooling system, non-combustion plants generally have significantly higher water use per MWh as compared to combustion plants.

Efficiency and, more generally, heat balance is one key aspect of water use at power plants; the other is the cooling system itself. The principal types of cooling system and their tradeoffs are discussed briefly below.

“Once-through cooling” (see Figure 2), also called open or open-loop cooling, involves withdrawing water from a surface water body, running it past a heat exchanger where it takes on the waste heat, and discharging it to the same water body, now some degrees warmer. The mechanism for water consumption in once-through cooling systems is increased evaporation due to the higher temperature of the discharged water. While this evaporation does not always occur within the physical boundaries of the plant, it is attributable to the cooling system and thus is often included in water consumption analyses.

Once-through cooling has the advantage of simplicity and low cost; where cool water is readily available it is also highly effective. The amount of water withdrawn is very large, however, and can have deleterious ecological impacts. Aquatic life may be “entrained” (sucked into the cooling system) or “impinged” on inlet grates; the increased temperature of the discharge may also have detrimental effects on the local ecosystem. For these reasons, once-through cooling systems have not been used in new plants in the US for some decades, and pending regulations under the US Clean Water Act are pressuring generators to phase out once-through cooling at existing plants.

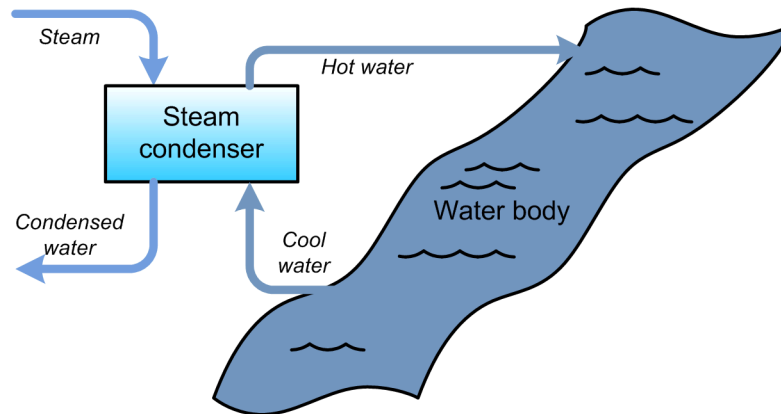


Figure 2: Diagram of once-through cooling system

“**Wet tower cooling**” (see Figure 3) uses a recirculating loop of cooling water. After running past the waste heat exchanger, the hot water is sprayed down through a cooling tower onto the “fill”, a block of lattice-like material that increases the surface area of the flow down through the tower. At the same time, a fan or natural draft draws air from the bottom of the tower up through the fill and out to the environment.

The flow of air and water acts as a heat exchanger, with convective, or “sensible,” heat transfer from the water to the air. Moreover, a small fraction of the water evaporates as it makes its way down through the tower, and the latent heat of this evaporation cools the remaining water as well. The cooled water collects at the bottom of the tower, from where it is pumped back to the waste heat loads.

Evaporation from the cooling tower is the principal consumption mechanism. In addition, smaller amounts of water are purged from the cooling water circuit to avoid build up of harmful contaminants. This “blowdown” water may be evaporated in holding ponds (in which case it is consumed) or discharged to the watershed (in which case it is not counted as consumed). A third water consumption mechanism is “drift,” spray that leaves the tower as liquid, but this may be considered negligible.

Wet towers withdraw far less water than once-through systems – about two orders of magnitude less. However, the water consumption of wet towers is somewhat more than once-through, and the cost and complexity is higher. In addition, cooling towers may elicit aesthetic objections; they produce vapor plumes under certain conditions, and natural draft cooling towers are huge structures hundreds of feet high.

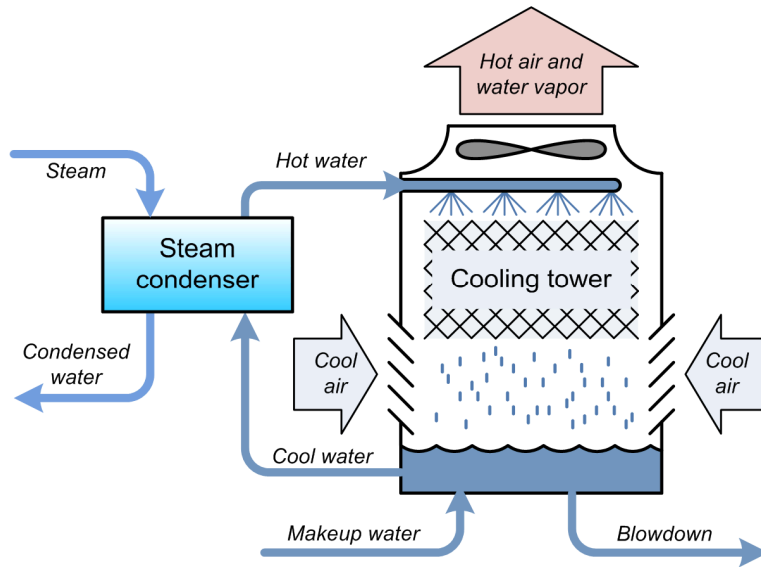


Figure 3: Diagram of wet cooling tower (mechanical draft)

“**Dry cooling**” (see Figure 4a), sometimes called air cooling, rejects waste heat to the atmosphere without relying on the evaporation of cooling water. Dry cooling withdraws and consumes no water, although other processes in a dry-cooled power plant may use water.

Dry cooling systems require a very large heat exchanger surface area – like an enormous radiator – to reject the power plant waste heat. As such, dry cooling is three or four times as expensive as an equivalent wet tower cooling system. Furthermore, the overall efficiency of the power plant depends on effective cooling; on hot days, the effectiveness of a dry cooling system decreases, and the plant efficiency decreases as well. Unfortunately, hot days usually coincide with high electricity demand (and high electricity prices).

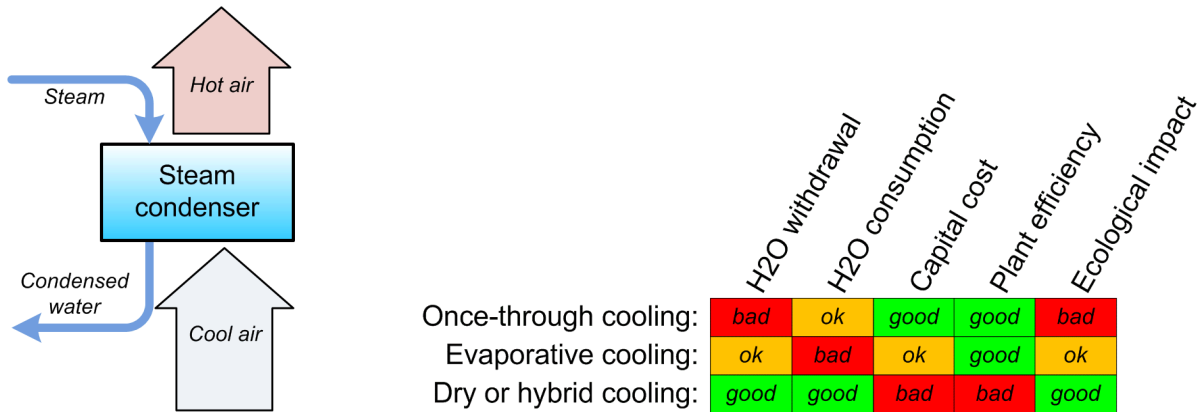


Figure 4: a) Diagram of dry cooling system; b) Cooling system tradeoffs in a nutshell

“**Hybrid cooling**” systems combine wet and dry cooling approaches. There are many flavors of hybrid cooling, but all are essentially compromises between wet and dry in terms of cost, performance, and water use.

“**Pond cooling**” entails a quasi-closed loop of cooling water, but uses a system of ponds or canals in place of a cooling tower. After running past the waste heat exchanger, the hot water is discharged to the pond, where it loses heat through evaporation and direct convection with the air, before ultimately being pumped back to the heat exchanger. Evaporation from the pond is the water consumption mechanism.

When considering pond cooling, it is necessary to define withdrawal and consumption more precisely, by defining the boundaries of a control volume for accounting water inflows and outflows. As an illustration, first consider a once-through cooling system (Figure 5). In the case of a once-through cooled plant on e.g. a river, the withdrawal control volume (B) is fairly obvious and agreed-upon, since it is a good metric for evaluating the impact on aquatic ecosystems, the principle concern for a once-through cooling system. Since the mechanism for consumption of a once-through cooling system is increased surface evaporation, the consumption control volume (A) thus makes sense from a regional water supply evaluation perspective since it accounts for this loss.

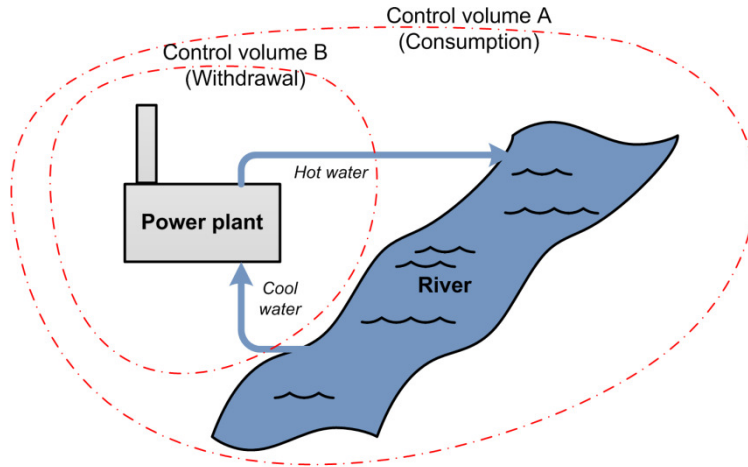


Figure 5: Control volume definitions for water withdrawal and consumption in a once-through-cooled power plant

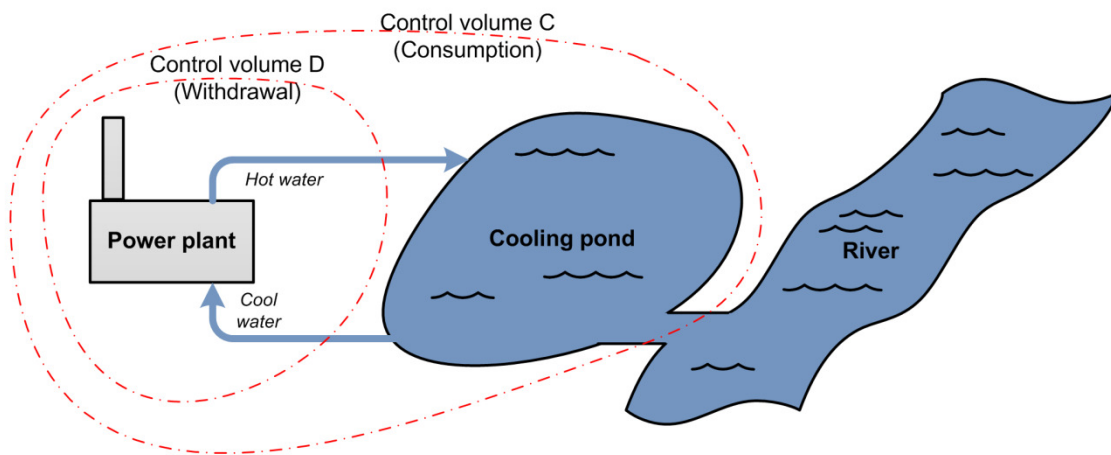


Figure 6: Control volume definitions for water withdrawal and consumption in a pond-cooled power plant. There is currently no standard convention for the withdrawal control volume.

Control volume issues are less clear-cut in the case of pond-cooled systems. Part of the issue is the wide variety of systems that fall under the header of “cooling pond;” it may refer to what is essentially a lake, a large aquatic habitat with overall moderate water temperatures; or it may be a highly structured series of canals, small and heavily-heated and intentionally devoid of wildlife; or anything in between.

Consider the diagram of a pond-cooled plant shown in Figure 6. The consumption control volume for a pond cooling system (C) is generally agreed upon, since it results in a useful number from both a regional-level and a plant-level water planning perspective. Modeling pond-cooling consumption generically is basically impossible since it is so site specific, but for a given heat load it can be safely bounded between consumption for wet-tower cooling on the high end and consumption for once-through cooling on the low end.

For defining withdrawal of a pond-cooled system, this thesis uses control volume D – the same as a once-through system – but there is no broader convention established for this. Across the literature, it is clear that some studies use control volume C for withdrawal while others use D. Which one is more appropriate for a given plant depends on the specifics of the site and the associated ecosystem.

The issue of control volumes raises an important point with regard to regional analysis. When analyzing water use over a given region, the relevant control volume is in fact the region in question. Water that evaporates from within the region effectively leaves the boundaries of the control volume; adding up consumption from multiple plants in the region results in a true cumulative quantity of water consumed. Water withdrawn within the region, however, may be discharged back to the watershed without ever leaving the regional control volume. Summing withdrawal from multiple plants in a region thus results in a number with ambiguous meaning.

Non-cooling processes: The water used by non-cooling plant processes, as noted above, is usually dwarfed by cooling water use. A typical wet cooling tower on a steam-cycle plant might consume 2000 L/MWh of water, while non-cooling processes are at least an order of magnitude below that. The primary water-using processes in various plant types are summarized in Table 1.

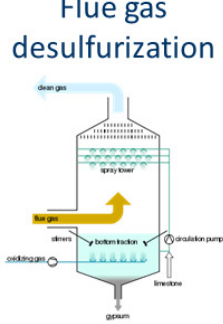


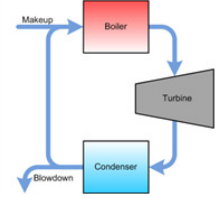
 <p style="text-align: center;">Flue gas desulfurization</p>	 <p style="text-align: center;">Bottom ash handling</p>	<p style="text-align: center;">Gasification / Water Gas Shift</p> $C + H_2O \rightarrow CO + H_2$ $CO + H_2O \rightarrow CO_2 + H_2$	 <p style="text-align: center;">Mirror / PV surface washing</p>	 <p style="text-align: center;">Boiler feedwater makeup</p>
Coal	Coal	IGCC (Coal or biomass)	Solar	All steam-cycle
~200 L/MWh (consumed)	~100 L/MWh (reusable)	~200 L/MWh (consumed)	~20 L/MWh (consumed)	~20 L/MWh (reusable)

Table 1: Non-cooling process water uses for various plant types, with order-of-magnitude-water use figures

Water as a Factor in Cost of Electricity

Water use at power plants is a highly regional issue; it matters much more in some places than in others. A useful guide is to assume that it matters when concerns over water use appear as a non-negligible factor in the levelized cost of electricity (LCOE) produced by for-profit power producers. There are several mechanisms through which this can occur:

- Direct costs of water – Water supply or disposal costs are themselves a non-negligible fraction of levelized electricity costs
- Capital costs – Water use concerns force investment in more expensive infrastructure (e.g. a dry or hybrid cooling system, discharged water treatment system, etc.), the amortized cost of which appears in the LCOE
- Operating costs – The cost of running water-conserving cooling systems or water treatment systems appears in the LCOE
- Capacity factor – Lack of available water forces plant shutdowns, driving the plant capacity factor down and the LCOE up
- Thermal efficiency – Water use concerns force the implementation of a plant system that decreases efficiency, increasing fuel required and thereby LCOE
- Regulated emissions – Water use concerns force the implementation of a plant system that results in increased regulated emissions, which must be offset by buying credits or paying taxes which raises LCOE
- Permitting delay – Water use concerns force delay in plant construction, prolonging scarcity and raising LCOE

In adopting this approach it is assumed that while the goal of the power producers is solely profit, the economic, regulatory and permitting environment in which the power producers operate perfectly reflects the priorities of that society. This is obviously not the case; there are inefficiencies in economic and legislative processes, and there are conflicts of interest within any society, be it municipal, national, or global. However, this approximation allows compression of a wide variety of variables onto a single axis (LCOE).

Because power plant costs and revenues depend on so many variables (which are often difficult to obtain), the work described in this thesis includes few specific economic analyses. By thinking along economic lines, however, the relative importance of various aspects of power plant water use can be considered in a unified fashion, and research guided accordingly.

Available Data Sources

All published data on water use for electricity generation is ultimately derived from two types of sources: models of water use based on physical laws, and field measurements at generation plants (see Figure 7). For the most part, published data sources can be traced back to one or both of these ultimate source types, although a few sources are “opaque,” providing little reference information on where their numbers are coming from.

The sources called out in Figure 7 are actually the majority of those that are closely tied to primary data and physical models. While there are many secondary data aggregations and augmentations of water use data, nearly all of them use some subset of the reports and papers listed in the figure as their principal data sources. There are only a handful of independently developed models and independently collected primary datasets.

To make matters worse, the available field datasets in the US suffer from limited granularity and poor quality, as addressed in the 2009 report by Mittal and Gaffigan, of the US Government Accountability Office (GAO). They interviewed various users of federal water use data, as well as representatives from the U.S. Energy Information Administration (EIA) and U.S. Geological Survey (USGS), the two organizations responsible for collecting that data.

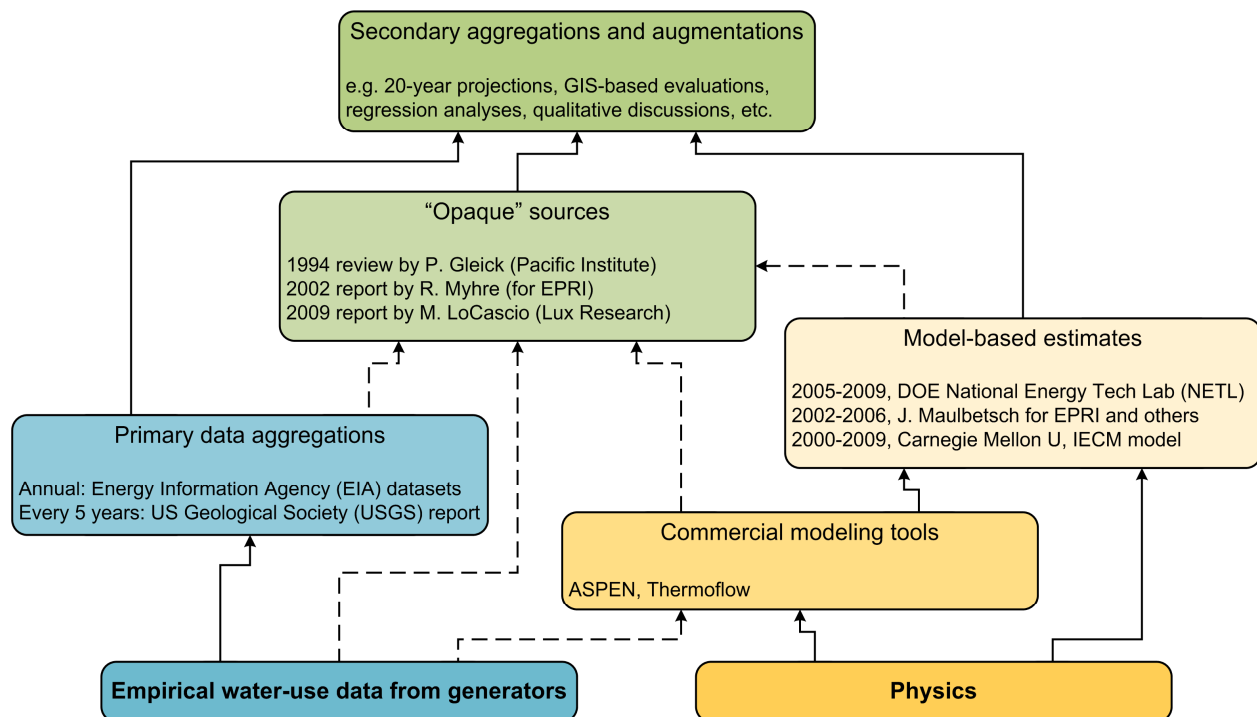


Figure 7: “Family tree” of US water-for-energy data and reports. There are very few primary sources.

The GAO identified significant limitations, notably including a lack of quality assurance on the data reported to the EIA: “Respondents may use different methods to measure or estimate data, and instructions may be limited or unclear. Respondents may make mistakes or have nontechnical staff fill out surveys.” Other limitations of the EIA and USGS datasets cited by the GAO include lack of consistency in USGS methods (in some states USGS draws heavily on EIA data); lack of seasonal data; and lack of detail on cooling system configurations and water sources.

Presumably as a result of such complaints, the EIA is in the process of improving its data collection processes, which will in time yield richer and higher-quality data sets. In the meantime, however, it is clear that to obtain estimates of US water use with a reasonable degree of resolution and accuracy, modeling is necessary.

Outside the US, available data is generally even more sparse. One notable exception, however, is South Africa. Eskom, the main public utility, maintains detailed accounts of water use at each of their power plants. A rich set of operational data from the Eskom fleet was requested and received, which was invaluable in the validation of the models developed in the following sections.

Part 1 – A System-Level Generic Model of Power Plant Water Use

Introduction

In many regions of the world, water use at thermoelectric power plants, predominantly for cooling, has a significant effect on the overall water supply and on the ecological health of surface water bodies. In some instances, permits for proposed plants have been denied because of water availability concerns or potentially adverse effects on aquatic life. In other instances proposed plants have opted for designs which include cooling systems that use less water but cost more and result in lower plant efficiency, or existing plants have been retrofitted with such cooling systems. During droughts, there have been cases in which generation plants have shut down because remaining operational would have left them in noncompliance with water use regulations. Water use at power plants is thus an issue that affects regional ecology and security of supply of both water and electricity. [1]-[5]

The importance of power plant water use is increasingly recognized, and several efforts have been made to analyze power plant water use in the US based on field data. Yang and Dziegielewski [6] performed statistical regressions on a water use dataset collected via survey from generators by the US DOE Energy Information Administration (EIA). The objective of the study was to identify major determinants of water withdrawal and consumption in terms of fuel types, cooling system types, operation conditions, and water sources. (“Withdrawal” refers to water taken from a watershed or aquifer, irrespective of whether it is ultimately discharged to the watershed. “Consumption” refers to water withdrawn that is specifically not discharged to the watershed. In this thesis, the term “water use” refers generically to both withdrawal and consumption.)

Feeley et al. [7] of the DOE National Energy Technology Laboratory (NETL) developed twenty-five-year forecasts of thermoelectric water use in the US using a set of “model plant profiles,” essentially categories broken out by plant and cooling system configuration. For each profile, associated water withdrawal and consumption factors were calculated, drawing on information from several sources but predominantly EIA survey data. Regional water use was then projected under various scenarios specifying electricity demand, generation mix (in terms of the model plants), and penetration of water use reduction technologies.

In a similar study, King, Duncan and Webber [8] projected power plant water use in the state of Texas over a ten-year timeframe. Their analysis was resolved to the level of individual plants and drew on field data from state agencies where available. Where field data was unavailable, default withdrawal and consumption factors were used, estimated with input from industry and regulatory stakeholders.

Data-focused research on power plant water use, however, has historically been hampered by the limited granularity and poor quality of the available field data. The two principal nation-wide sources of power plant water use data in the US, respectively published by the US EIA and US Geological Survey (USGS), are acknowledged to suffer from significant inaccuracies, inconsistency, and incompleteness [4],[5]. While the data collection and quality assurance tools used by the EIA and USGS are improving, the quality of these datasets is still fundamentally limited: the US fleet contains a wide variety of power plant configurations, and there are currently no standardized methods for measuring or estimating water usage. In many other countries, moreover, power plant water use data is simply unavailable.

Model-focused research on water use at power plants has generally revolved around detailed reference models of individual plants. A series of studies [9]-[11] published by NETL used detailed process models of state-of-the-art fossil-fuel power plants to benchmark various aspects of plant performance, including water use. The US DOE National Renewable Energy Laboratory (NREL) took a similar approach in assessing water use in parabolic trough concentrated solar plants [12]. The Integrated Environmental Control Model (IECM), a fossil-fuel power plant model developed by Rubin et al. [13], includes a water use submodel; recent work by Zhai [14],[15] applies IECM to assessing the effect of carbon capture on water use. Because of the targeted nature and fine level of detail of these models, however, it is difficult to apply them generically to generate estimates of regional power plant water use or to evaluate the potential effects of new technologies or policies.

A system-level generic model (S-GEM) of water use at wet tower-cooled power plants was recently introduced by the author and colleagues [16] to address these deficiencies. The S-GEM applies to fossil, nuclear, geothermal and solar thermal plants, using either steam or combined cycles. Drawing on related treatments in the literature (Maulbetsch [17], Zhai [18]), the S-GEM was developed with the objectives of capturing the essential physics of the processes involved while minimizing computational complexity and number of input parameters. The basis of input parameters was selected such that each parameter has a clear physical meaning that can be related to plant operating conditions and performance metrics, ideally those that are specified for large numbers of plants in readily-available datasets. Part 1 of this thesis presents a methodology for estimating those parameters, validates the S-GEM against water consumption data from the literature and from the field, and concludes with a discussion of the implications of S-GEM for reducing water consumption at wet tower-cooled power plants.

The System-level Generic Model (S-GEM)

The outputs of the S-GEM are values for water withdrawal and water consumption intensity, in units of L/MWh. These intensities represent the ratio of the volume of water withdrawn or consumed to the net electrical energy produced.

At the highest level, the S-GEM divides water withdrawal or consumption intensity I into cooling use intensity I_{cool} and process use intensity I_{proc} :

$$I = I_{cool} + I_{proc} \quad (1.1)$$

For most plants with wet tower cooling systems, I_{cool} is larger than I_{proc} by at least an order of magnitude, for both withdrawal and consumption. The S-GEM therefore leaves I_{proc} as a standalone coefficient reflecting the water use of all non-cooling processes in the plant, such as boiler feedwater makeup, cleaning, ash handling, and flue gas desulfurization (FGD). The value of I_{proc} is accounted net of any internal recycling streams; a non-cooling process whose wastewater was then used as makeup water for the cooling system would not count towards I_{proc} . Similarly, a non-cooling process whose water source consisted of cooling tower blowdown would not count towards I_{proc} . For the purposes of the S-GEM, I_{proc} is considered the same for both withdrawal and consumption; it is assumed that any non-cooling process wastewater streams discharged to the watershed, as opposed to evaporated or recycled, are negligible.

To determine I_{cool} , it is necessary to characterize the cooling system heat load. A Sankey diagram showing the energy flow for a generic thermoelectric power plant is shown in Figure 8.

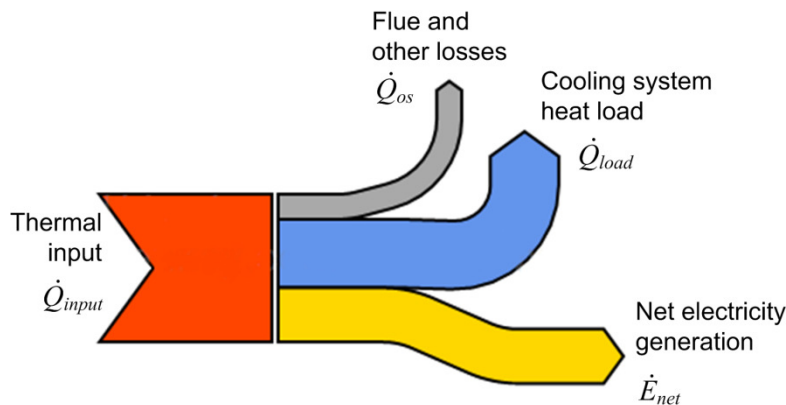


Figure 8: Heat flow through a generic steam-cycle or combined-cycle power plant

Referencing the Sankey diagram, the net efficiency η_{net} can be defined:

$$\eta_{net} \equiv \frac{\dot{E}_{net}}{\dot{Q}_{input}} \quad (1.2)$$

where \dot{E}_{net} is the net electricity generation rate and \dot{Q}_{input} is the rate of thermal input to the plant, both in units of MW. The dimensionless coefficient k_{os} , representing the fraction of heat lost to sinks other than the cooling system, is defined as:

$$k_{os} \equiv \frac{\dot{Q}_{os}}{\dot{Q}_{input}} \quad (1.3)$$

where \dot{Q}_{os} is the rate of thermal loss up the flue and to other sinks, in units of MW. The heat loss mechanisms encompassed by \dot{Q}_{os} include heat rejected directly to the atmosphere (not counting any such heat transfer in the cooling system) and heat lost due to a difference in enthalpies of the input and output streams (net of any difference in enthalpies of formation that is accounted for by the heating value of the fuel in \dot{Q}_{input}).

An energy balance results in the following expression for the heat load on the cooling system \dot{Q}_{load} :

$$\dot{Q}_{load} = \dot{Q}_{input} (1 - \eta_{net} - k_{os}) \quad (1.4)$$

The two most common means of rejecting waste heat at US power plants are wet tower cooling systems and once-through cooling systems [7]. The mechanisms of water use in these two system types are quite different, so a separate version of the S-GEM was developed for each.

S-GEM for wet tower-cooled plants

Wet tower cooling (see Figure 9) uses a recirculating loop of cooling water. In a typical cooling tower, hot water from the condenser and any other heat loads flows into the top of the tower. This hot water is sprayed onto the “fill,” a block of lattice-like material that increases the surface area of the flow down through the tower. At the same time, a fan or natural draft draws air from the bottom of the tower up through the fill and out to the environment.

The flow of air and water acts as a heat exchanger, with convective, or “sensible,” heat transfer from the water to the air. Moreover, a small fraction of the water evaporates as it makes its way down through the tower, and the latent heat of this evaporation cools the remaining water as well. The cooled water collects at the bottom of the tower, from where it is pumped back to the condenser and other heat loads.

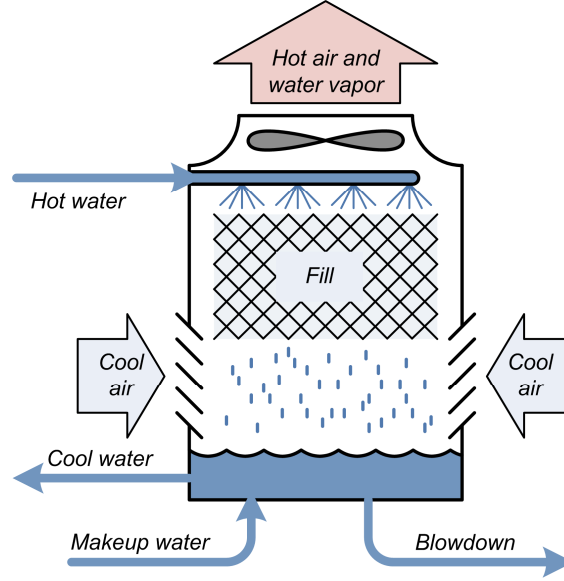


Figure 9: Schematic of wet cooling tower (induced draft)

Evaporation from the cooling tower is the principal mechanism through which water is consumed. In addition, smaller amounts of water are purged from the cooling water circuit to avoid build-up of harmful contaminants. This “blowdown” water may be evaporated in holding ponds (in which case it is consumed) and/or discharged to the watershed (in which case it is not counted as consumed). A third water consumption mechanism is “drift,” spray that leaves the tower as liquid, but this may safely be considered negligible. [17]

The fraction of heat load rejected through sensible heat transfer is denoted here as k_{sens} , and depends on the temperature of the incoming air, and to a lesser extent on the design of the cooling tower and the ambient humidity and atmospheric pressure. The remainder of the heat load is rejected through evaporation, such that the evaporation losses \dot{W}_{evap} in units of kg/s can be expressed as:

$$\dot{W}_{evap} = \frac{\dot{Q}_{load} (1 - k_{sens})}{h_{fg}} \quad (1.5)$$

where h_{fg} is the latent heat of vaporization of water, assumed constant at 2.45 MJ/kg.

The rate of blowdown $\dot{W}_{blowdown}$ can be related to the rate of evaporation \dot{W}_{evap} in terms of the number of cycles of concentration n_{cc} , a parameter that describes the concentration of impurities in the circulating water relative to that of the makeup water:

$$\dot{W}_{blowdown} = \dot{W}_{evap} \left(\frac{1}{n_{cc} - 1} \right) \quad (1.6)$$

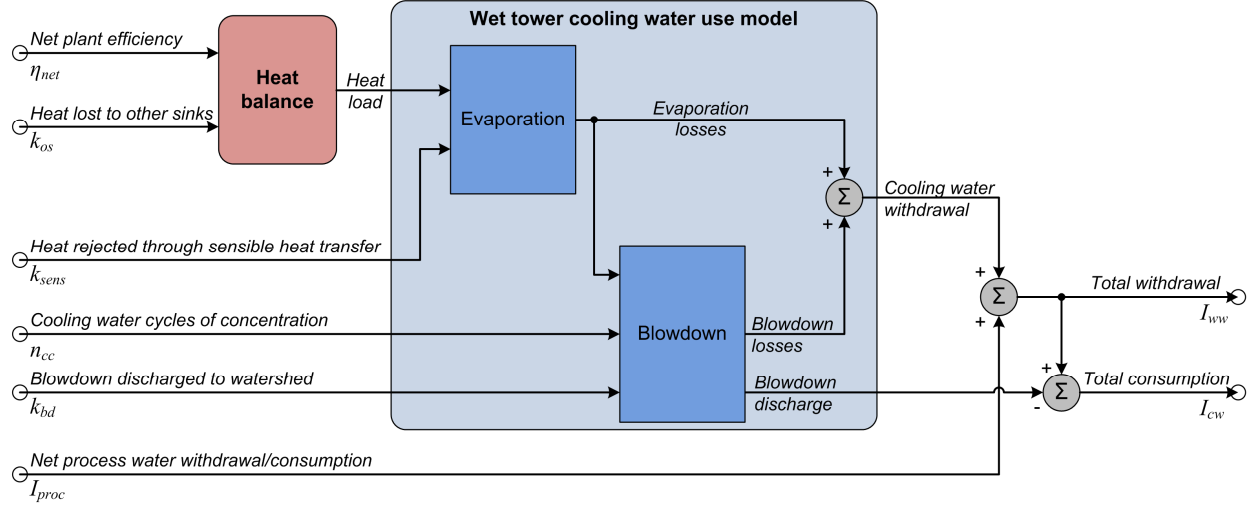


Figure 10: Block diagram of S-GEM for wet tower-cooled power plant

Derivations of this relation appear in [17] and [18], so it is not presented here. The purer the input stream, the more cycles of concentration can be tolerated before mineral impurities reach unacceptable levels; typical values for n_{cc} in the US fall between 2 and 10 [9],[19].

Combining Equations 1.4, 1.5, and 1.6 yields an expression for the total cooling tower water loss \dot{W}_{cool} in units of kg/s:

$$\dot{W}_{cool} = \dot{Q}_{input} (1 - \eta_{net} - k_{os}) \frac{(1 - k_{sens})}{h_{fg}} \left(1 + \frac{1}{n_{cc} - 1} \right) \quad (1.7)$$

Converting the above into an expression for cooling water withdrawal intensity in L/MWh is accomplished by dividing through by net electricity generation \dot{E}_{net} and water density ρ_w (assumed constant at 0.998 kg/L), and multiplying by 3600 to convert between seconds and hours. Adding the resulting expression to the non-cooling process intensity coefficient I_{proc} yields the final equation for withdrawal:

$$I_{ww} = 3600 \frac{(1 - \eta_{net} - k_{os}) (1 - k_{sens})}{\eta_{net} \rho_w h_{fg}} \left(1 + \frac{1}{n_{cc} - 1} \right) + I_{proc} \quad (1.8)$$

The delta between withdrawal and consumption hinges on how blowdown is dispatched. At one extreme is zero liquid discharge (ZLD), where none of the blowdown is discharged back to the watershed, in which case withdrawal and consumption are identical. If some fraction k_{bd} of the blowdown is treated and discharged, however, the S-GEM equation for consumption intensity in L/MWh becomes:

$$I_{cw} = 3600 \frac{(1 - \eta_{net} - k_{os}) (1 - k_{sens})}{\eta_{net} \rho_w h_{fg}} \left(1 + \frac{1 - k_{bd}}{n_{cc} - 1} \right) + I_{proc} \quad (1.9)$$

assuming that I_{proc} is the same for both withdrawal and consumption as discussed above. The overall model is diagrammed in Figure 10.

S-GEM for once-through-cooled plants

Once-through cooling, sometimes called open or open-loop cooling, involves withdrawing water from a surface water body, running it past a heat exchanger where it takes on the waste heat, and discharging it to the same water body, now some degrees warmer. The mechanism for water consumption in once-through cooling systems is increased evaporation due to the higher temperature of the discharged water. While this evaporation does not always occur within the physical boundaries of the plant, it is attributable to the cooling system and thus is often included in water consumption analyses.

The system-level generic model for once-through cooling can be developed by realizing that the flow rate of the once-through cooling water through the condenser, \dot{W}_{cond} [kg/s], can be expressed as:

$$\dot{W}_{cond} = \frac{\dot{Q}_{load}}{c_{p,w} \Delta T_{cond}} \quad (1.10)$$

where ΔT_{cond} is the inlet/outlet temperature difference of the cooling water and $c_{p,w}$ is the specific heat of water [MJ/kg-K]. Combining equations 1.4 and 1.10:

$$\dot{W}_{cond} = \dot{Q}_{input} (1 - \eta_{net} - k_{os}) \left(\frac{1}{c_{p,w} \Delta T_{cond}} \right) \quad (1.11)$$

Dividing through by net electricity generation \dot{E}_{net} and water density ρ_w , multiplying by 3600 to convert between seconds and hours, and adding the non-cooling process intensity coefficient I_{proc} yields:

$$I_{wo} = 3600 \frac{(1 - \eta_{net} - k_{os})}{\eta_{net}} \frac{1}{\rho_w c_{p,w} \Delta T_{cond}} + I_{proc} \quad (1.12)$$

To obtain an expression for consumption, the “downstream evaporation” coefficient k_{de} is introduced, representing the fraction of discharged water that undergoes forced evaporation as a result of having been warmed. The value of k_{de} is typically on the order of 1% [19]. Then

$$I_{co} = 3600 \frac{(1 - \eta_{net} - k_{os})}{\eta_{net}} \frac{k_{de}}{\rho_w c_{p,w} \Delta T_{cond}} + I_{proc} \quad (1.13)$$

assuming that I_{proc} is the same for both withdrawal and consumption. The overall model is diagrammed in Figure 4.

As will be established in Part 2 of this thesis, k_{de} and ΔT_{cond} are proportional to one another, such that it is possible to define a k_{sens} term for once-through cooled plants. This enables a direct comparison of water consumption between once-through and wet-tower cooled plants.

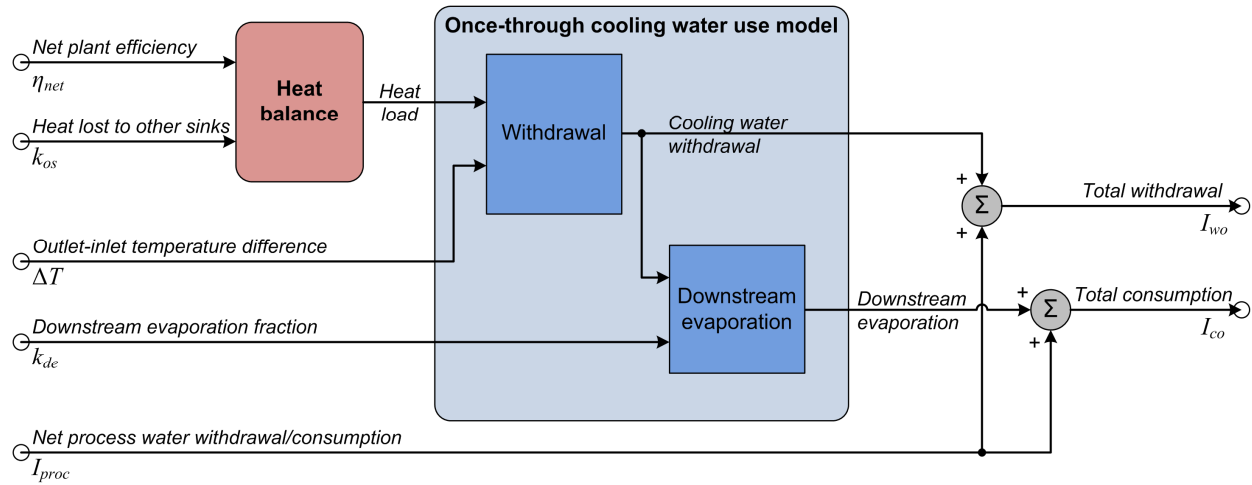


Figure 11: Block diagram of S-GEM for once-through cooled power plant

S-GEM Validation: U.S. Wet Tower Cooled Plants

As a preliminary validation of the S-GEM across generation technologies, data from several sources were used to produce plant-by-plant estimates of water consumption for wet tower-cooled coal, nuclear, and combined-cycle gas plants in the US generation fleet, as well as one binary geothermal plant and one parabolic-trough solar thermal plant. These S-GEM-generated results were then compared to water consumption intensities presented in a recent meta-study by Macknick et al. of DOE-NREL [3].

The primary references for S-GEM parameter estimation were the 2010 EIA-860 and EIA-923 datasets [20],[21], respectively containing specifications and operations data for the US generation fleet. The total set of US plants was first filtered to retain coal, nuclear, and combined cycle gas plants that use only wet towers for cooling. Plants with zero or negative net generation for the year were eliminated. Combined-heat-and-power (CHP) plants and non-utility plants were also eliminated, as the difficulty of separately attributing fuel to electrical generation and heat production in such plants makes calculated efficiency values unreliable. Collectively, the 288 retained plants account for 1360 TWh of net generation in 2010, 33% of the US total. In addition, the SEGS-8/9 parabolic trough solar thermal plant in Harper Lake, CA

and the Second Imperial binary geothermal plant in Heber, CA were selected as renewable generation case studies, based on the availability of relevant data.

For each coal and combined-cycle gas power plant in the dataset, net efficiency η_{net} was calculated from the EIA-923 values of thermal input (based on fuel quantity and higher heating value, or HHV) and net electricity output. The EIA reports only nominal thermal input values for nuclear plants, so a 2010 DOE report on nuclear power plant cooling [22] was used as a source for nuclear plant efficiencies. A histogram of the aggregated efficiencies is shown in Figure 12 (four outlying plants with net efficiencies less than 15% were omitted from the dataset). The average net efficiency of the SEGS-8/9 solar thermal plant was estimated at 29% [23] and that of the Second Imperial geothermal plant at 10.5% [24].

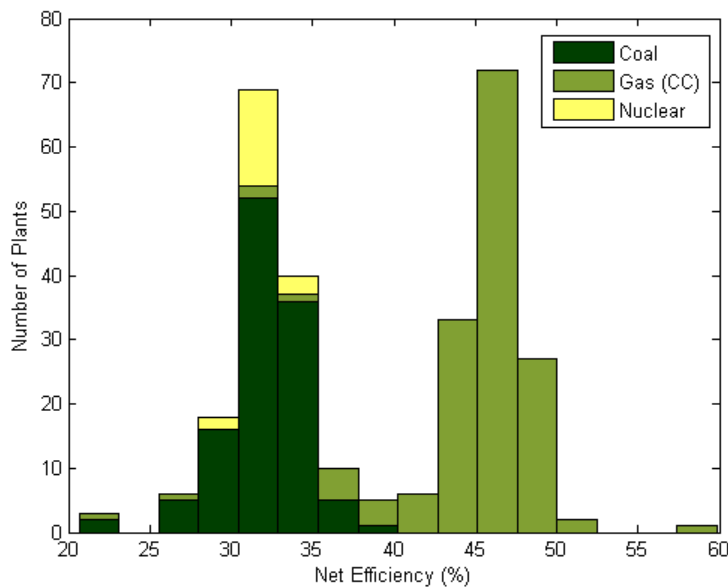


Figure 12: Histogram of net efficiency η_{net} for US wet tower-cooled power plants (2010 data)

A value for k_{os} , the fraction of thermal input lost to sinks other than the cooling system, was set for each plant based on generation technology. For fossil plants, these values were derived from the energy balances of NETL reference models [10] of combined-cycle gas and subcritical pulverized coal plants. Dividing the flue losses by the higher heating value of the fuel input yielded k_{os} values of 12% for coal and 20% for combined-cycle gas. Since non-combustion plants have no flue losses, k_{os} was assumed to be 0% for nuclear, solar thermal and geothermal plants.

To estimate k_{sens} , the fraction of heat load rejected through sensible heat transfer, a correlation was developed based on the Poppe cooling tower model as implemented by Kloppers and Kroger [25]. According to this model, k_{sens} depends on six cooling tower parameters: inlet air temperature, inlet air humidity, inlet water temperature, outlet water temperature, ambient pressure, and water/air mass flow

ratio. Of these, k_{sens} is most sensitive to inlet air temperature. A series of model runs was executed varying air temperature while holding the other tower parameters constant; the results were fit to a cubic equation as shown in Figure 13a. (The model runs assumed standard atmospheric pressure at 0m elevation, air inlet relative humidity of 60%, air/water mass flow ratio of 1, and water inlet temperature of 40°C. The water outlet temperature was determined such that its “approach” to the air inlet wet bulb temperature was 40% of the difference between the water inlet temperature and the air inlet wet bulb temperature.) More sophisticated applications of the Poppe model, which take into account local worst-case weather conditions as well as variation in ambient humidity and atmospheric pressure, can result in more accurate and finer-grained estimates of k_{sens} . The computational expense of such methods is considerable, however, hindering their use with large datasets. Ongoing research seeks to reduce this expense, but for the purposes of this analysis the simple cubic correlation was used.

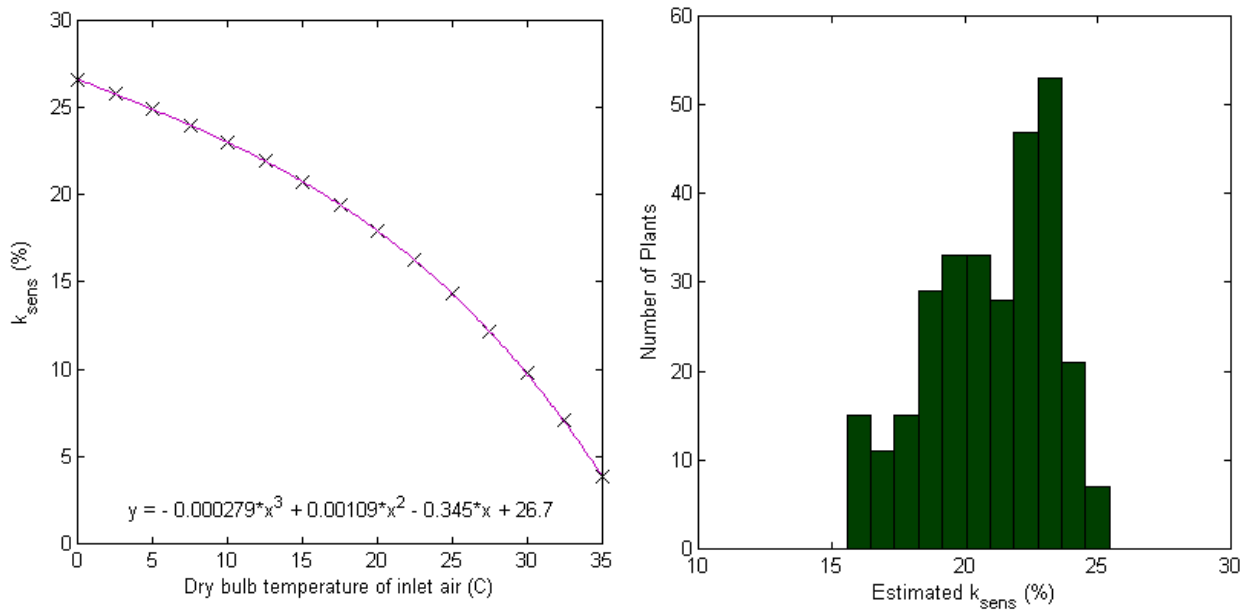


Figure 13: a) Correlation between k_{sens} and ambient dry-bulb temperature derived using the Poppe cooling tower model; b) Histogram of k_{sens} values for US power plants calculated using NCDC temperature normals

To estimate the air inlet temperature for each plant, the approximate latitude and longitude of the plant were found based on 5-digit ZIP code [26], and the nearest weather station registered with the US National Climatic Data Center (NCDC) was located. The overall mean normal air temperature at that station [27] was then used to estimate k_{sens} based on the cubic correlation. A similar approach to the estimation of k_{sens} has been taken by Zhai [18]. A histogram of the k_{sens} estimates at the plants in the dataset is shown in Figure 13b.

The blowdown discharge fraction k_{bd} was assumed equal to 1, effectively eliminating blowdown from the consumption calculation. The EIA-923 and EIA-860 datasets do not contain information on cooling water cycles of concentration (n_{cc}) or blowdown discharge (k_{bd}). In theory, a plant with low values of n_{cc} and k_{bd} would have very high water consumption intensities, as shown by the sensitivity plot in Figure 17b. Typically, however, plants in regions with plentiful water are able to legally discharge most of their cooling tower blowdown to the watershed (values of k_{bd} approaching 1), although n_{cc} may be low. Conversely, plants in regions where water is scarce may have values of k_{bd} approaching 0, but tend to run at higher n_{cc} to conserve water. This inverse correlation between n_{cc} and k_{bd} could be expected to keep the blowdown consumption term in Equation 1.9 to a small if non-negligible fraction.

A value for non-cooling process water use I_{proc} was set for each plant based on generation technology. Coal plants were assumed to use wet FGD units, with a resulting I_{proc} of about 200 L/MWh, while nuclear, gas, and geothermal plants were assumed to use very little non-cooling process water, on the order of 10 L/MWh, for boiler feedwater makeup and miscellaneous uses [10]. A value of 100 L/MWh was assumed for solar thermal case study, due to the water required for washing the parabolic troughs [12].

After estimating the S-GEM input parameters for each plant, the water consumption intensity I_{cw} was calculated using Equation 1.9. A histogram of the results is shown in Figure 14. Shown above the histogram are the median and extreme literature values of water consumption intensity for wet tower-cooled power plants of each type, as given in the 2011 meta-study by Macknick et al. [3]. This meta-study collected and presented estimates of water withdrawal and consumption intensity for various generation technologies in the US, taken unmodified from a comprehensive search of the published primary literature. The results of S-GEM calculations for the renewable generation case studies are shown in Figure 15, again with the meta-study medians and ranges displayed above. Comparison with the meta-study results suggests that the S-GEM for wet tower-cooled plants, as well as the methodology used to estimate S-GEM input parameters in this analysis, is reasonably effective.

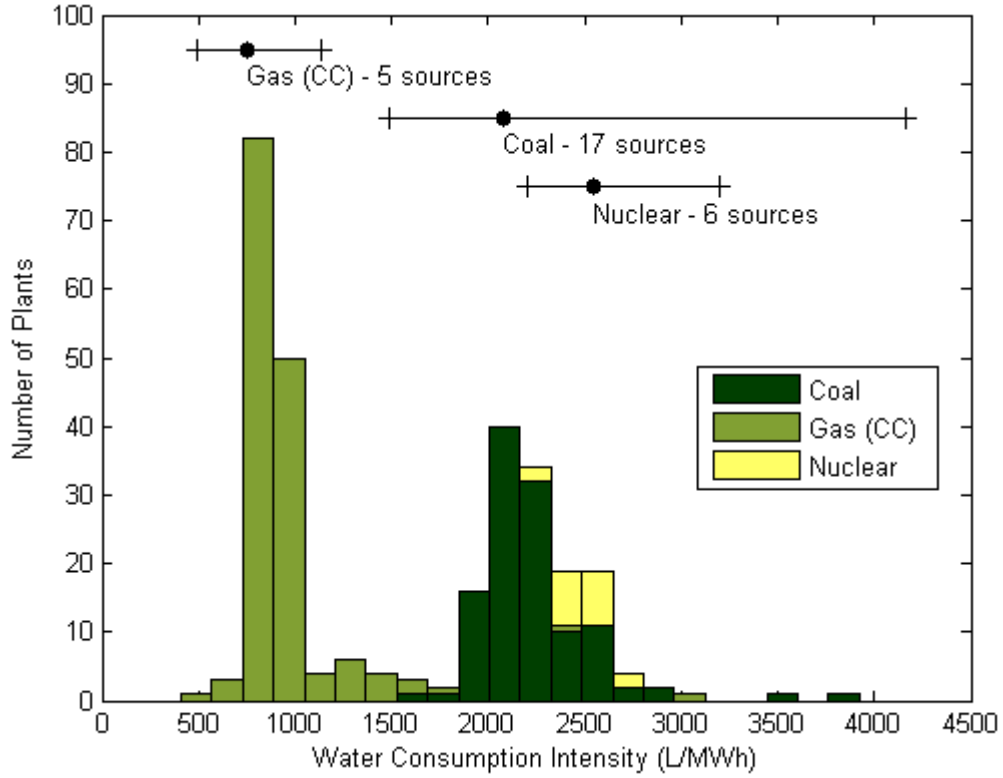


Figure 14: Histogram of S-GEM estimates of plant water consumption intensity, with medians and ranges of values from a meta-study of the literature [3]

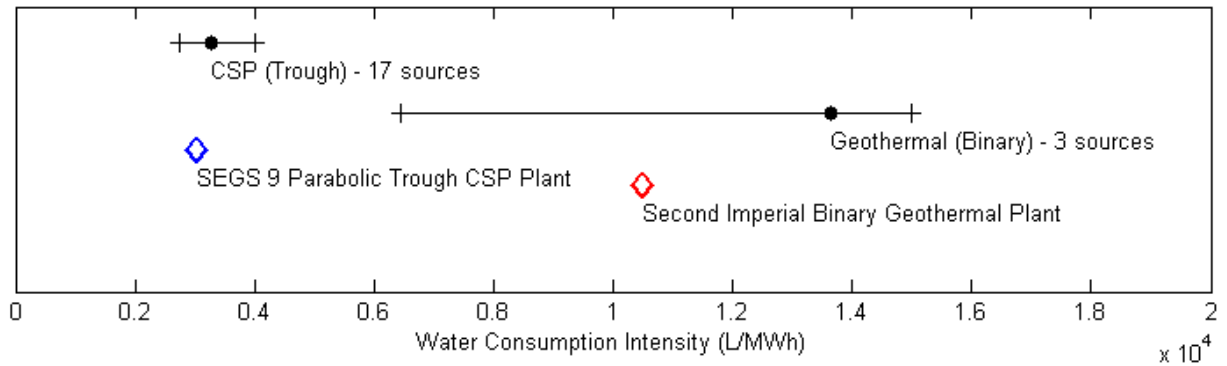


Figure 15: S-GEM estimates of plant water consumption intensity for solar thermal and geothermal case studies, again with data from the meta-study

S-GEM Validation: Eskom Coal Plants

Following the cross-technology validation described above, a finer-grained validation was performed using a dataset from Eskom, the main public utility in the water-scarce nation of South Africa. Eskom maintains detailed accounts of water use at each of their power plants; they provided monthly data from ten coal-fired plants, including net electricity output, net efficiency and water consumption, from April 2006 to March 2011. [28] The plants in the dataset are summarized in Table 2. The water consumption intensities and efficiencies listed are median values of the monthly data.

Plant	Cooling system type	n_{cc}	Measured I_c (L/MWh)	Measured η_{net} (HHV)	Calculated k_{os} ($I_{proc} = 0$ L/MWh)	Calculated k_{os} ($I_{proc} = 150$ L/MWh)
Arnot	Wet tower	20	2074	32.6%	12.6%	16.6%
Duvha	Wet tower	20	2005	33.6%	11.0%	15.1%
Hendrina	Wet tower	20	2327	30.5%	12.4%	16.2%
Kendal	Indirect dry	--	136	32.7%	--	--
Kriel	Wet tower	35	2202	33.8%	3.7%	7.9%
Lethabo	Wet tower	39	1819	34.9%	12.8%	17.3%
Majuba	Hybrid	--	974	33.1%	--	--
Matimba	Direct dry	--	106	33.5%	--	--
Matla	Wet tower	14	1994	34.8%	10.3%	14.4%
Tutuka	Wet tower	39	1915	35.0%	9.4%	13.9%

Table 2: Coal-fired power plants in the Eskom data set, with median values of measured water consumption intensity, measured net efficiency, and back-calculated k_{os}

Analysis of the Eskom data included three key goals: validation of the overall S-GEM; validation of the methodology for estimating k_{sens} ; and confirmation of typical values of I_{proc} and k_{os} for coal plants.

In the analysis of the Eskom data, k_{bd} was zero; all Eskom plants follow a ZLD policy, so withdrawal and consumption are identical. The value of n_{cc} was given for each plant, and the value of η_{net} was given for each plant by month. The remaining unknowns in Equation 1.9 were thus k_{sens} , I_{proc} , and k_{os} .

To estimate k_{sens} , historical information on ambient temperature was required. The latitude, longitude, and elevation of each of the seven wet-cooled plant sites was first identified using Google Earth [29]. Since these sites are all located within 100 miles of the Ermelo weather station, historical mean temperature data at Ermelo for each month in the timeperiod of interest was obtained using Weather Underground [30]. The temperatures at each site were then corrected for elevation using an ASHRAE correlation [31] and input to the cubic correlation discussed above to estimate k_{sens} for each plant-month.

Values of I_{proc} were not known for the wet-cooled plants in question, but bounds could be established. An upper bound was estimated using the water use field data from two dry-cooled plants (Kendal and Matimba), for which the only water use is non-cooling process use. Adding margin for variation between plants, the upper bound of I_{proc} was estimated to be 150 L/MWh. The lower bound was taken to be 0 L/MWh; lacking FGD systems, the largest process water streams in these plants are related to ash handling, and with rigorous recycling schemes the associated losses can be minimal.

Having field data for I_{cw} and experimentally-grounded values for every S-GEM parameter except k_{os} , values of k_{os} could then be back-calculated for each plant-month using Equation 1.9. The median results are given in the last two columns of Table 2.

One clear outlier among these results is plant Kriel, with a k_{os} range that does not overlap with any other plants. There is no other characteristic or parameter along which Kriel is particularly anomalous, and this fact combined with unusually high variance in the efficiency and water intensity field data (see Table 3) may suggest a data quality issue at this particular plant.

To complete the validation, a series of S-GEM calculations was conducted using parameter estimation methods of increasing fidelity. First, a baseline calculation was run assuming a value for each parameter that would be typical for a wet-cooled coal plant in a dry location: $\eta_{net} = 34\%$, $k_{os} = 12\%$, $k_{sens} = 15.5\%$, $n_{cc} = 10$, $k_{bd} = 0$, $I_{proc} = 75$. (The baseline value of k_{sens} is that implicitly assumed by the NETL studies [10].) This “Method 0” resulted in a baseline consumption value of 2266 L/MWh, which falls among the median measured values listed in Table 2.

Calculations for each plant-month were then run using “Method 1,” in which values for η_{net} and n_{cc} given in the Eskom data were used, but all other parameters remained at their baseline values. The result is shown on the top row of Figure 16, with the left-hand plot showing data for individual plant-months and the right-hand plot showing median values for each plant. Net efficiency explains much of the variation in consumption intensity; agreement with measured values is fairly good, particularly for the median values at each plant. Within the data each plant, however, Method 1 falls short. The points from plant Tutuka, for example, do not trend well along the line of perfect agreement.

Method 2, in which estimated values of k_{sens} for each plant-month were used in addition to those for η_{net} and n_{cc} , does a better job of capturing the variation within the data for each plant, as illustrated in the difference between the first and the second rows of Figure 16 and the corresponding columns in Table 3. This shows that the methodology for k_{sens} estimation, i.e. for capturing the effects of ambient weather conditions on water consumption, works fairly well, even knowing nothing about the design of the

cooling tower, the atmospheric pressure, or the relative humidity. In addition, the median values of Method 2 fall closer to the line of perfect agreement than Method 1, suggesting that the k_{sens} baseline value of 15.5% is an underestimate for the climate near Ermelo.

Method 3 calculations (third row of Figure 16) used the estimated parameter values of Method 2, as well as values of k_{os} tuned for each plant (the means of the upper and lower estimates shown in Table 2). To be clear, the result is a calculated as opposed to predicted value of water consumption, since the tuning of k_{os} relies on knowledge of measured water consumption values. Unsurprisingly, Method 3 produces the best fit. Future research may result in methods for generating refined plant-by-plant estimates of k_{os} without *a priori* knowledge of water consumption, based on available plant design specifications such as boiler efficiency and flue gas exit temperature. With the exception of plant Kriel, however, the differences between the results of Methods 2 and 3 are relatively small, suggesting that the k_{os} baseline value of 12% is a good one for most coal plants.

Plant	Standard deviation of efficiency (%)	Standard deviation of consumption (L/MWh)	Method 1 correlation coefficient	Method 2 correlation coefficient	Method 3 correlation coefficient
Arnot	0.88	105	0.24	0.45	0.45
Duvha	0.81	106	-0.10	0.06	0.06
Hendrina	1.32	117	0.16	0.29	0.29
Kriel	1.38	292	0.07	0.21	0.21
Lethabo	0.66	95	0.29	0.55	0.54
Matla	0.62	104	0.30	0.47	0.47
Tutuka	1.01	87	0.52	0.69	0.69

Table 3: Standard deviation values for field data on plant efficiency and water consumption intensity, with correlation coefficients between calculated and measured values of water consumption intensity

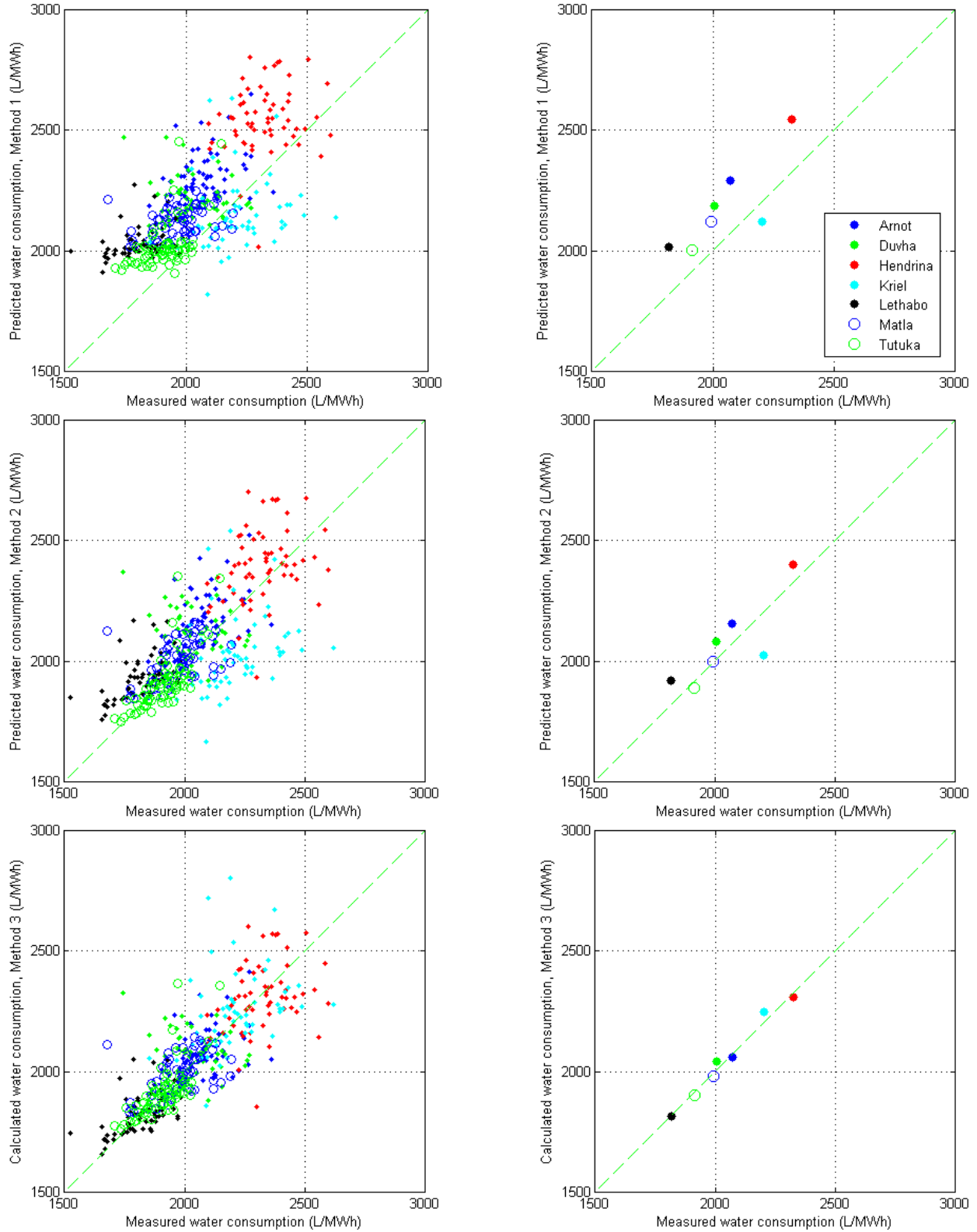


Figure 16: Accuracy of water consumption calculations using three parameter estimation methods. Individual plant-month data are shown on the left-hand charts, medians for each plant on the right-hand charts. Four outlying plant-months (3 from Kriel, 1 from Hendrina) fall outside the plotted range and are thus not shown in the left-hand charts.

Discussion

The above validations suggest that the S-GEM accurately predicts water consumption at wet tower-cooled power plants. As such, it can be used as a quality assurance tool to vet field data on power plant water use, or as a data synthesis tool where field data is unavailable. Along similar lines, it can be used to project the water use profile of a power plant, or a fleet of power plants, under hypothetical demand, climate, and technology deployment scenarios.

More broadly, S-GEM serves as a consistent, quantitative framework to examine the levers that control power plant water use, thus illuminating the most effective means of reducing water consumption. Figure 17 shows the sensitivity of water consumption intensity I_{cw} to various pairs of S-GEM parameters, all other parameters remaining constant at the baseline values used in the South Africa validation.

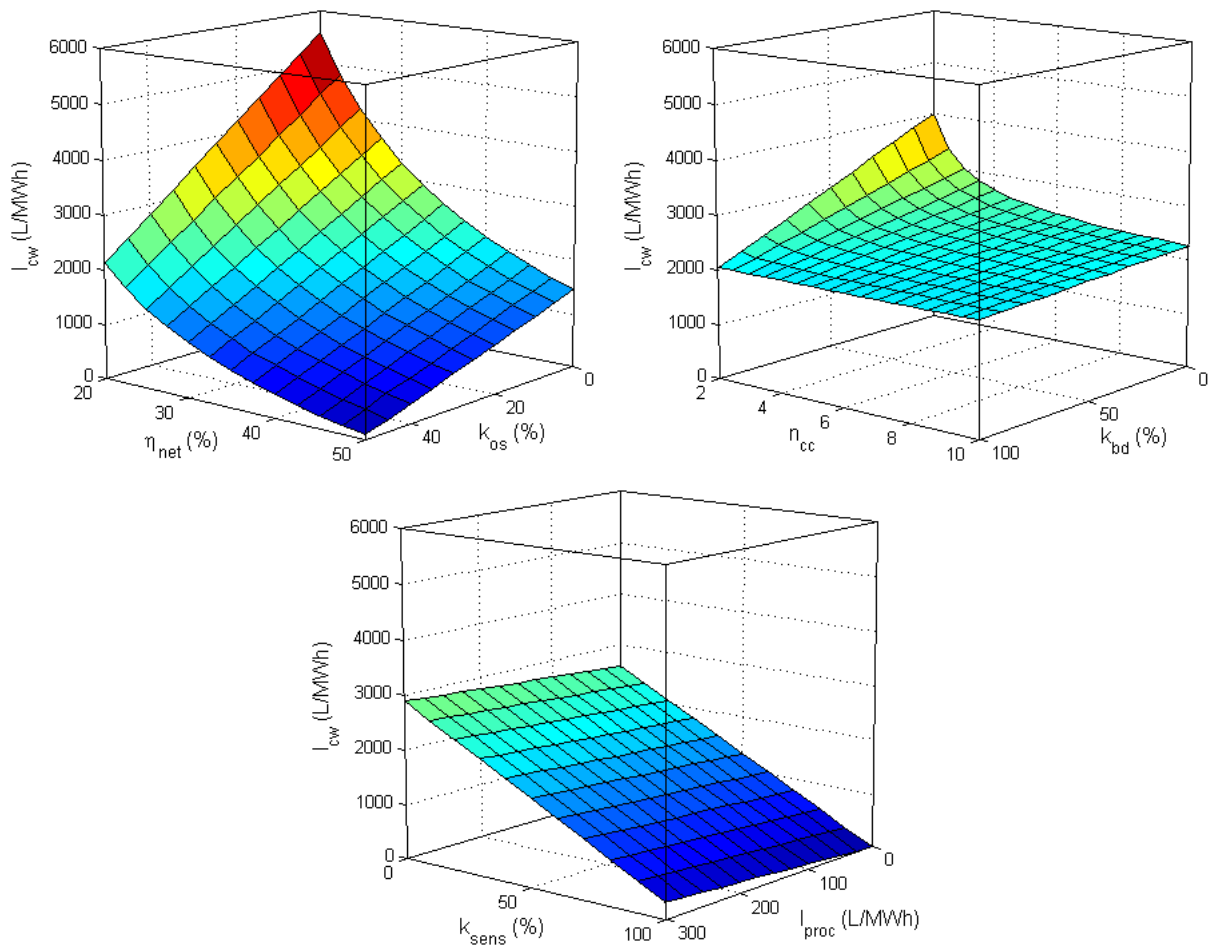


Figure 17: Bivariate sensitivity of water consumption intensity I_{cw} to (a) heat balance parameters η_{net} and k_{os} ; (b) blowdown parameters n_{cc} and k_{bd} ; and (c) parameters k_{sens} and I_{proc}

As Figure 17a shows, the heat balance parameters are very strong levers with respect to water consumption. A wet-cooled binary geothermal plant with $\eta_{net} = 10\%$ and $k_{os} = 0\%$ consumes vastly more

water than a combined-cycle gas plant with $\eta_{net} = 50\%$ and $k_{os} = 20\%$. As the validations have shown, differences in net efficiency in fact explain much of the variation in water use between plants, both within and across generation technologies. Improving the efficiency of a power plant, e.g. by reblading an aging turbine, will result in commensurate reduction in water use. Furthermore, topping-cycle cogeneration plants, in which waste heat is sent out for district or process heating, can achieve very high values of k_{os} . Where there is sufficient demand, cogeneration can greatly reduce the load on the cooling system and thus the amount of cooling water required.

The effect of the blowdown parameters n_{cc} and k_{bd} is illustrated in Figure 17b. Treating the cooling makeup water to enable increased values of n_{cc} can decrease blowdown, but this has somewhat limited scope for reducing water consumption. As discussed above, plants running at low values of n_{cc} often discharge most of their cooling tower blowdown to the watershed. Plants already running at high values of n_{cc} can obtain only incremental water savings by pushing it yet higher.

Figure 17c shows the significance of k_{sens} . For wet tower-cooled systems, k_{sens} typically falls within a fairly narrow range (see Figure 13b). The effect on water consumption is fairly weak and anyways mostly beyond the control of the tower designer. Changing the cooling technology altogether, however, can have dramatic effects on k_{sens} and thus on water consumption. Once-through cooling systems have substantially higher values of k_{sens} , while hybrid wet/dry cooling systems can be higher still. In the limiting case of a dry-cooled plant, all waste heat is rejected through sensible heat transfer; k_{sens} is equal to 100% and the only remaining water use is for non-cooling processes.

The above sensitivity analyses reveal that of the possible means of reducing water consumption at power plants, many yield only incremental results. Tuning a wet tower-cooled plant for efficiency, implementing blowdown and process water recycling schemes, and using dry FGD and ash handling all result in reduced water consumption, but on the order of perhaps 5-20% collectively. To achieve water consumption reductions of a factor of two or more, there are essentially only three options: switch to a much more thermally efficient generation technology; implement topping-cycle cogeneration, or use a different type of cooling system.

Part 2 – Water Consumption in Power Plant Cooling Systems: A Review

Introduction

Freshwater consumption in thermoelectric power plant cooling systems is increasingly cited as a concern in water-stressed regions. Water consumption has therefore emerged as one of the factors that drive build, retrofit, and retirement decisions about cooling systems and even entire power plants. [1]-[5] Existing field data on power plant water consumption, however, is sparse and of poor quality. [4],[5] Furthermore, although the mechanisms of water consumption in cooling systems are reasonably well understood, most relevant models in the literature are esoteric and difficult to apply, inhibiting quantitative discussion on this important topic, particularly at a resource planning or policymaking level.

This review places the water consumption of various cooling systems on a common quantitative analytical footing, enabling direct comparison of water consumption between cooling system types, and examining the factors that affect water consumption within each cooling system type. To frame water consumption in the larger context of engineering tradeoffs, this review also qualitatively summarizes the cost, performance, and environmental impact considerations associated with once-through, pond, wet tower, and wet/dry hybrid cooling technologies.

A broadly-applicable metric for water consumption intensity

Fundamentally, the purpose of all cooling systems is to reject a waste heat load \dot{Q}_{load} [MW] to the environment. In the case of a thermoelectric power plant, the primary heat load comes from the heat exchanger that condenses the steam on the far side of the turbine; auxiliary loads include waste heat from pumps and generators. In the cooling system, this heat load is rejected through a combination of “sensible” heat transfer, i.e. direct conduction or convection to the environment; and “latent” heat transfer, i.e. mass transfer of water evaporated by the waste heat. The fraction of \dot{Q}_{load} rejected through sensible heat transfer is here denoted k_{sens} , while the fraction rejected through latent heat transfer is denoted k_{lat} . The two fractions sum to 1, such that:

$$k_{lat} = 1 - k_{sens} \quad (2.1)$$

By definition, the latent heat in the water evaporated (i.e. consumed) by the cooling system must equal the waste heat rejected through latent heat transfer:

$$\dot{W}_{evap} h_{fg} = k_{lat} \dot{Q}_{load} \quad (2.2)$$

where \dot{W}_{evap} is the rate of water consumption [kg/s] and h_{fg} is the latent heat of vaporization of water [MJ/kg]. Since h_{fg} is approximately constant, it can be seen that the evaporation rate \dot{W}_{evap} is directly

proportional to k_{lat} for a given heat load \dot{Q}_{load} . For the purposes of this review, k_{lat} will thus serve as a proxy for water consumption intensity that cuts across all cooling system scales and types: the higher k_{lat} , the more water consumed per unit of heat rejected.

Note that the performance of the power plant cooling system can have a direct impact on plant efficiency, which affects the amount of waste heat that must be rejected (\dot{Q}_{load}) and in turn the amount of water consumed. The link between efficiency and water use is quantified in Part 1 of this thesis, while the link between cooling performance and efficiency is discussed later in Parts 2 and 3.

Once-Through and Pond Cooling

Once-through cooling (see Figure 18) involves withdrawing water from a surface water body, running it past a heat exchanger where it takes on the waste heat, and discharging it to the same water body, now some degrees warmer. Once-through cooling has the advantage of simplicity and low cost; where cool water is readily available it is also highly effective. [17]

The amount of water withdrawn is very large, however, and can have deleterious ecological impacts. Aquatic life may be “entrained” (sucked into the cooling system) or “impinged” on inlet grates; the increased temperature of the discharge may also have detrimental effects on the local ecosystem. For these reasons, once-through cooling systems have not been used in new plants in the US for some decades, and pending regulations under the US Clean Water Act are pressuring generators to phase out once-through cooling at existing plants. Thorough reviews of the literature on once-through environmental impacts have been conducted by the U.S. Environmental Protection Agency [32] and the California Energy Commission [33] in support of such legislation.

Power plants with once-through cooling systems have in some instances been forced to shut down during heat waves, as remaining operational would have left them in noncompliance with discharge temperature limits. In times of drought, once-through systems have shut down because the water level dropped below the cooling system intakes. [5] Saline once-through systems do not have these problems, however, since the temperature and level of the ocean are fairly stable.

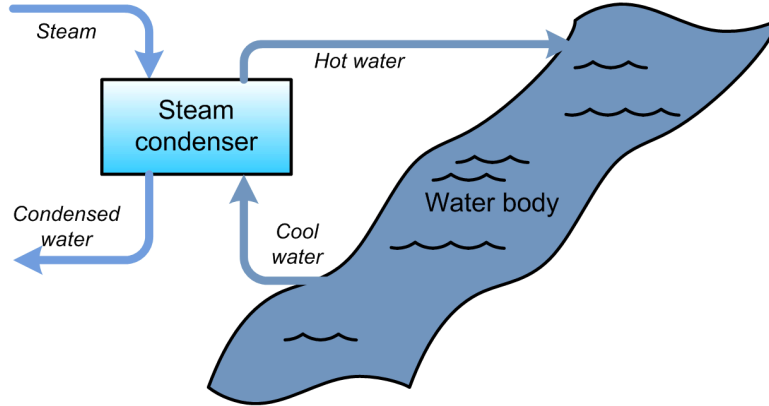


Figure 18: Diagram of a once-through cooling system

The rate of water withdrawal by a once-through cooling system, i.e. the flow rate through the condenser, \dot{W}_{cond} [kg/s], is given by

$$\dot{W}_{cond} = \frac{\dot{Q}_{load}}{c_{p,w} \Delta T_{cond}} \quad (2.3)$$

where ΔT_{cond} is the temperature rise across the condenser [K] and $c_{p,w}$ is the specific heat of water [MJ/kg-K], which is approximately constant. This relationship has important ecological implications. When ΔT_{cond} and thus the outlet temperature of the cooling water is low, the quantity of water run through the system is high, increasing aquatic organism mortality through entrainment and impingement. When ΔT_{cond} is high, entrainment and impingement are reduced, but hotter water is discharged to the water body, potentially damaging heat-sensitive species. The point of least evil from an ecological standpoint is highly site-specific, and may even vary over the course of a year with the life cycles of the local fauna.

The mechanism for water consumption in freshwater once-through cooling systems is increased (“forced”) evaporation due to the higher temperature of the discharged water. While this evaporation does not always occur within the physical boundaries of the plant, it is attributable to the cooling system and thus is typically included in water consumption analyses. Once-through saline systems are considered to consume no freshwater.

Forced evaporation can be modeled using heat and mass transfer theory. First developed by Harbeck in the late 1950s, it has not been substantially improved upon since; Diehl [34] gives a thorough review of the relevant literature. The treatment presented here follows that of Stolzenbach [35], but with certain simplifying assumptions de-emphasized.

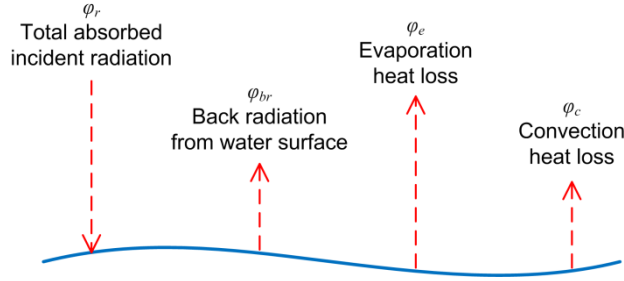


Figure 19: Heat transfer processes at the surface of a water body

The core of the analysis is a heat balance around the surface of the water body, as shown in Figure 19. The net surface heat transfer flux out of the water body φ_n can be expressed

$$\varphi_n = \varphi_r + \varphi_{br} + \varphi_e + \varphi_c \quad (2.4)$$

where φ_r is the total absorbed incident radiation, φ_{br} is the back radiation from the water surface, φ_e is the evaporation heat loss, and φ_c is the convection heat loss, all in units of MW/m^2 and defined such that a positive value represents heat transfer out of the water body.

The total absorbed incident radiation φ_r comprises both solar and atmospheric incident radiation, net of radiation that is reflected from the water surface. It is a function only of ambient weather conditions, independent of the temperature of the water surface. In contrast, the back radiation from the water surface φ_{br} is a function only of the surface temperature T_s [K], independent of ambient weather conditions, per the grey-body radiation law:

$$\varphi_{br} = \varepsilon\sigma T_s^4 \quad (2.5)$$

where ε is the emissivity of the water surface, assumed to be 0.9, and σ is the Stefan-Boltzmann constant, equal to $5.67 \times 10^{-14} \text{ MJ/m}^2\text{-s-K}^4$.

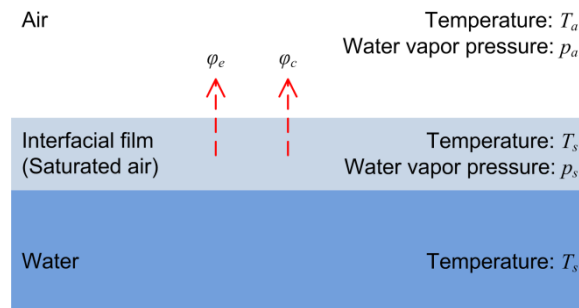


Figure 20: Relevant fluid properties at the air-water interface

The evaporation heat flux φ_e is equal to the latent heat of water vapor lost through mass transfer. Raoult's law is assumed to apply, meaning that the air/water interface is a film of saturated air at the temperature

of the water surface (see Figure 20). The mass transfer flux of water vapor \dot{w}_{evap} [kg/m²-s] can then be expressed:

$$\dot{w}_{evap} = f_v (p_s - p_a) \quad (2.6)$$

where p_s [Pa] is the partial pressure of water vapor in the interfacial film, i.e. the saturation pressure at the surface temperature, and p_a [Pa] is the partial pressure of water vapor in the ambient air. The “windspeed function” f_v [kg/s-m²-Pa] is a mass transfer coefficient that is correlated versus windspeed v [m/s].

The water evaporated draws the latent heat of vaporization from the water body, resulting in the following expression for evaporative heat loss:

$$\varphi_e = h_{fg} f_v (p_s - p_a) \quad (2.7)$$

The expression for convection heat flux φ_c is analogous to that for mass flux, where the driving force is a difference in temperature rather than concentration. The heat transfer coefficient governing the convection process is directly proportional to the mass transfer coefficient f_v , such that the convection and evaporation heat flux can be related as follows:

$$\frac{\varphi_c}{\varphi_e} = \gamma \frac{T_s - T_a}{p_s - p_a} \quad (2.8)$$

where T_a is the ambient air temperature [K] and γ is the psychrometric constant [Pa/K], which changes slightly depending on atmospheric pressure.

Substituting Equations 2.5, 2.7 and 2.8 into the main energy balance (Equation 2.4) yields:

$$\varphi_{n'} \equiv \varphi_n - \varphi_r = \varepsilon \sigma T_s^4 + h_{fg} f_v [(p_s - p_a) + \gamma (T_s - T_a)] \quad (2.9)$$

where the quantity $(\varphi_n - \varphi_r)$ can be considered the “adjusted” net heat flux out of the water body, here denoted $\varphi_{n'}$ for concision. Recall that the total absorbed incident radiation φ_r is constant for a given set of meteorological conditions; since the concern here is an increase in evaporation as opposed to the total evaporation, its absolute value is unimportant.

Given the temperature, relative humidity and atmospheric pressure of the ambient air, its water vapor pressure p_a can be calculated using psychrometrics, the thermodynamics of moist air. (Reviews of psychrometric relationships may be found in many treatments of cooling systems, including Kroger [36], Cheremisinoff [37], and ASHRAE [31].) The vapor pressure of the saturated interfacial film p_s is purely a function of surface temperature T_s , as shown in the lower plot of Figure 21. If the mass transfer

coefficient f_v is known, Equation 2.9 can then be used to calculate the adjusted net flux out of the water body (φ_n) as a function of T_s , as illustrated in the upper plot of Figure 21.

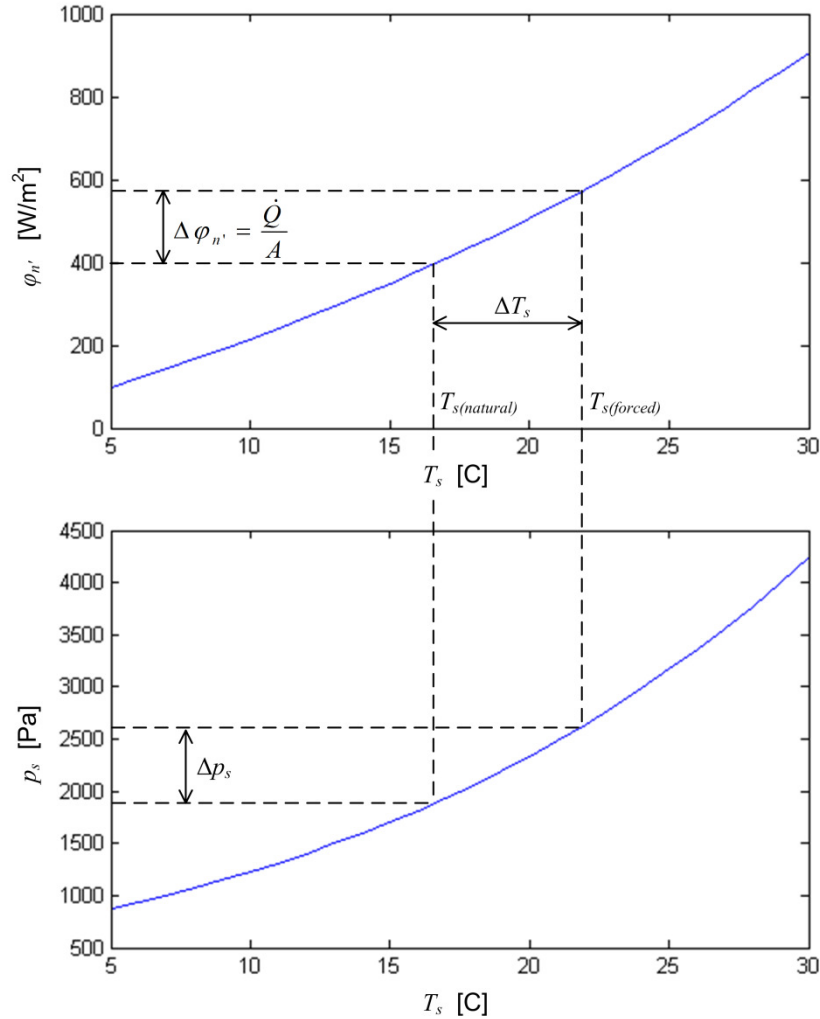


Figure 21: Adjusted net heat flux (top) and surface vapor pressure (bottom) plotted as functions of surface temperature, illustrating solution of forced evaporation due to a given waste heat load

Now consider a well-mixed water body of area A [m²] with a water temperature of $T_{s(natural)}$ in the absence of any thermal load. If we introduce a thermal load of \dot{Q}_{load} from a once-through cooling system on this water body, the water temperature will increase, as will the heat flux out of its surface, until at steady state the increased heat flux out of the surface exactly equals the thermal load per unit surface area (see top plot of Figure 21):

$$\frac{\dot{Q}_{load}}{A} = \varphi_n \Big|_{T_s=T_{s(forced)}} - \varphi_n \Big|_{T_s=T_{s(natural)}} \equiv \Delta\varphi_n \quad (2.10)$$

The surface vapor pressure at $T_{s(\text{forced})}$ is higher than that at $T_{s(\text{natural})}$ by some interval Δp_s (see bottom plot of Figure 21). Per Equation 2.6, this results in a mass flux that is higher by $\Delta \dot{w}_{\text{evap}}$:

$$\Delta \dot{w}_{\text{evap}} = f_v \Delta p_s \quad (2.11)$$

This increase in mass flux as a result of the thermal load is the forced evaporation, i.e. the water consumed by the cooling system. Multiplying through by area A yields an expression for total cooling water consumption rate:

$$\dot{W}_{\text{evap}} = A \Delta \dot{w}_{\text{evap}} = A f_v \Delta p_s \quad (2.12)$$

For a water body of finite area A , the quantity \dot{W}_{evap} can be determined numerically by 1) using Equations 2.9 and 2.10 to find the forced surface temperature increase ΔT_s that corresponds to the specified heat load \dot{Q}_{load} ; 2) using psychrometric relations to find the vapor pressure increase Δp_s that corresponds to that ΔT_s ; then 3) using Equation 2.12 to calculate \dot{W}_{evap} .

As A approaches infinity, however, ΔT_s approaches zero (refer to Figure 21) and a differential form of this relationship arises:

$$\lim_{A \rightarrow \infty} (A \Delta T_s) = \frac{\dot{Q}}{\left(\frac{\partial \phi_{n'}}{\partial T_s} \right)} = \frac{\dot{W}_{\text{evap}}}{f_v \left(\frac{dp_s}{dT_s} \right)} \quad (2.13)$$

This permits an analytical solution which will result in a closed-form expression for k_{lat} . Equations 2.2 and 2.13 can first be combined to yield:

$$k_{\text{lat}} = h_{fg} f_v \frac{\left(\frac{dp_s}{dT_s} \right)}{\left(\frac{\partial \phi_{n'}}{\partial T_s} \right)} \quad (2.14)$$

Expressions for the two derivatives can then be obtained as follows. Recall that p_s is purely a function of T_s ; this allows definition of a thermodynamically constant function β [Pa/K] such that:

$$\beta(T_s) \equiv \frac{dp_s}{dT_s} \quad (2.15)$$

and taking the partial derivative of Equation 2.9 with respect to T_s yields:

$$\frac{\partial \varphi_{n'}}{\partial T_s} = 4\varepsilon\sigma T_s^3 + h_{fg} f_v (\beta + \gamma) \quad (2.16)$$

Substituting Equations 2.15 and 2.16 into Equation 2.14 yields the final expression for k_{lat} for a once-through cooling system on a large water body:

$$k_{lat} = \left(1 + \frac{\gamma}{\beta} + \frac{4\varepsilon\sigma T_s^3}{h_{fg} f_v \beta} \right)^{-1} \quad (2.17)$$

For a given windspeed function, the above expression is dependent only on water temperature (T_s), windspeed (v), and to a lesser extent on elevation, as γ is a function of atmospheric pressure. (ASHRAE [31] gives a correlation for standard atmospheric pressure as a function of elevation.) Note, however, that the above derivation assumes that the mass transfer is out of the water body, i.e. that the vapor pressure of the ambient air is lower than that at the water surface. If this condition is not satisfied, k_{lat} may be considered 0.

There is little consensus in the literature concerning the mass transfer coefficient f_v , which has been fit to linear or quadratic windspeed functions on the basis of various site-specific studies [34]. Figure 22a shows several such windspeed functions as reviewed in Stolzenbach [35]. For the purposes of this review, a simple middle-of-the-road linear windspeed function was selected, shown as a dashed line in Figure 22a:

$$f_v = (1.0 + v) \times 10^{-8} \quad (2.18)$$

A sensitivity analysis of k_{lat} to water temperature, windspeed and elevation was conducted using Equations 2.17 and 2.18, as shown in Figure 22b. While elevation is a weak effect, both water temperature and windspeed are very strong determinants of k_{lat} ; water consumption can easily vary by a factor of two or more depending on ambient conditions. It is also worth emphasizing that k_{lat} does not depend at all on the temperature rise across the condenser, the incident radiation, or the temperature and humidity of the ambient air (as long as the condition regarding vapor pressure is satisfied as discussed above).

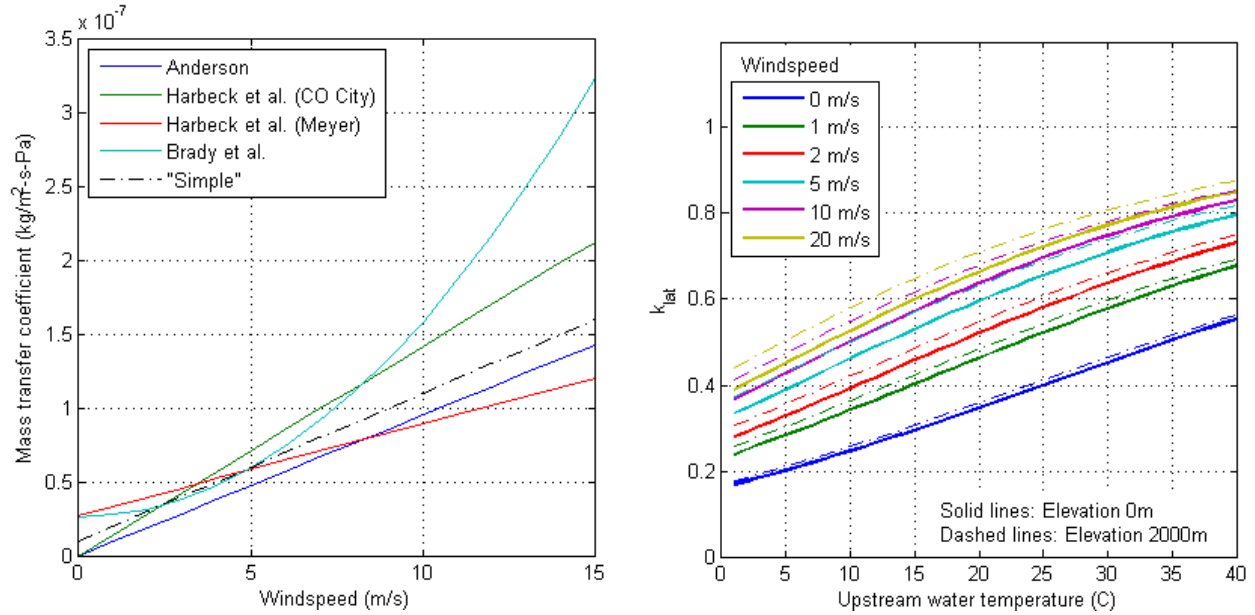


Figure 22: a) Comparison of mass transfer windspeed functions in the literature; b) Sensitivity of k_{lat} to water temperature, windspeed, and elevation.

Pond cooling

Pond cooling can refer to a wide variety of system types, including large artificial lakes that are for all intents and purposes equivalent to once-through cooling systems. As discussed here, however, pond cooling entails a recirculating loop of cooling water moving through a system of ponds or canals. After running past the waste heat exchanger, the hot water is discharged to the pond, where it loses heat through evaporation and direct convection with the air, before ultimately being pumped back to the heat exchanger. Cooling ponds share many of the cost advantages of once-through cooling systems, and are exempt from once-through environmental regulations in cases where they are lined and/or too small to be considered habitat. They do have high land use requirements, however, and only some sites are geographically suitable. [17]

Water is consumed through evaporation from the surface of the cooling pond, so it can be modeled as in the once-through cooling case described above. However, two of the assumptions made for the once-through model – namely, that the surface area of the water body is large, and that the water body is well-mixed – may not hold. The effect of these non-idealities is a surface temperature (T_s) that is higher than in the once-through case. As a result, the vapor pressure at the surface (p_s) is higher (refer to Figure 21), and k_{lat} is commensurately higher. The extent of the increase depends strongly upon the specifics of the pond, but the value of k_{lat} can confidently be bounded between a once-through cooling system and a wet cooling tower under equivalent conditions.

Wet Tower Cooling

Wet tower cooling uses a recirculating loop of cooling water. Hot water from the condenser flows into the top of the tower. This hot water is sprayed onto the “fill,” a block of lattice-like material that increases the surface area of the flow down through the tower. A fan or natural draft draws air through the fill and out to the environment.

The flow of air and water acts as a heat exchanger, with convective (sensible) heat transfer from the water to the air. Moreover, a small fraction of the water evaporates as it flows down through the tower, and the latent heat of this evaporation also cools the remaining water. The cooled water collects at the bottom of the tower, from where it is pumped back to the condenser. The temperature difference between the inlet and outlet water streams is known as the “range.” As in many treatments, it is assumed here that the pipes between the condenser and cooling tower are adiabatic, such that the range is equal to the temperature rise across the condenser; ΔT_{cond} will therefore be used to denote range.

Wet towers withdraw far less water than once-through systems, almost two orders of magnitude less. However, as will be illustrated shortly, the water consumption of wet towers is somewhat more than once-through, and the cost and complexity is higher. The cooled water can in principle approach the wet bulb temperature of the air, so cooling towers are reasonably effective except in environments which are both hot and humid.

Evaporation from the cooling tower is the principal mechanism through which water is consumed. In addition, smaller amounts of water are purged from the cooling water circuit to avoid build-up of harmful contaminants. This “blowdown” may be evaporated in holding ponds (and thus consumed) and/or discharged to the watershed (not counted as consumed). This discussion will not consider blowdown, as this is a system-level issue (see Part 1 of this thesis for the effect of blowdown on water consumption). A third water consumption mechanism is “drift,” spray that leaves the tower as liquid, but this may safely be considered negligible. [17]

Cooling towers are primarily classified according to the direction of the airflow, and the source of the draft (see Figure 23). Each configuration has engineering advantages and disadvantages, as discussed in Kroger [36], Cheremisinoff [37], and Kennedy [38]. Counterflow towers, where the air is drawn upwards, counter to the water flow, are thermodynamically favorable to crossflow towers, so they can in principle achieve better performance in the same footprint. However, crossflow towers, where the air is drawn across the water flow, are somewhat easier to implement in practice. The water distribution system in a crossflow tower can be gravity-fed, requiring less pumping power and creating a more uniformly distributed flow as compared to the sprayer systems used in counterflow towers. Crossflow towers are

also favorable in that the air pressure drop across the fill in is independent of tower height, and the fill support structures do not interfere with the airflow.

Natural draft towers, which rely on the chimney effect to create the air flow, do not require fans and so have low running costs and make little noise. However, natural draft towers must be hundreds of feet high to create a suitable draft; mechanical draft (fan-driven) towers are much more compact, so are preferred from an aesthetic and capital cost standpoint. Mechanical draft towers are sometimes subclassified into “induced draft,” where the fan is situated at the outlet, and “forced draft,” where the fan is at the inlet. Forced draft towers require less fan power, while induced draft towers are less prone to recirculation of exhaust air. Natural draft towers, because of their great height, have a minimal risk of recirculation.

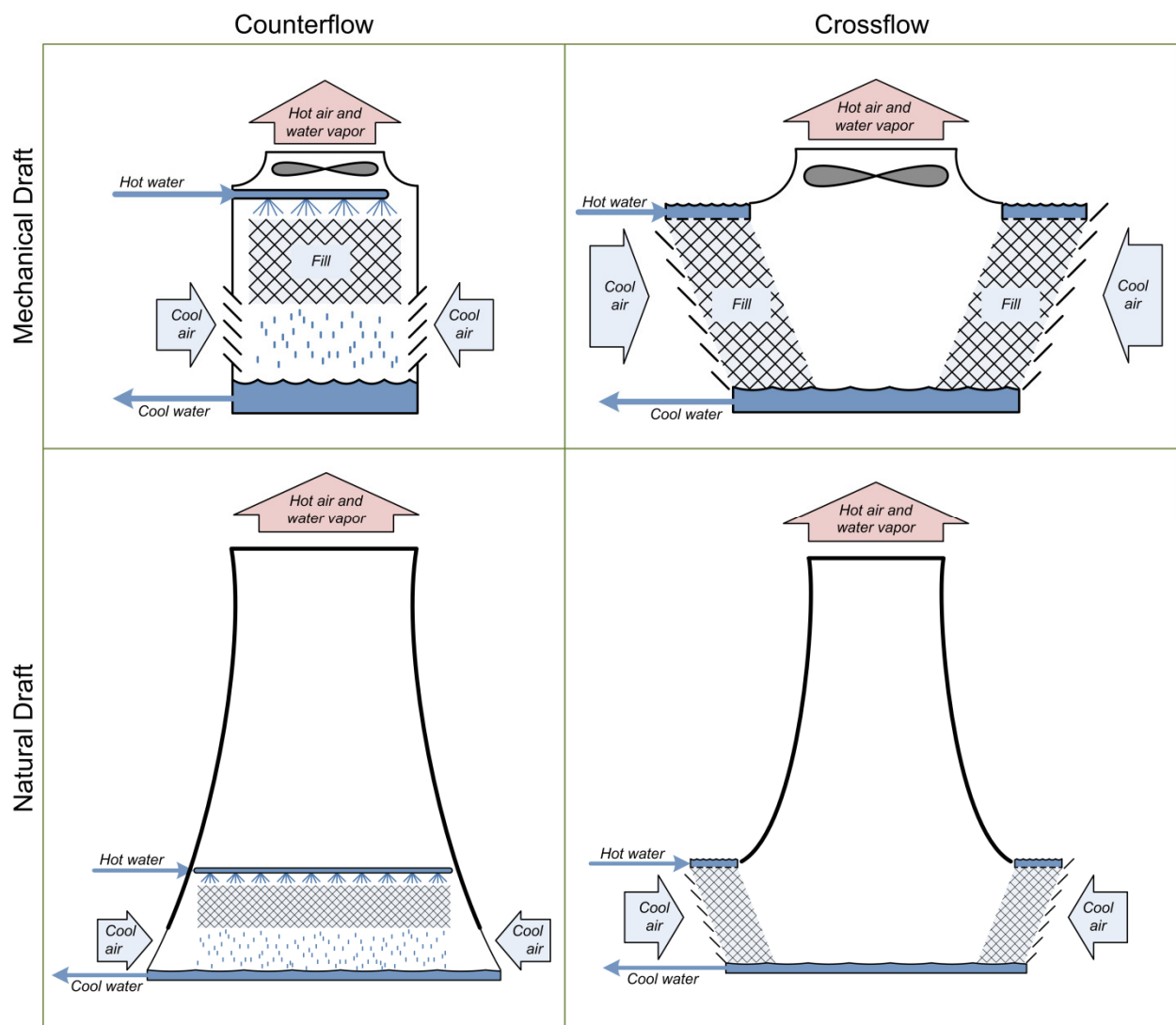


Figure 23: Wet cooling tower taxonomy

Interestingly, while the engineering tradeoffs between tower configurations are certainly important to the system designer, they do not have a significant impact on water consumption (see Lefevre [39]). The below discussion of water consumption in a counterflow mechanical draft tower may generally be considered applicable to crossflow and natural draft towers as well.

Cooling towers have been the subject of theoretical analysis since shortly after their invention in the late 19th century. Baker [40] gives a thorough review of early developments, while Kloppers and Kroger [25] review more recent advances. The focus of most cooling tower analysis, however, is cooling performance as opposed to water evaporation. The literature specifically focusing on cooling tower water consumption is much more limited, and is reviewed below.

The simplest treatments of cooling tower evaporation are rules of thumb that assume a constant value of k_{lat} . “One pound of water evaporated per 1000 Btu of heat transferred” [41] implies a k_{lat} of approximately 1, as can be seen by applying Equation 2.2 with appropriate unit conversions.

Other industry rules of thumb define k_{lat} implicitly using a relationship between evaporation losses \dot{W}_{evap} and circulating water flow rate \dot{W}_{cond} :

$$\dot{W}_{evap} = k_{evap} \dot{W}_{cond} \quad (2.19)$$

The dimensionless constant k_{evap} that relates evaporation losses to circulating water flow rate can be used to determine k_{lat} , by combining Equations 2.2, 2.3, and 2.19 to yield

$$k_{lat} = k_{evap} \frac{h_{fg}}{c_{p,w} \Delta T_{cond}} \quad (2.20)$$

The ASHRAE rule of thumb [42] states that “the evaporation rate at typical design conditions is approximately 1% of the water flow rate for each 12.5°F of water temperature range,” i.e. $k_{evap} = 1\% \times \Delta T_{cond} / 7^\circ\text{C}$, implying a constant k_{lat} of 0.84.

ASHRAE also mentions, however, that k_{sens} increases (k_{lat} decreases) as entering air temperature decreases. This effect is captured to first order by Leung and Moore [41], who perform a heat-and-mass balance around the entire tower with the critical assumption that the air exiting the tower is fully saturated.

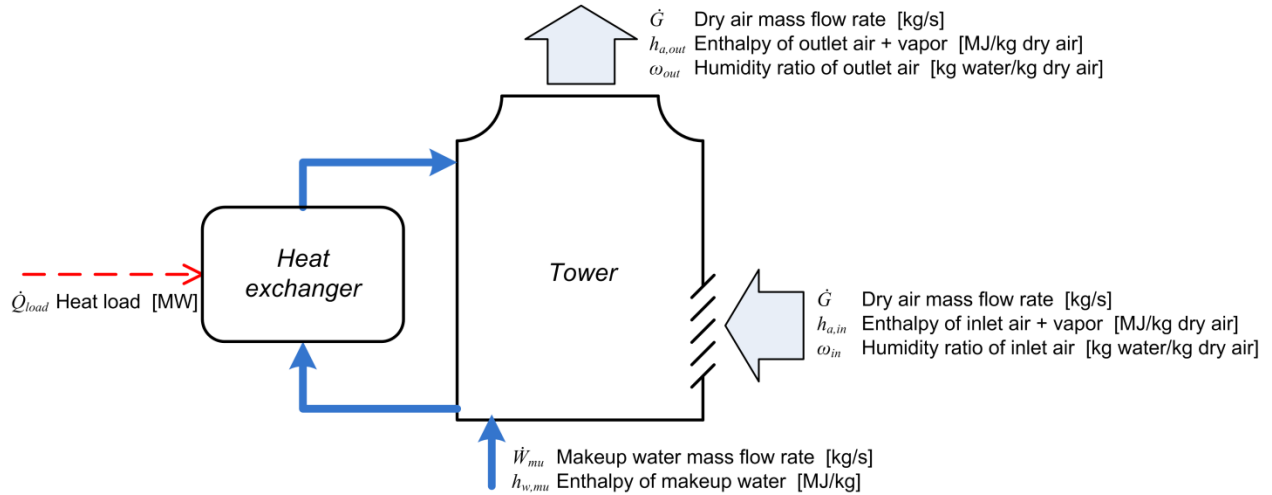


Figure 24: Heat and mass balance around wet tower cooling system, as treated in Leung and Moore [41]

The wet tower cooling system as modeled by Leung is shown in Figure 24. A heat balance around the system yields

$$\dot{Q}_{load} + \dot{W}_{mu} h_{w,mu} = \dot{G} (h_{a,out} - h_{a,in}) \quad (2.21)$$

where \dot{Q}_{load} [MW] is again the system heat load, \dot{W}_{mu} [kg/s] and $h_{w,mu}$ [MJ/kg] are the mass flow rate and enthalpy of the makeup water; \dot{G} [kg/s] is the mass flow rate of dry air through the tower; and $h_{a,in}$ and $h_{a,out}$ [MJ/kg] are the enthalpies of the inlet and outlet air, including water vapor but accounted per unit dry air.

A mass balance around the system yields

$$\dot{W}_{mu} = \dot{W}_{evap} = \dot{G} (\omega_{out} - \omega_{in}) \quad (2.22)$$

where ω_{in} and ω_{out} [kg water/kg dry air] are the humidity ratios of the inlet and outlet air.

Leung assumes that the heat load (\dot{Q}_{load}), dry air mass flow rate (\dot{G}) and makeup water enthalpy ($h_{w,mu}$) are known. Additionally given the ambient temperature, relative humidity and atmospheric pressure, psychrometric relations can be applied to calculate the inlet air enthalpy ($h_{a,in}$) and humidity ratio (ω_{in}). This leaves three unknowns ($h_{a,out}$, ω_{out} , \dot{W}_{mu}) with only two equations. However, given the assumption that the outlet air is fully saturated, there is a one-to-one psychrometric correspondence between outlet air enthalpy ($h_{a,out}$) and outlet humidity ratio (ω_{out}). This essentially constitutes a third equation, and the system can be solved. Equation 2.2 can then be applied to calculate k_{lat} .

Rather than specifying $h_{w,mu}$ directly, it is more convenient to specify makeup water temperature, as there is a one-to-one relationship between the two. Similarly, rather than specifying \dot{G} directly, it is more

convenient to use cooling range (ΔT_{cond}) and inlet water/air mass flow ratio (\dot{W}_{cond}/\dot{G}). For a given heat load, \dot{G} can be determined from ΔT_{cond} and \dot{W}_{cond}/\dot{G} using Equation 2.3. The value of ΔT_{cond} for power plant cooling towers typically falls between 5-15°C. The value of \dot{W}_{cond}/\dot{G} is typically of order 1, and has a thermodynamically bounded maximum value: there must be enough air mass flow to absorb the heat load, given that the temperature of the air-side flow can never exceed the water-side inlet temperature.

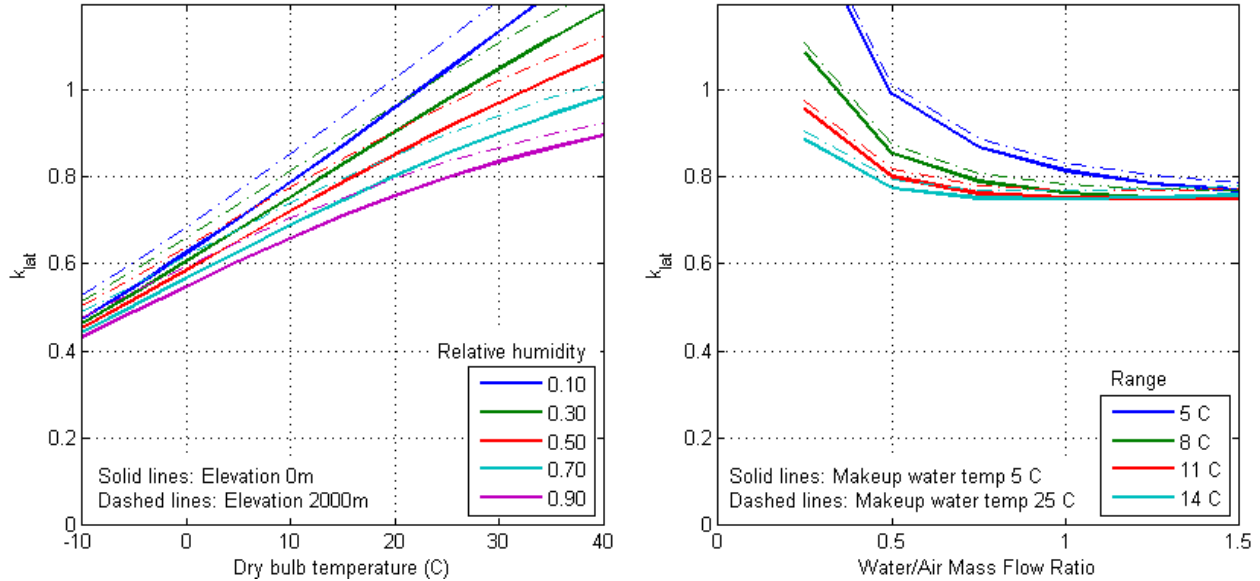


Figure 25: Sensitivity of k_{lat} to various parameters according to the cooling tower model of Leung and Moore. a) Ambient temperature, humidity and elevation; b) Cooling range, water/air mass flow ratio, and makeup water temperature

The sensitivity of k_{lat} to ambient temperature, humidity, and elevation as predicted by the Leung model was assessed holding the other parameters constant ($\dot{W}_{cond}/\dot{G}=0.8$; $\Delta T_{cond}=11^\circ\text{C}$; $T_{w,mu}=15^\circ\text{C}$). The result is shown in Figure 25a. Temperature is clearly the strongest determinant, though both elevation and humidity also have significant effects. As with once-through cooling systems, the value of k_{lat} varies over a large range depending on ambient conditions. Under very hot and dry conditions, k_{lat} may even be greater than 1: in addition to rejecting essentially all of the heat load through latent heat transfer, some evaporative cooling of the air stream itself necessarily takes place.

A second sensitivity analysis was performed of k_{lat} to ΔT_{cond} , \dot{W}_{cond}/\dot{G} and $T_{w,mu}$, assuming 15°C ambient dry bulb temperature, 0.6 relative humidity and 0m elevation. The results are shown in Figure 25b. As ΔT_{cond} and \dot{W}_{cond}/\dot{G} approach zero, the air mass flow rate \dot{G} blows up, which, given the assumption of saturated exit air, results in very high values of k_{lat} . This suggests that Leung may not be appropriate for towers operating with short ranges and/or low \dot{W}_{cond}/\dot{G} ratios. The effect of makeup water temperature can be seen in the difference between the dashed and dotted lines in Figure 25b; it is barely significant even over a 20°C variation, since \dot{Q}_{load} in Equation 2.21 is large compared to $\dot{W}_{mu}h_{w,mu}$.

The next level of cooling tower modeling fidelity is a one-dimensional model that eliminates the assumption that the exit air is saturated. Such a model underlies the water use submodel in Carnegie Mellon's Integrated Environmental Control Model [18], and presumably the Cooling Tower Institute's commercial software package as well. The model of Poppe and Rogener [43] is considered to be the most accurate; the version summarized here is that presented by Kloppers and Kroger [25].

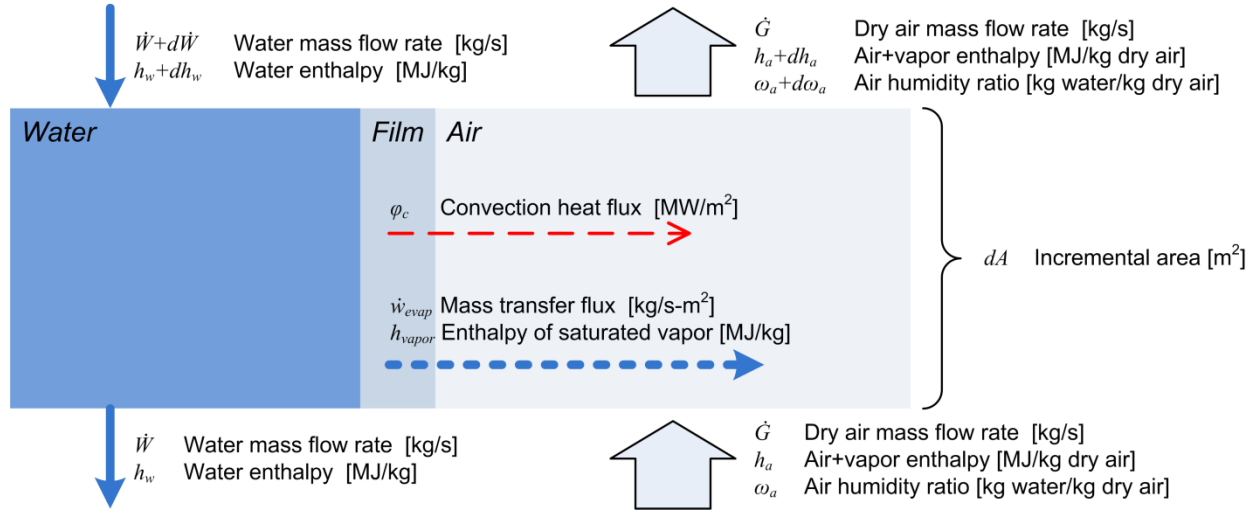


Figure 26: Heat and mass balance around an incremental section of wet cooling tower, as treated in Kloppers and Kroger [25]

The Poppe model considers both the water-side and air-side streams within incremental sections of the tower (see Figure 26). It is a one-dimensional model, so the air and water flows are assumed to be perfectly uniform at any given height within the tower, and it additionally assumes that there is no heat or mass transfer through the walls of the tower. Poppe considers a mass balance over the entirety of a section:

$$d\dot{W} = \dot{G}d\omega_a \quad (2.23)$$

the heat balance over the entirety of the section:

$$(\dot{W} + d\dot{W})(h_w + dh_w) = \dot{W}h_w + \dot{G}dh_a \quad (2.24)$$

a mass balance over the air-side of the section:

$$\dot{w}_{evap}dA = \dot{G}d\omega_a \quad (2.25)$$

and a heat balance over the air-side of the section:

$$\dot{w}_{evap}h_{vapor}dA + \phi_c dA = \dot{G}dh_a \quad (2.26)$$

where h_a [MJ/kg dry air] and h_w [MJ/kg] are the air-side and water-side enthalpies; ω_a is the air-side humidity ratio [kg water/kg dry air]; and \dot{W} is the water-side mass flow rate [kg/s], all at the bottom of the incremental section. Over the section, which has a total surface area of dA , these terms change by dh_a , dh_w , $d\omega_a$, and $d\dot{W}$. Because the air-side mass flow rate \dot{G} is accounted in terms of dry air, it is constant throughout the tower, which explains the absence of a $d\dot{G}$ term. As in Leung and Moore, the air-side enthalpy h_a includes the enthalpy of water vapor in the air but is accounted per kg of dry air. The term h_{vapor} is the enthalpy of the saturated vapor at the interfacial film, while φ_c and \dot{w}_{evap} are the convective heat flux and evaporative mass flux, as in the once-through cooling analysis.

The heat and mass transfer processes at the water-air interface are closely analogous to the once-through cooling case, with the interfacial film assumed to be saturated air at the temperature of the water per Raoult's law. Radiation is neglected, however, and the mass transfer is now expressed in terms of a gradient in humidity ratio as opposed to vapor pressure:

$$\dot{w}_{evap} = K_D (\omega_s - \omega_a) \quad (2.27)$$

where K_D is a mass transfer coefficient [kg/m²-s] and ω_s is the humidity ratio of the saturated interfacial film. The convective heat transfer is given by

$$\varphi_c = K (T_w - T_a) \quad (2.28)$$

where K is a heat transfer coefficient [MW/m²-K], and T_a and T_w are air-side and water-side temperatures [K]. The relationship between the heat and mass transfer coefficients is given by the Lewis factor (Le_f):

$$Le_f = \frac{K}{K_D c_{p,a}} \quad (2.29)$$

where $c_{p,a}$ is the specific heat of air. The approach used in the once-through cooling case implicitly assumes that $Le_f=1$. In the Poppe model, however, the Bosnjakovic relation is used to estimate Le_f instead. For a given atmospheric pressure, thermodynamic relations can be used to define h_w , h_{vapor} and ω_s as functions of T_w ; and h_a as a function of ω_a and T_a .

Given T_w , T_a and ω_a at the bottom of the tower, T_w and \dot{W} at the top of the tower, \dot{G} and atmospheric pressure, the resulting system of differential equations can be integrated numerically over the water temperature range. The result is a set of profiles for T_w , T_a and ω_a throughout the tower, as well as the Merkel number (Me), a dimensionless group typically of order 1 that is a rough proxy for relative tower size:

$$Me = \frac{K_D A}{\dot{W}} \quad (2.30)$$

Once the outlet air humidity ratio is known, Equation 2.22 can be applied to calculate \dot{W}_{evap} , and Equation 2.2 to calculate k_{lat} .

The sensitivity of k_{lat} to ambient temperature, humidity, and elevation as predicted by the Poppe model was examined, holding the other parameters constant ($\dot{W}_{cond}/\dot{G}=0.8$; $\Delta T_{cond}=11^\circ\text{C}$; $Me=1.5$), as shown in Figure 27a. The results are similar to the Leung model, with temperature being the strongest determinant followed by humidity and finally elevation. The slopes of k_{lat} with respect to temperature are less severe than Leung, however. At high ambient temperatures, Poppe predicts subsaturated exit air, implying lower values of k_{lat} than Leung, while at low ambient temperatures, Poppe predicts supersaturated exit air, implying higher values of k_{lat} than Leung.

A second sensitivity analysis (Figure 27b) was performed of k_{lat} to cooling range and inlet water/air mass flow ratio, assuming 15°C ambient dry bulb temperature, 0.6 relative humidity, 0m elevation, and a Merkel number of 1.5. As would be expected, the degree of increase in k_{lat} at high air mass flow rates is much less marked than in the Leung analysis, since the assumption of saturated output air is not applied in Poppe.

A third sensitivity analysis (Figure 27c) was performed varying Merkel number (relative tower size) and inlet dry bulb temperature, holding the other parameters constant at the same baseline values as above. While increasing tower size reduces k_{lat} at lower air temperatures, it actually increases k_{lat} at high air temperatures. This makes some physical sense; since warm air can hold so much more water than cool air, making the tower increasingly bigger in a warm environment means increasingly more water evaporating into the warm air. Since most water-scarce places are hot as opposed to cool, and since increasing tower size linearly yields diminishing increases in k_{sens} even at cooler air temperatures, it seems unlikely that sizing a tower larger than optimal for cooling performance and cost would ever result in an overall reduction in water consumption substantial enough to warrant doing so.

For completeness, it is worth mentioning that various groups have conducted two- and three-dimensional computational fluid dynamic (CFD) modeling of cooling towers over the last decade, mostly in the context of hyperbolic natural draft towers (e.g. [44],[45]). The goals of these studies have included prediction and improvement of water and air distribution, fill performance, and reduction of crosswind and recirculation effects. In terms of k_{lat} , however, these issues are not particularly significant, so they are not explored further in this review.

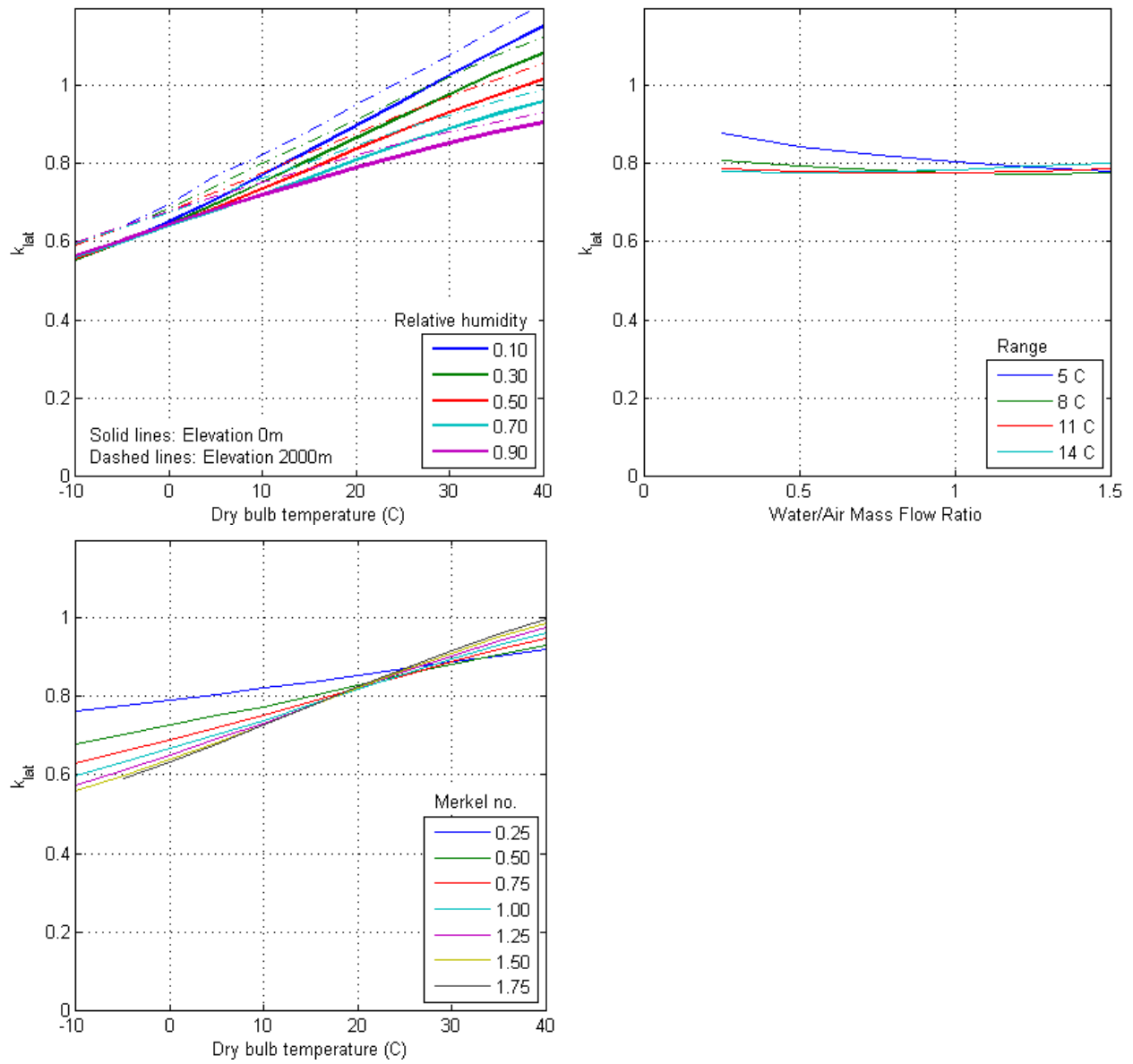


Figure 27: Sensitivity of k_{lat} to various parameters according to the Poppe cooling tower model. a) Ambient temperature, humidity and elevation; b) Cooling range and water/air mass flow ratio; c) Ambient temperature and Merkel number (relative tower size)

Dry and Hybrid Cooling

Dry cooling, sometimes called air cooling, rejects waste heat to the atmosphere without relying on the evaporation of cooling water. Dry cooling withdraws and consumes no water, although other processes in a dry-cooled power plant may use water.

Dry cooling systems require a very large heat exchanger surface area to reject the power plant waste heat. As such, dry cooling is three or four times as expensive as an equivalent wet tower cooling system. Furthermore, the overall efficiency of the power plant depends on effective cooling; on hot days, the effectiveness of a dry cooling system decreases, and the plant efficiency decreases as well. Unfortunately, hot days often coincide with high electricity demand (and high electricity prices), resulting in a substantial economic penalty.

Hybrid cooling systems combine wet and dry cooling approaches. There are many varieties of hybrid cooling, but all are essentially compromises between wet tower and dry cooling in terms of cost, performance, and water use. Values of k_{lat} can range from zero, as in a fully dry cooling system, to near that of a wet tower. The following sections will summarize the design space of dry and hybrid cooling systems in terms of these parameters, drawing on recent work by Ashwood and Bharathan [46] as well as other sources.

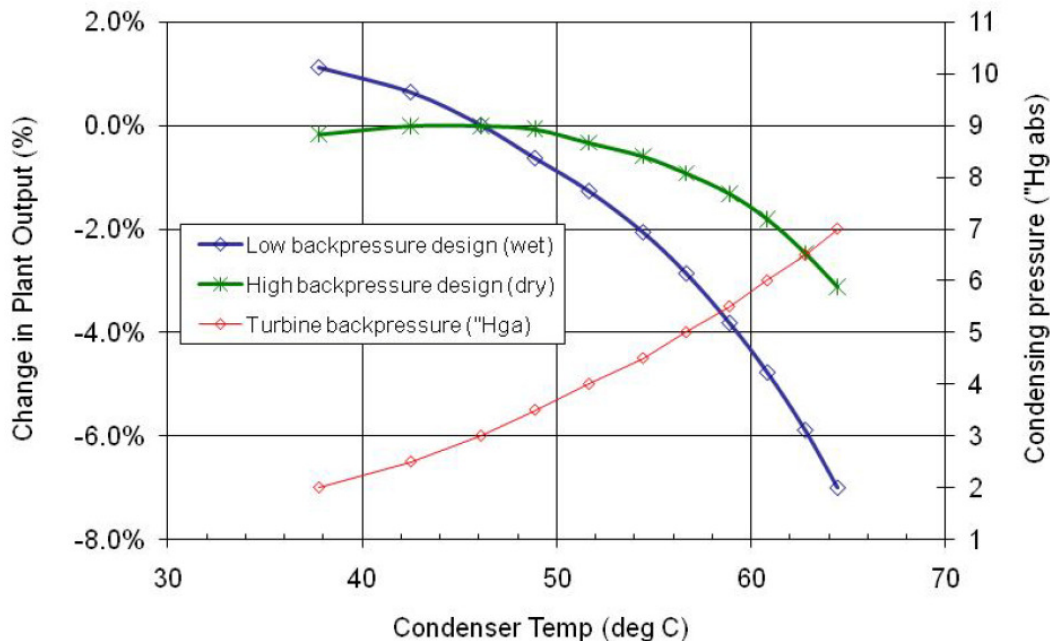


Figure 28: Turbine output vs. condenser temperature for low- and high-backpressure turbine designs (NREL [12])

First, however, a more rigorous definition of cooling system performance is needed. The key figure of merit is the temperature of the condensing steam on the low-pressure side of the turbine. Because this steam is in a saturated two-phase state, the temperature of the condensing steam uniquely determines its absolute pressure: the lower the temperature, the lower the pressure. The lower the pressure on the far side of the turbine (“backpressure”), the larger the pressure difference across the turbine and the higher the mechanical and electrical output of the power plant.

Different turbines have different output profiles with respect to backpressure, depending on turbine design, as shown in Figure 28. Turbines typically used in wet-cooled plants have high efficiencies at low backpressures (low steam condensing temperatures), but output falls off rapidly as the backpressure increases. The “high backpressure” or “extended backpressure” turbines typically used in dry-cooled plants suffer less of a penalty at higher backpressures, but are not as efficient at lower backpressures.

A discussion of steam condensing temperature must start with the condenser itself, of which there are three basic types: the air-cooled condenser (ACC), surface condenser, and direct contact condenser (DCC). In an air-cooled condenser (ACC), the steam to be condensed is piped directly into a heat exchanger that is cooled by a fan-driven flow of air. While conceptually simple (see Figure 29a), an ACC is physically enormous; the capital cost is considerable, as is the operational cost of running the fans. Additional engineering challenges include designing the piping and ductwork to handle large volumetric flows of steam at sub-atmospheric pressure, and minimizing adverse aerodynamic effects from ambient winds.

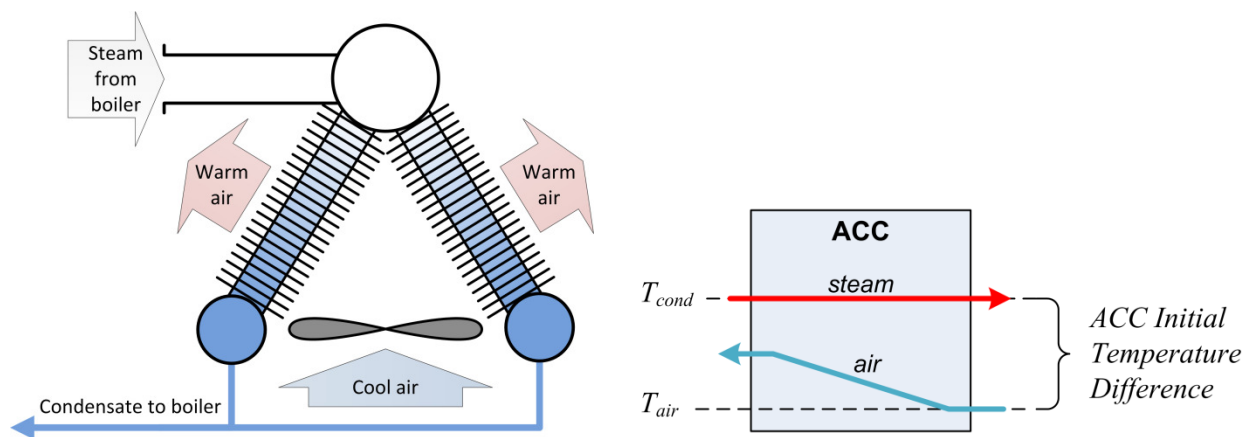


Figure 29: a) Schematic of an air-cooled condenser (ACC); b) Temperature diagram of an ACC

The temperature difference between the incoming air and the steam condensing temperature is known as the initial temperature difference (ITD), as shown in Figure 29b (note that the saturated steam, being at constant pressure, remains at constant temperature throughout the condenser). The larger the heat

exchange surface of the ACC and/or the faster the airflow, the smaller the ITD and the lower the condensing temperature, but the higher the capital and/or running costs. A typical ITD is on the order of 15°C.

In a surface condenser (see Figure 30a), hot steam flows over and condenses around tubes filled with a flow of cooling water. This is the type of condenser typically used in once-through and wet tower cooling systems, but it can also be used in dry and hybrid systems. It is by far the most common condenser type.

In a direct-contact condenser (DCC), sometimes called a barometric condenser, cooling water is sprayed directly into the condensing steam (see Figure 30b). In a system using a DCC, the cooling water circuit must be completely closed, with no pond or wet cooling tower in the loop. Since the steam and cooling water mix in a DCC, exposing the cooling water to the outside world would introduce unacceptably high levels of contaminants to the steam circuit. Furthermore, DCCs cannot be used with nuclear plants, since the steam circuit must be kept isolated from the cooling water for radiation safety reasons.

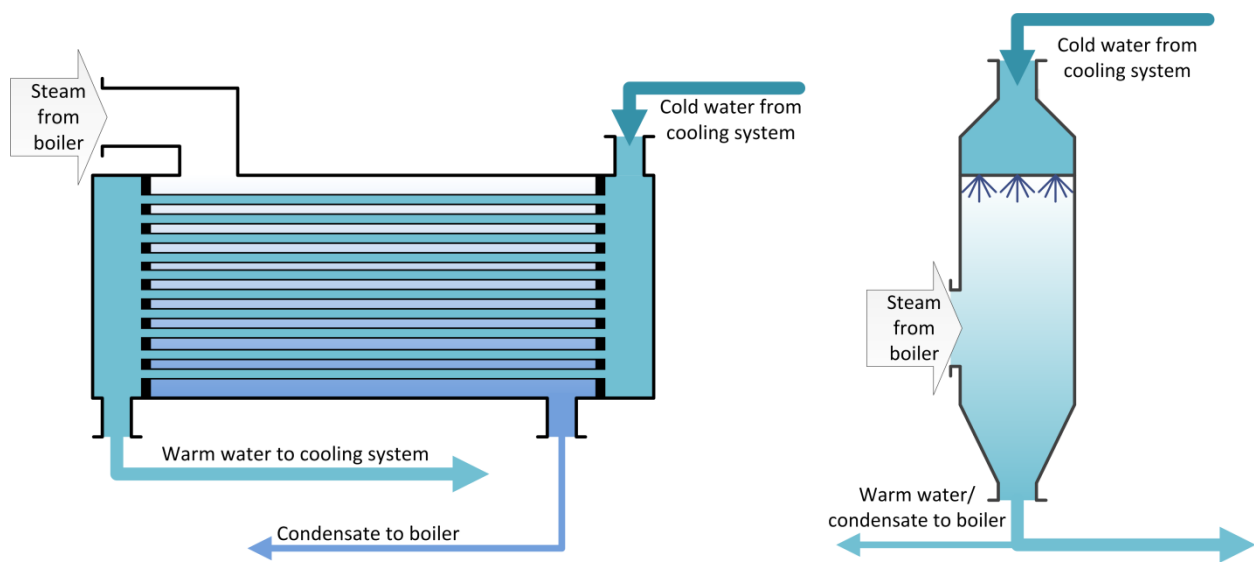


Figure 30: a) Schematic of surface condenser; b) Schematic of direct-contact condenser (DCC)

The nature of the temperature interval between the condensing steam and the incoming air is somewhat more complicated in a cooling system using a surface condenser or a direct-contact condenser than one using an ACC. Specifically, it is the sum of three smaller intervals (see Figure 31): the terminal temperature difference, cooling range, and approach.

The terminal temperature difference (TTD) is the difference between the temperature of the condensing steam and that of the cooling water leaving the condenser. For a surface condenser with a given cooling water flow rate, the TTD is a function of condenser size; a typical value of surface condenser TTD might be 5°C. A direct-contact condenser, on the other hand, has a TTD of less than 1°C, since the intimate

mixing of cooling water and steam enables very efficient heat transfer. This is the primary advantage of a DCC.

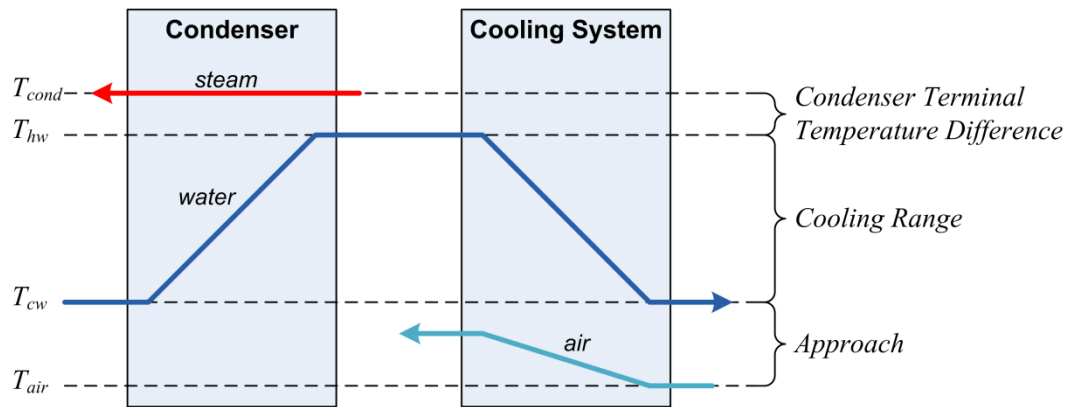


Figure 31: Temperature diagram of a cooling system using a surface or direct contact condenser and a recirculating loop of cooling water

As discussed earlier, the cooling range is the cooling water temperature rise across the condenser – also equal to the cooling water temperature fall across the water cooling system. For a given heat load and cooling water flow rate, Equation 2.3 shows that the range is fixed; a realistic value for a power plant is 10°C. The “approach” is the temperature difference between the incoming air and the water leaving the water cooling system; it is generally a function of cooling system size (the larger the cooling system, the smaller the approach).

Systems using air-cooled condensers

An air-cooled condenser by itself constitutes a viable dry cooling system, and indeed these “direct” dry cooling systems are increasingly used in South Africa, the U.S. and elsewhere (though still a small percentage of the overall fleet). A few examples include the Chuck Lenzie combined-cycle gas plant outside Las Vegas, the Wyoak coal plant in Wyoming, and the Mystic plant outside Boston.

To lower the steam condensing temperature, the size and flow rate of the ACC can be increased, thus decreasing the initial temperature difference, to the extent that makes economic sense. Alternatively, the temperature of the incoming air itself can be lowered by spraying it with water; this spray inlet cooling constitutes one form of hybrid system. If the incoming air becomes completely saturated, it will have reached its wet-bulb temperature, which is the temperature approached by the cooling water in a conventional wet tower system. ACC spray inlet cooling has been successfully piloted at the Crockett combined-cycle gas plant in California [47], but is still a technology under development.

Spray inlet cooling is attractive in that it lowers the steam condensing temperature while adding minimal capital cost to the cooling system. However, getting the entire spray to evaporate is an engineering challenge. Often some water reaches the ACC as liquid, causing corrosion on the finned surfaces of the heat exchanger as well as wasting water that drips off and soaks into the ground. Higher water pressures and fogging nozzles can generate fine sprays that evaporate more completely, but this quickly becomes uneconomical. Ultimately, low-cost spray inlet cooling is a good hybrid option for occasional use in peak summer; if more regular use is anticipated, a parallel hybrid system is a better choice.

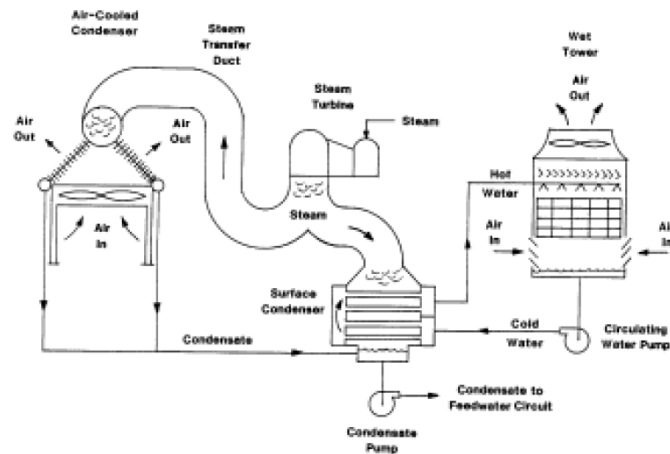


Figure 32: a) Pilot installation of spray inlet cooling [47]; b) Diagram of parallel hybrid cooling system [17]

In a parallel hybrid system, the steam flow can be split between an ACC and a surface condenser whose water is cooled by a wet tower. When the ambient air temperature is low, all steam goes to the ACC and the system operates dry. When the ambient air temperature rises above a certain point, some steam is diverted to the surface condenser; this reduces the load on the ACC, increasing its relative size and decreasing the ITD and thus the steam condensing temperature. Parallel hybrids are the most common variety of hybrid cooling systems used at power plants today; one large example is the Comanche 3 coal plant in Pueblo, CO. The amount of water conserved vs. a wet tower system depends on how often the wet tower is deployed. A recent study by NREL [12] on solar thermal power plant cooling arbitrarily pegged the conservation at 50% compared to a standard wet tower.

A final ACC hybrid variant is wetted media inlet cooling, where air flowing into an ACC first flows through a lattice of wet material. Wetted media inlet cooling is generally considered less attractive than spray inlet cooling, being somewhat expensive to install, awkward to operate and maintain, and incurring a significant pressure drop in the air flow path which increases the required fan horsepower. [46] It has not been deployed on a power plant to date.

Systems using surface condensers

A surface condenser combined with an air-cooled heat exchanger (ACHEX) constitutes an “indirect” dry cooling system, so called because the heat load is first transferred to the cooling water before being rejected to the air. In practice, however, indirect dry systems rarely use surface condensers. The relatively large terminal temperature difference of the condenser means that a prohibitively large ACHEX would be required to match the steam condensing temperature achievable with an ACC. Indirect dry systems using surface condensers are therefore not used in power plants.

When it comes to hybrid systems, however, the use of a surface condenser allows a series hybrid configuration, where the hot water first passes through an air-cooled heat exchanger before entering a wet tower where it rejects the remainder of the heat load. This hybrid configuration has been occasionally used for water conservation, and somewhat more often for plume abatement (see Figure 33a). In a series hybrid design, as with a conventional wet tower, the air temperature approached by the cooling water is the wet bulb temperature. The design principles behind series hybrids are reviewed by Lindahl [48], and several real-life examples are given, though water conservation data are absent and the plants are not identified by name.

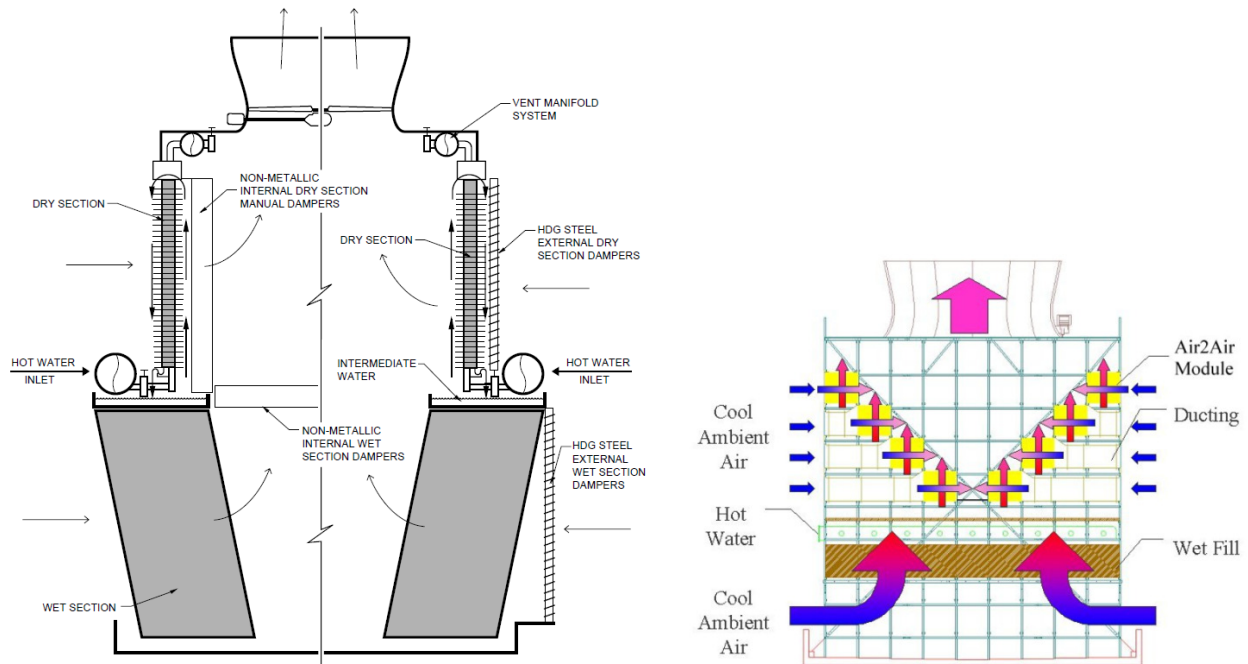


Figure 33: a) Schematic of series-hybrid cooling tower for plume abatement [48]; b) Schematic of Air2Air moisture recovery hybrid cooling tower [49]

One particularly unusual variation of hybrid cooling is known as Air2Air [49], under development at SPX Cooling. It is essentially a conventional wet tower fitted with “condensing modules” that recover moisture

from the outlet airstream by using a secondary draft of ambient air (see Figure 33b). Water recovery rates in a pilot study at the San Juan coal plant in New Mexico ranged from 15-25%. This technology is interesting in that there may be potential for hydrophilic engineered surfaces to increase the water recovery rate substantially. As with a conventional wet tower, Air2Air would be employed in conjunction with a surface condenser.

Systems using direct-contact condensers

Combining a direct-contact condenser with an air-cooled heat exchanger results in a form of indirect dry cooling system known as a Heller system, after its inventor Laszlo Heller. Because the terminal temperature difference in a DCC is minimal, the required heat exchange surface is much smaller than for an indirect dry system using a surface condenser. Moreover, since a Heller system is running hot water through the ACHEX (as opposed to steam in an ACC), the pipes and ductwork involved are physically smaller and can be run farther away from the plant. This allows the ACHEX to be configured to take advantage of natural drafts, reducing or eliminating the required fan power. While no Heller systems have been constructed in the US to date, there are quite a few installations elsewhere, such as the Gebze and Adapazari plant in Turkey, the Al Zara plant in Syria, and the Kendal plant in South Africa. As with an ACC, spray inlet cooling can be used to reduce steam condensing temperature on hot days; one of the few existing examples is the Sochi gas combined cycle plant in Russia. [50]

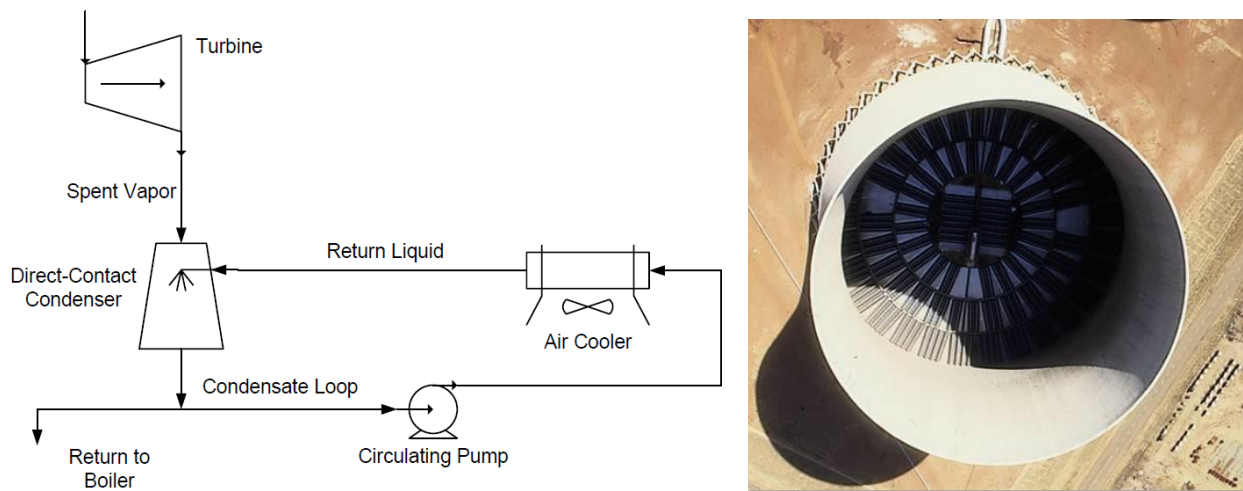


Figure 34: a) Simplified diagram of Heller indirect-dry cooling system [46]; b) Aerial view of a Heller cooling tower, showing arrangement of air-cooled heat exchangers in a natural draft tower [51]

Wet surface air coolers and condensers

Wet surface air coolers are essentially air-cooled heat exchangers that are continuously deluged with water, resulting in an intrinsically hybrid heat rejection scheme. Deluging of ACCs as a very low-capital wet assist during hot weather has been investigated, but the technique was found to cause unacceptable corrosion on the highly finned surface of the ACC. Coolers and condensers with coated or finless tubes specifically designed for wet-surface heat rejection have been developed by several companies. While not commonly used for power plant applications, they have attracted some attention in the context of low-quality water. A pilot study has been conducted at the San Juan coal plant in New Mexico [52].

Discussion

This review has expressed the water consumption of various power plant cooling systems in terms of a common normalized parameter, k_{lat} , and summarized the other engineering tradeoffs involved. As a very general rule, k_{lat} is highest for wet cooling towers, followed sequentially by cooling ponds, once-through systems, wet/dry hybrids, and fully dry cooling systems. However, k_{lat} can vary widely within each class of cooling systems, depending primarily on ambient temperature and humidity in the case of wet towers; water temperature and windspeed in the case of once-through systems and cooling ponds; and aggressiveness of wet subsystem deployment in the case of hybrid wet/dry systems.

The strong determinants of water consumption for tower, pond, and once-through systems are meteorological, and lie beyond human control. This suggests that when evaluating cooling options at a specific site, reliable and fine-grained meteorological normals must be obtained in order to estimate hypothetical water consumption with any reasonable degree of accuracy. It further suggests that in situations which demand strictly limited water consumption, hybrid or dry cooling is likely the only viable option.

Improving the economics and performance of dry and hybrid cooling systems is indeed one of the two most active areas of research with respect to decreasing freshwater consumption in power plants. The other major area of research is the use of nontraditional water for cooling, such as municipal wastewater, brackish and saline groundwater, seawater, minepool water, and water produced during oil and gas extraction. The use of such nontraditional waters presents special challenges with regard to equipment corrosion and fouling; related research focuses on water treatment techniques and equipment modifications to withstand degraded water. Ongoing programs of R&D to reduce freshwater consumption in power plants are reviewed by the Electric Power Research Institute [53] and the National Energy Technology Laboratory [54],[55].

Part 3 – Cold-Side Thermal Energy Storage for Dry-Cooled Concentrating Solar Power Plants

Introduction

Concentrating solar power (CSP) plants rely on the concentration of direct sunlight to heat a fluid, which serves as the “hot side” of a steam power cycle. CSP plants are therefore typically sited in arid regions which get lots of direct sunlight, such as the U.S. Southwest. Unfortunately, these regions often lack sufficient water resources to support the use of wet cooling towers. Dry and hybrid cooling systems are therefore increasingly viewed as a necessary component of future CSP plants.

Dry cooling, however, has two major drawbacks, as discussed in the previous section. First, it carries a high capital cost due to the large heat transfer surface area required in what is essentially an enormous radiator. Second, the efficiency of an air-cooled CSP plant is less than that of an equivalent wet-cooled plant: as ambient air temperature increases, a dry cooling system is unable to maintain a low steam condensing temperature, so the pressure drop across the turbine decreases, as does the turbine output.

Since high ambient air temperatures typically coincide with plentiful sunlight and high wholesale energy prices, the dry cooling efficiency rolloff decreases plant output during the most potentially lucrative hours of the year. The overall economic penalties associated with dry-cooled CSP are thus significant, corresponding to a levelized cost of electricity (LCOE) that is 2-10% higher than a wet-cooled plant. CSP, a technology struggling to be economically competitive, can ill afford such penalties.

Hybrid cooling most often entails a dry cooling system with an auxiliary wet tower for use when the ambient air temperature is high. A 2010 study [12] by WorleyParsons and the National Renewable Energy Laboratory (NREL) created several optimized models of hypothetical CSP plants sited near Las Vegas: some wet-cooled, some dry-cooled, and some hybrid-cooled. While the hybrid-cooled models indicated a plant efficiency close to that of the equivalent wet-cooled cases, the overall LCOE was generally about halfway between the wet- and dry-cooled cases, owing to the additional capital cost of the hybrid cooling infrastructure. The water savings achieved using the hybrid system was set at 50% of the wet-cooled case. It is dubious whether a water-scarce community that rejected a proposed 100MW plant consuming 900 million liters (ML) of water annually would consider 450 ML/year an acceptable compromise; in some cases dry cooling will be a necessity.

Cold side thermal energy storage (CS-TES) is recommended here as a variant of dry cooling ideally suited to CSP plants. CS-TES rests on a fundamentally simple idea: cool a thermal storage medium at

night, when ambient temperatures are low, the sun is down and the plant is inactive, then use it during the day when temperatures is high, the sun is out and the plant is active.

The cooling system architecture investigated here is diagrammed below in Figure 35. It is essentially an indirect dry cooling system with a large cooling water storage reservoir in the loop. An air-cooled heat exchanger would be used to chill water overnight while the plant is inactive, storing the chilled water in the lower portion of a large stratified thermocline tank (Figure 36). During the day when the plant was operating, the cooling water would be piped to the condenser and the warmed water returned to the upper portion of the thermocline tank (Figure 37).

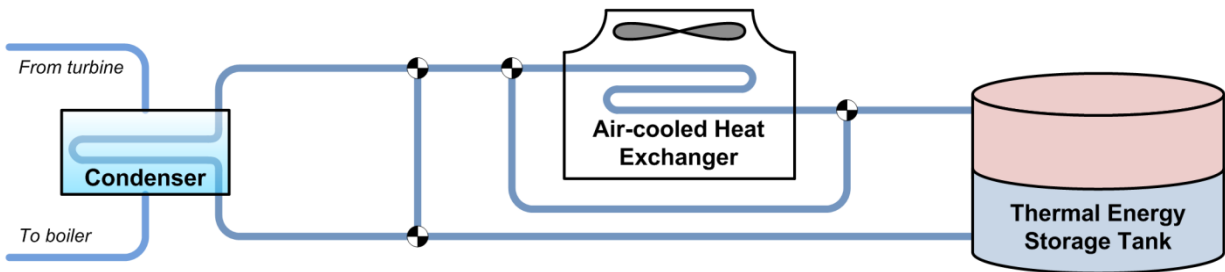


Figure 35: The cold-side thermal energy storage (CS-TES) cooling system architecture

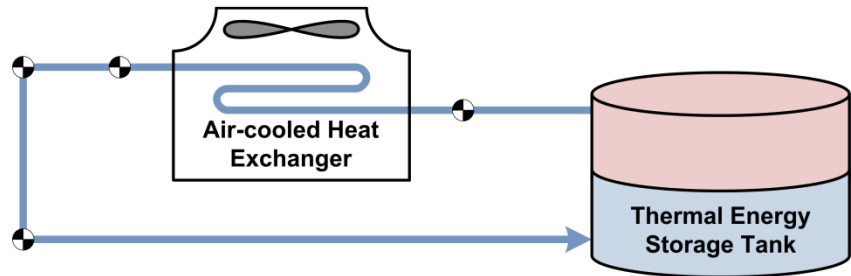


Figure 36: CS-TES operational mode: Overnight cooling

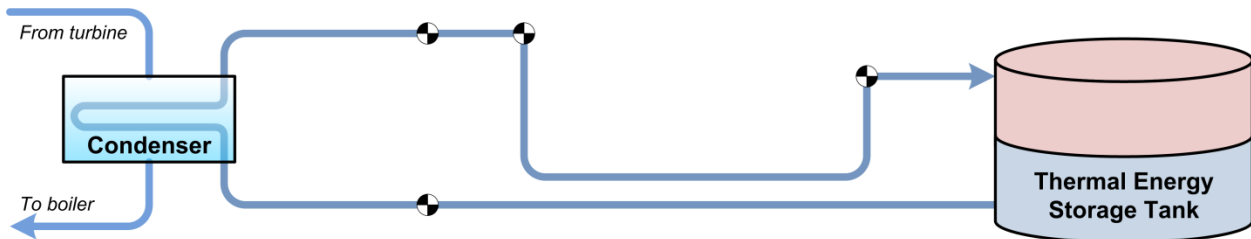


Figure 37: CS-TES operational mode: Daytime operation

Arid regions experience very large diurnal temperature swings; in Las Vegas, for example, there is normally a 10-15°C difference between the maximum and minimum temperature over a given 24 hour period (see Figure 38). CS-TES could take full advantage of this phenomenon, using cool nighttime air to reject the bulk of the heat load. Furthermore, a plant using CS-TES would not have to cool in “real time;” it would have the flexibility to reject e.g. 8 hours’ heat load over the course of say 10 hours overnight.

The use of CS-TES would therefore enable smaller (less expensive) air cooling equipment and higher plant efficiencies. In addition, any fans used for cooling would be running at night, when electricity is less expensive than it is during the day.

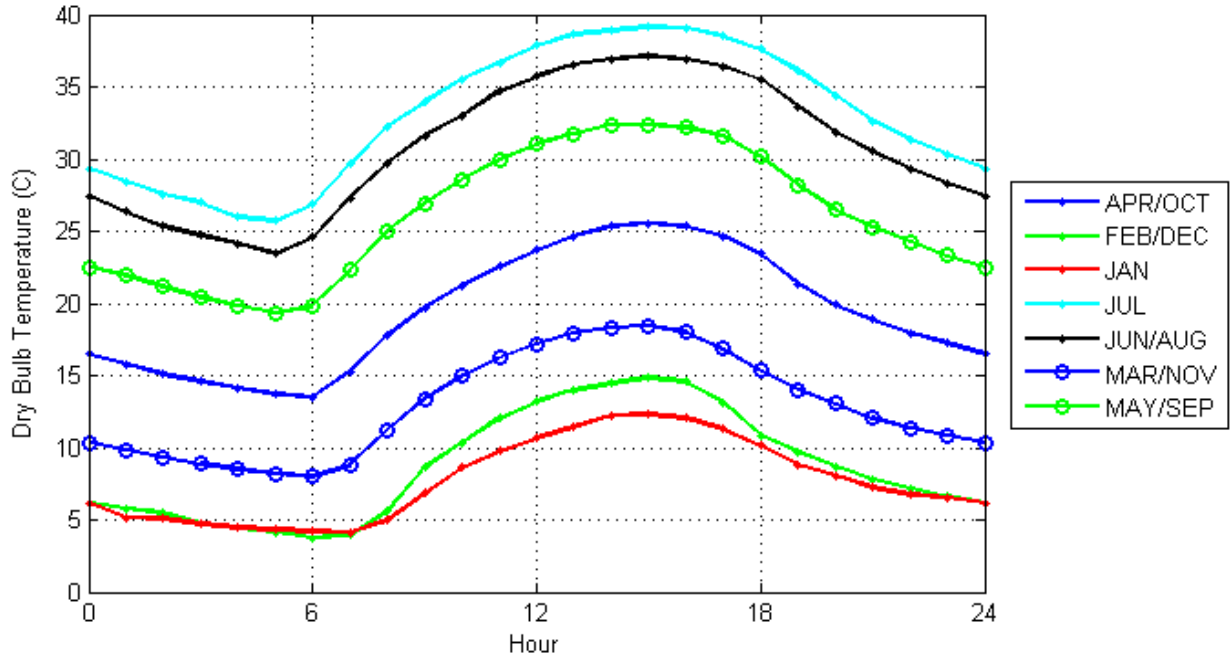


Figure 38: Average hourly dry bulb temperatures near Las Vegas (NREL TMY3 data [56])

The concept of thermal energy storage for cooling is not new; it is often used for HVAC cooling, and for turbine inlet cooling of combustion turbines. [57] CS-TES was mooted for condenser dry-cooling as early as 1976 by Guyer and Golay of MIT [58], who investigated its potential use in nuclear plants. A following study by Drost and Allemann of Pacific Northwest National Laboratory [59] conducted a techno-economic analysis of CS-TES for a dry-cooled coal plant but found that it did not result in a significant overall benefit. Realizing that the intrinsic diurnal cycle of CSP is much better suited to CS-TES, compared to a baseload plant like coal or nuclear, later work by Guyer and Golay [60] focused on fluid-dynamic design of a CS-TES system for CSP. The storage medium in these early studies was water in an enclosed canal, relying on plug flow to keep the hot and cold water separate.

CS-TES for condenser cooling then disappeared from the literature for some thirty years, re-emerging only very recently. Pistocchini and Motta [61] investigated the techno-economic feasibility of CS-TES in a CSP plant using a phase-change material as the storage medium. They found that, even with optimistic assumptions about the behavior of the phase-change material, such a system would not yield a significant economic advantage as compared to a standard air-cooled condenser (ACC). However, their conclusions identified CS-TES using water as the storage medium as a potentially more promising option. Munoz et al

[62] considered a CSP plant using a water-based CS-TES system similar to that investigated here. They found a significant increase in plant efficiency as compared to a reference plant using an ACC. However, their assumptions around day-night temperature variations were drastically larger than those found even in desert areas, and no attempt at techno-economic analysis was made.

The Munoz study also assumed separate tanks for hot and cold water, which requires twice as much tank space as compared to a thermocline tank. While two tanks are often used in high-temperature TES, since the high thermal conductivity of molten salts and liquid metals preclude their use in a thermocline tank, there is no good reason to use two-tank TES with water. Indeed, several companies sell large prestressed concrete or welded steel tanks with laminar diffusers on the inlets, specifically designed for thermocline TES applications. Compared to ice-based (latent heat) cold TES systems, water-based (sensible heat) systems have ~20% lower capital and operating costs. [57] Compared to plug flow ponds, thermocline tanks have a much smaller footprint. [60]

As a preliminary quantitative evaluation of the benefits of cold-side thermal energy storage in dry-cooled CSP plants, a case study of a 100MW plant was conducted. Roughly based on one of the NREL/WorleyParsons case studies, the plant was assumed to be a parabolic trough CSP plant with no hot-side TES, sited near Las Vegas. The two key figures of merit considered were net present value (NPV) of cooling system costs, and steam condensing temperature.

Case Study Design Basis

A total of five cooling system cases were evaluated: a wet cooling tower; an air-cooled condenser; a Heller indirect dry system; and two indirect dry systems using CS-TES. The first CS-TES case assumed a direct-contact condenser (DCC). As discussed above in Part 2, a DCC has the advantage of extremely efficient heat transfer between steam and cooling water, leading to a near-zero terminal temperature difference. The cooling water must be kept very clean, however; it remains to be seen whether a practical water treatment scheme can be devised to permit use of a DCC with a very large storage reservoir in the loop. A second CS-TES case using a shell-and-tube surface condenser was therefore included as well. All cases were assumed to use mechanical drafts.

For this initial analysis, a static design point was considered, corresponding to a worst-case day in mid-July: an 8-hour “daytime” with temperatures of 40°C dry bulb and 20°C wet bulb, and a 10-hour “nighttime” with a dry bulb temperature of 30°C. During the daytime, the plant was assumed to be running at full capacity, producing an invariant 200MW(th) condensing heat load. In the CS-TES cases,

daytime plant operation was assumed to run entirely using stored chilled water, and the entire nighttime was assumed to be used for cooling water recharge.

Heat exchanger thermo-hydraulics

The design basis for heat exchanger thermo-hydraulics drew on several sources, mainly the NREL study [12], Maulbetsch [17], and an industry handbook [63]. The key design assumptions for each case are outlined below.

Wet tower case: The wet tower design point was taken directly from the NREL study, with an approach (to the wet bulb temperature) of 5.5°C, a cooling range of 11°C, and a surface condenser terminal temperature difference (TTD) of 4°C. The air mass flow rate was assumed to be 5,000 kg/s, corresponding to a water/air mass flow ratio of 0.9. The water-side pressure drop across the condenser and the pressure head required for the cooling tower risers were assumed to be 50kPa and 75kPa respectively. The air pressure drop through the tower was assumed to be 175Pa.

Air-cooled condenser case: The ACC design point was also taken directly from the NREL study, with an initial temperature difference of 14°C. The ACC was modeled as a single-stream heat exchanger [64], since the steam-side remains at near-constant temperature, and the air mass flow rate was assumed to be 20,000 kg/s, corresponding to a heat exchanger effectiveness of 0.7. The air pressure drop across the ACC was assumed to be 175Pa.

Indirect dry cooling cases: For direct contact condensers, the TTD was assumed to be 0.3°C and the water pressure drop 100kPa. For surface condensers, the TTD was assumed to be 4°C and the water pressure drop 50kPa. The air-cooled heat exchangers (ACHEX) were modeled as counterflow heat exchangers [64], with a water-side pressure drop of 100kPa and an air-side pressure drop of 175Pa. For each case, the approach (to the dry bulb temperature), cooling range, and air flow rate were tuned to minimize cost subject to a steam condensing temperature constraint, or vice versa, as described below.

Costing and economics

The capital costs considered in this study included, as applicable by case, the surface condenser, DCC, ACC, wet tower, ACHEX, and TES tank. The operational costs included pumping power, fan power, and water consumed. Daily operational costs were annualized by multiplying through by 365, thus assuming an entire year of “design point days.” Net present value (NPV) was then calculated for each case, following the assumptions of the NREL study: a three-year construction period in which all capital costs were accrued the first year, and an operational life of 30 years, with an annual discount rate of 5.25%. The estimation methodology for each cost component is outlined below.

Condenser and wet tower capital costs: The capital costs of an appropriately sized surface condenser (\$0.8m) and wet tower (\$2.0m) were estimated based on relevant costing information in Maulbetsch. Lacking more specific information, a direct-contact condenser was assumed to cost roughly the same as a surface condenser (\$0.8m). The cost of an ACC with a 14°C ITD was estimated at \$27.3m, based on a power law correlation fitted to data provided in Maulbetsch.

Air-cooled heat exchanger capital costs: The capital costs of the ACHEX were estimated using a metric of heat exchanger capacity [MW/K] based on a counterflow heat exchanger model [64]. This capacity was obtained by multiplying the heat exchanger NTU by the lower of the two flow capacities. The capacity metric was then converted to capital cost using a factor of \$625,000/MW/K, obtained by fitting to two Heller case studies presented in Maulbetsch.

TES tank capital costs: Conversations with three vendors of thermocline TES tanks consistently yielded a cost estimate of \$0.11/L for large tanks. In CS-TES cases involving a DCC, the estimate was set at \$0.14/L to account for any additional water purification and treatment plant required to keep the boiler feedwater at a suitable level of quality.

Pumping and fan power: The electric power required for pumping water and air through condensers, cooling tower, and ACHEX was estimated by multiplying volumetric flow rate by pressure drop, and dividing by overall efficiency (assumed to be 70% for water pumps and 65% for fans). The daytime wholesale electricity rate, representing the opportunity cost of daytime pumping and fan loads, was assumed to be \$75/MWh, based on the part-peak summer rate from a PG&E schedule [65]. The nighttime wholesale electricity rate, representing the real cost of nighttime loads, was assumed to be \$63/MWh, based on the off-peak summer rate from the same schedule.

Cost of water: The annual water consumption of the wet tower and ACC cases were taken from the NREL study, with 935,000m³ consumed annually by the wet tower plant and 75,000m³ consumed annually by the ACC plant (mainly for washing the parabolic mirrors). The CS-TES cases were assumed to consume 95,000m³ annually since there may be some blowdown and makeup required to maintain the quality of the thermal storage water supply. The assumed cost of water of \$0.36/m³ was taken from the NREL report.

Case Study Results and Discussion

Two sets of cases were examined. In the first set, the steam condensing temperature was held constant at 54°C, the same as the ACC reference case. The approach, cooling range, and air flow rate of the Heller and CS-TES cases were then tuned to minimize net present value (NPV) of cooling system costs. The results are shown in Figure 39. (The wet tower case, included for reference, has a steam condensing temperature of 40.5°C.) The results are promising. As compared to the ACC case, both cases using CS-TES result in reduced capital and operating costs, with the CS-TES incorporating a DCC coming in lowest. The cost of the TES tank is more than offset by the reduction in ACHEX size.

The total installed capital cost of the parabolic trough plants in the NREL study ranges from \$528m to \$550m, with the NPV of total plant costs falling between \$644m and \$661m. The cost savings associated with CS-TES vs. the ACC reference case, on the order of \$5m NPV, are thus significant but small in the context of the overall plant. The application of CS-TES to reducing steam condensing temperature, and so increasing plant electricity output, is perhaps more interesting.

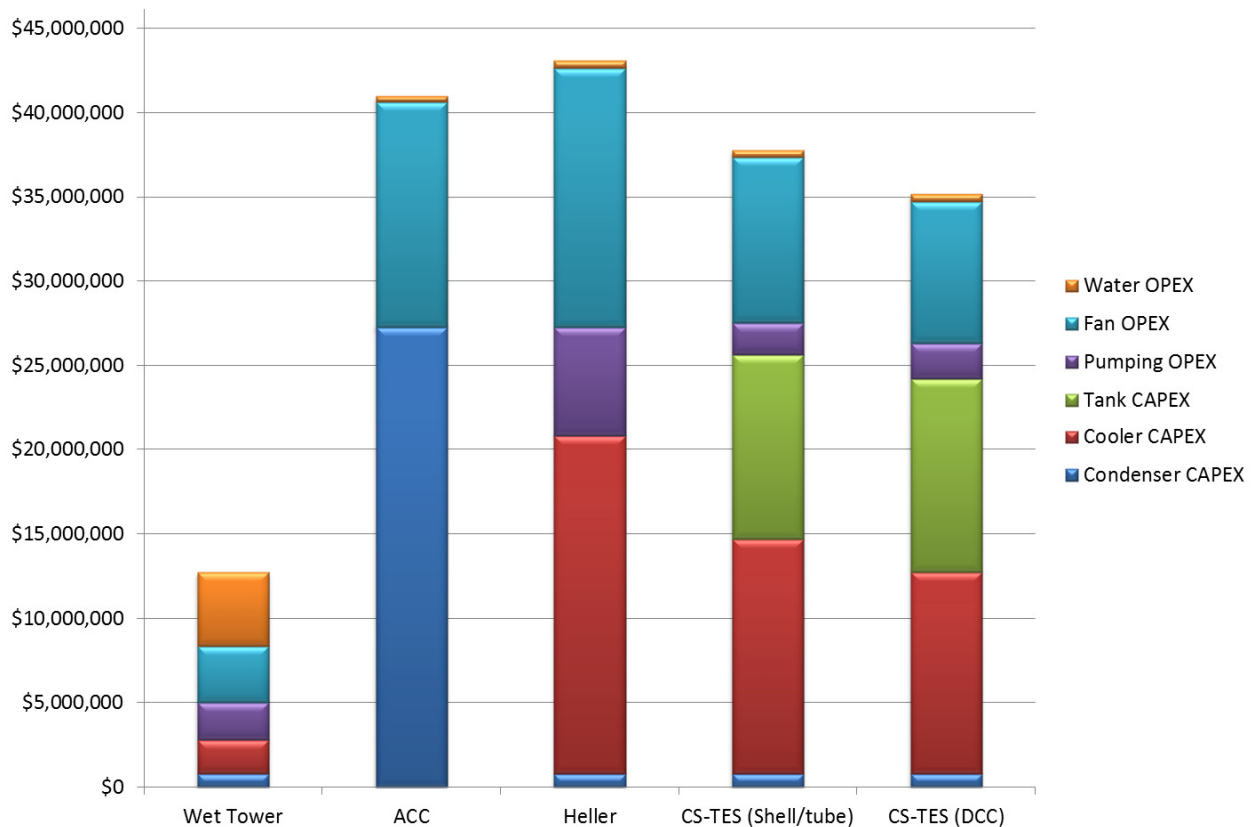


Figure 39: Case study NPV of cooling system costs, optimized with steam condensing temperature constant at 54°C

In the second set of cases, the NPV of cooling system costs was held constant at \$41m, as in the ACC case; the tuning parameters were then adjusted to minimize steam condensing temperature. The results are shown in Figure 40. (The wet tower case, again included for reference, has a cooling cost NPV of \$13m.) Below the results is a plot from the NREL study showing turbine output characteristics as a function of condensing temperature. For a fixed cooling cost NPV, the use of CS-TES shows a significant decrease in design-point steam condensing temperature, again with the DCC case showing the most promise. Given that this analysis was conducted at a worst-case mid-summer design point, these results suggest that dry-cooled systems incorporating CS-TES may permit the use of a low backpressure turbine, yielding substantial gains in output over the course of the year.

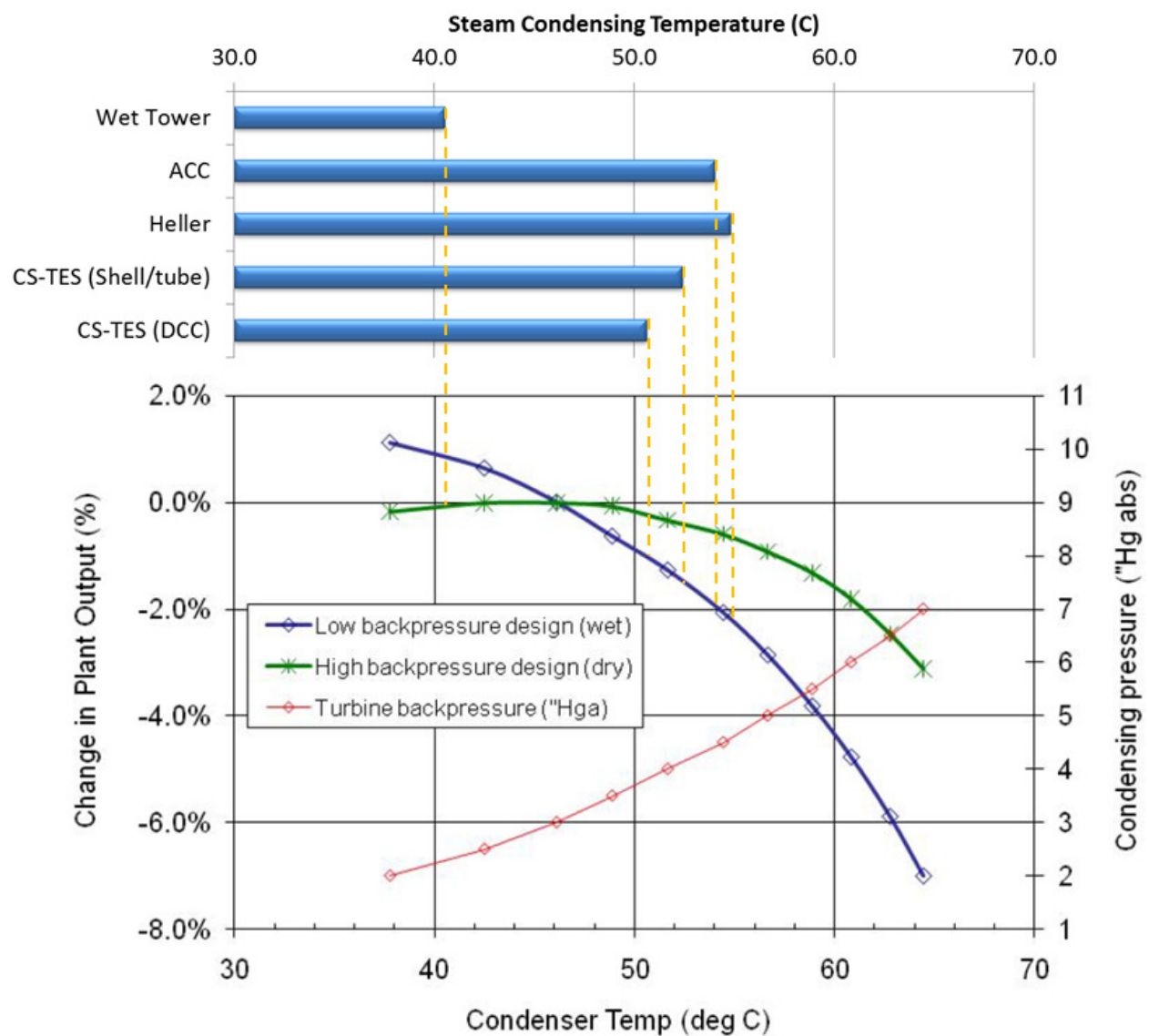


Figure 40: Case study steam condensing temperatures, optimized with NPV of cooling system costs constant at \$41m, shown with typical turbine output curves (NREL [12])

Across both sets of cases, the size of the required TES tank optimized out to between 80 and 110 ML. This is a lot of storage, to be sure, but within the realm of industry experience. The tank vendors contacted have built individual TES tanks holding upwards of 50 ML, and water storage tanks holding 150 ML. It is also possible that the tank size could be reduced through the inclusion of other operational modes such as “real-time cooling,” in which the cooling circuit closes without the TES tank in the loop, operating as a standard indirect dry cooling system during hours when the sun is out but the ambient air is sufficiently cool. This would reduce the maximum amount of daily thermal storage required and thus the size of the TES tank.

Several aspects of the presented analysis may be considered conservative with respect to the benefits of CS-TES. First, the small electricity price difference between night and day reflects a regulated rate schedule; in a deregulated wholesale market, the difference can span a factor of two in peak summer. Second, the invariant heat load of 200MW(th) does not reflect changes in turbine efficiency. In actuality, reducing the steam condensing temperature increases turbine efficiency, reducing condenser heat load. This in turn increases relative cooling system size, further reducing steam condensing temperature, creating a “virtuous cycle” not reflected in this analysis. Finally, CS-TES creates a buffer against transient wind effects that often plague performance of air-cooled condensers; this benefit is likewise not captured in these results.

Future studies should quantify the above effects, creating a finer grained model that takes into account an actual meteorological year with a corresponding wholesale electricity price profile, rather than a static design point, and an actual power island instead of a static heat load. The interactions between CS-TES and hot-side TES should be explored, and the potential benefits of CS-TES with natural draft cooling – generally not feasible with an ACC but frequently used with an ACHEX – should be examined. A preliminary design by Abengoa Solar (see Figure 41) shows a natural draft dry cooling tower integrated with the collector structures of a power tower CSP plant [66], which has interesting implications for the economics of natural draft.

In summary, CS-TES shows significant promise to reduce the capital, operational, and performance costs of dry cooling in CSP plants. The system including CS-TES with a direct-contact condenser is most encouraging, if the water quality requirements of a DCC system can be met. The component technologies involved – thermocline TES tanks and indirect dry cooling – are already mature and could be incorporated into plants built in the near future. Finer-grained analysis, perhaps in the context of specific plants in the pipeline, should be conducted.

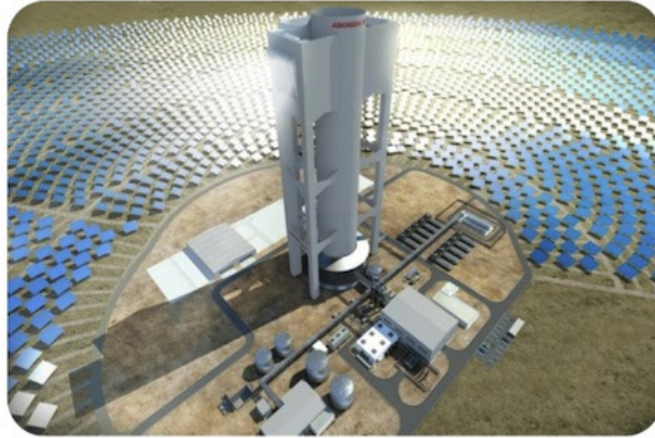


Figure 41: Natural draft dry cooling tower integrated into collector structures of power tower [66]

Details of Case Study Analysis

The details of the case study analysis are tabulated on the following page.

Parameter	Units	Reference		Constant Condensing Temperature			Constant Net Present Value		
		Wet Tower	ACC	Heller	CS-TES (Surf.)	CS-TES (DCC)	Heller	CS-TES (Surf.)	CS-TES (DCC)
Design point									
Wet bulb air temp	°C	20.0	n/a	n/a	n/a	n/a	n/a	n/a	n/a
Dry bulb air temp	°C	n/a	40.0	40.0	30.0	30.0	40.0	30.0	30.0
Approach	°C	5.5	n/a	7.7	6.0	6.7	8.6	5.7	6.1
Cooling range	°C	11.0	n/a	6.0	14.0	17.0	5.9	12.7	14.2
Condenser term. temp diff	°C	4.0	n/a	0.3	4.0	0.3	0.3	4.0	0.3
ACC initial temp diff	°C	n/a	14.0	n/a	n/a	n/a	n/a	n/a	n/a
Steam condensing temp	°C	40.5	54.0	54.0	54.0	54.0	54.8	52.4	50.6
Condenser									
		Surface	ACC	DCC	Surface	DCC	DCC	Surface	DCC
Operating duty	hr/day	8	8	8	8	8	8	8	8
Heat load	MW	201	201	201	201	201	201	201	201
Water mass flow rate	kg/s	4371	n/a	8014	3435	2829	8150	3786	3386
Water volume flow rate	m3/s	4.41	n/a	8.08	3.46	2.85	8.22	3.82	3.41
Water pressure drop	Pa	50,000	n/a	100,000	50,000	100,000	100,000	50,000	100,000
Pump efficiency	%	70%	n/a	70%	70%	70%	70%	70%	70%
Pumping power	MW(e)	0.31	n/a	1.15	0.25	0.41	1.17	0.27	0.49
Pump electricity rate	\$/MWh	\$75	n/a	\$75	\$75	\$75	\$75	\$75	\$75
Pumping OPEX	\$/year	\$68,934	\$0	\$252,757	\$54,162	\$89,208	\$257,041	\$59,706	\$106,799
Surface cost	\$/MW/K	n/a	\$1,088,388	n/a	n/a	n/a	n/a	n/a	n/a
CAPEX	\$	\$800,000	\$27,272,122	\$800,000	\$800,000	\$800,000	\$800,000	\$800,000	\$800,000
Cooler									
		Wet tower	None	ACHEX	ACHEX	ACHEX	ACHEX	ACHEX	ACHEX
Operating duty	hr/day	8	n/a	8	10	10	8	10	10
Heat load	MW	201	n/a	201	161	161	201	161	161
Water mass flow rate	kg/s	4371	n/a	8014	2748	2263	8150	3029	2709
Water volume flow rate	m3/s	4.41	n/a	8.08	2.77	2.28	8.22	3.05	2.73
Water flow capacity	MW/K	18.3	n/a	33.5	11.5	9.5	34.1	12.7	11.3
Water pressure drop	Pa	75,000	n/a	100,000	100,000	100,000	100,000	100,000	100,000
Pump efficiency	%	70%	n/a	70%	70%	70%	70%	70%	70%
Pumping power	MW(e)	0.47	n/a	1.15	0.40	0.33	1.17	0.44	0.39
Pump electricity rate	\$/MWh	\$75	n/a	\$75	\$63	\$63	\$75	\$63	\$63
Pumping OPEX	\$/year	\$103,401	\$0	\$252,757	\$90,992	\$74,935	\$257,041	\$100,307	\$89,711
Surface cost	\$/MW/K	n/a	n/a	\$625,000	\$625,000	\$625,000	\$625,000	\$625,000	\$625,000
CAPEX	\$	\$2,000,000	\$0	\$20,002,025	\$13,891,530	\$11,923,068	\$18,884,783	\$15,024,806	\$13,536,352
Air draft									
		Mechanical	Mechanical	Mechanical	Mechanical	Mechanical	Mechanical	Mechanical	Mechanical
Air mass flow rate	kg/s	5000	20000	23000	14000	12000	21000	15000	14000
Air volume flow rate	m3/s	4425	17699	20354	12389	10619	18584	13274	12389
Air flow capacity	MW/K	n/a	20.2	23.2	14.1	12.1	21.2	15.2	14.1
Air outlet temperature	°C	n/a	50.0	48.7	41.4	43.3	49.5	40.6	41.4
Air pressure drop	Pa	175	175	175	175	175	175	175	175
Fan efficiency	%	65%	65%	65%	65%	65%	65%	65%	65%
Fan power	MW(e)	1.19	4.77	5.48	3.34	2.86	5.00	3.57	3.34
Fan electricity rate	\$/MWh	\$75	\$75	\$75	\$63	\$63	\$75	\$63	\$63
Fan OPEX	\$/year	\$260,892	\$1,043,567	\$1,200,102	\$767,022	\$657,447	\$1,095,745	\$821,809	\$767,022
Water Consumption									
Water consumption	m3/yr	934,993	75,244	94,980	94,980	94,980	94,980	94,980	94,980
Cost of water	\$/m3	\$0.36	\$0.36	\$0.36	\$0.36	\$0.36	\$0.36	\$0.36	\$0.36
Water OPEX	\$/yr	\$341,100	\$27,450	\$34,650	\$34,650	\$34,650	\$34,650	\$34,650	\$34,650
ACC/ACHEX analysis									
		None	Single-stream	Counterflow	Counterflow	Counterflow	Counterflow	Counterflow	Counterflow
Min flow capacity	MW/K	n/a	20.2	23.2	11.5	9.5	21.2	12.7	11.3
Capacity ratio	d.l.	n/a	n/a	0.69	0.81	0.78	0.62	0.84	0.80
Max heat transfer	MW	n/a	283	318	230	224	308	233	230
Effectiveness	d.l.	n/a	0.71	0.63	0.70	0.72	0.65	0.69	0.70
NTU	d.l.	n/a	1.2	1.4	1.9	2.0	1.4	1.9	1.9
Heat transfer capacity	MW/K	n/a	25.1	32.0	22.2	19.1	30.2	24.0	21.7
TES Tank									
Tank size	ML	n/a	n/a	n/a	100	82	n/a	110	98
Tank cost/liter	\$/L	n/a	n/a	n/a	\$0.11	\$0.14	n/a	\$0.11	\$0.14
Tank CAPEX	\$	\$0	\$0	\$0	\$10,968,955	\$11,496,872	\$0	\$12,091,761	\$13,763,861
Total costs									
Total OPEX	\$/year	\$774,326	\$1,071,017	\$1,740,266	\$946,826	\$856,241	\$1,644,477	\$1,016,472	\$998,181
Total CAPEX	\$	\$2,800,000	\$27,272,122	\$20,802,025	\$25,660,484	\$24,219,941	\$19,684,783	\$27,916,567	\$28,100,213
Total NPV	\$	\$12,711,372	\$40,981,140	\$43,077,427	\$37,779,863	\$35,179,819	\$40,734,090	\$40,927,409	\$40,876,934

Nomenclature

A	Water surface area	[m ²]
$c_{p,a}$	Specific heat of air	[MJ/kg-K]
$c_{p,w}$	Specific heat of water	[MJ/kg-K]
\dot{E}_{net}	Net electricity generated	[MW]
f_v	Windspeed function (mass transfer coefficient)	[kg/m ² -s-Pa]
\dot{G}	Air mass flow rate	[kg/s]
h_a	Enthalpy of moist air	[MJ/kg]
$h_{a,in}$	Enthalpy of moist air at tower inlet	[MJ/kg]
$h_{a,out}$	Enthalpy of moist air at tower outlet	[MJ/kg]
h_{fg}	Latent heat of water	[MJ/kg]
h_{vapor}	Enthalpy of saturated water vapor	[MJ/kg]
h_w	Enthalpy of water	[MJ/kg]
$h_{w,mu}$	Enthalpy of makeup water	[MJ/kg]
I	Total water use intensity	[L/MWh]
I_{co}	Water consumption intensity, once-through	[L/MWh]
I_{cool}	Water use intensity of cooling processes	[L/MWh]
I_{cw}	Water consumption intensity, wet	[L/MWh]
I_{proc}	Water use intensity of non-cooling processes	[L/MWh]
I_{wo}	Water withdrawal intensity, once-through	[L/MWh]
I_{ww}	Water withdrawal intensity, wet	[L/MWh]
k_{bd}	Fraction of blowdown discharged to the watershed	[d.l.]
k_{de}	Fraction of withdrawal that evaporates downstream	[d.l.]
k_{evap}	Fraction of circulating water lost to evaporation	[d.l.]
k_{lat}	Fraction of heat load rejected through latent heat transfer	[d.l.]
k_{os}	Fraction of thermal input lost to non-cooling system sinks	[d.l.]
k_{sens}	Fraction of heat load rejected through sensible heat transfer	[d.l.]
K	Heat transfer coefficient	[MW/m ² -K]
K_D	Mass transfer coefficient	[kg/m ² -s]
Le_f	Lewis factor	[d.l.]
Me	Merkel number	[d.l.]
n_{cc}	Number of cycles of cooling water concentration	[d.l.]
p_a	Vapor pressure of ambient air	[Pa]
p_s	Vapor pressure at water surface	[Pa]
\dot{Q}_{input}	Thermal input to power plant	[MW]
\dot{Q}_{load}	Heat load on cooling system	[MW]
\dot{Q}_{os}	Heat lost to sinks other than the cooling system	[MW]
T_a	Temperature of ambient air	[K]
T_s	Temperature of water surface	[K]
ΔT_{cond}	Cooling range; inlet/outlet temperature difference	[K]

v	Windspeed	[m/s]
\dot{W}_{evap}	Mass flux of water vapor from water surface	[kg/m ² -s]
$\dot{W}_{blowdown}$	Mass flow rate of cooling water lost to blowdown	[kg/s]
\dot{W}_{cond}	Mass flow rate of cooling water through condenser	[kg/s]
\dot{W}_{cool}	Total mass flow rate of cooling water lost	[kg/s]
\dot{W}_{evap}	Mass flow rate of cooling water lost to evaporation	[kg/s]
\dot{W}_{mu}	Mass flow rate of cooling water makeup	[kg/s]
β	Slope of saturated vapor pressure curve	[Pa/K]
γ	Psychrometric constant	[Pa/K]
ε	Emissivity of water surface	[d.l.]
η_{net}	Net efficiency	[d.l.]
ρ_w	Density of water	[kg/L]
σ	Stefan-Boltzmann constant	[MJ/m ² -s-K ⁴]
φ_n	Net heat flux out of water surface	[MW/m ²]
$\varphi_{n'}$	Adjusted net heat flux	[MW/m ²]
φ_r	Total absorbed incident radiation heat flux	[MW/m ²]
φ_{br}	Back radiation heat flux	[MW/m ²]
φ_e	Evaporation (latent) heat flux	[MW/m ²]
φ_c	Convection (sensible) heat flux	[MW/m ²]
ω_a	Humidity ratio	[kg water/kg dry air]
ω_{in}	Humidity ratio at tower inlet	[kg water/kg dry air]
ω_{out}	Humidity ratio at tower outlet	[kg water/kg dry air]

References

- [1] U.S. Department of Energy, 2006, “Energy Demands on Water Resources: Report to Congress on the Interdependency of Energy and Water,” U.S. Department of Energy, Washington, DC.
- [2] Barker B, 2007, “Running Dry at the Power Plant,” *EPRI Journal*, Summer 2007, pp. 26-35.
- [3] Macknick J, Newmark R, Heath G and Hallett KC, 2011, “A Review of Operational Water Consumption and Withdrawal Factors for Electricity Generating Technologies,” Technical Report No. NREL/TP-6A20-50900, U.S. DOE National Renewable Energy Laboratory, Boulder, CO.
- [4] Mittal A and Gaffigan M, 2009, “Energy-Water Nexus: Improvements to Federal Water Use Data Would Increase Understanding of Trends in Power Plant Water Use,” Report no. GAO-10-23, U.S. Government Accountability Office, Washington, DC.
- [5] Averyt K, Fisher J, Huber-Lee A, Lewis A, Macknick J, Madden N, Rogers J and Tellinghuisen S, 2011, “Freshwater use by US plants: Electricity’s thirst for a precious resource,” Union of Concerned Scientists, Cambridge, MA.
- [6] Yang X and Dziegielewski B, 2007, “Water Use by Thermoelectric Power Plants in the United States,” *J. Am. Water Resour. Assoc.*, **43**(1), pp. 160-169.
- [7] Feeley TJ, Skone TJ, Stiegel GJ, McNemar A, Nemeth M, Schimmoller B, Murphy JT and Manfredo L, 2008, “Water: A Critical Resource in the Thermoelectric Power Industry,” *Energy*, **33**(1), pp. 1-11.
- [8] King C, Duncan I and Webber M, 2008, “Water Demand Projections for Power Generation in Texas,” Contract no. 0704830756, Texas Water Development Board, Austin, TX.
- [9] Klett MG, Kuehn NJ, Schoff RL, Vaysman V and White JS, 2007, “Power Plant Water Usage and Loss Study” (May 2007 Revision), National Energy Technology Laboratory, Pittsburgh, PA.
- [10] National Energy Technology Laboratory, 2010, “Cost and Performance Baseline for Fossil Energy Plants; Volume 1: Bituminous Coal and Natural Gas to Electricity,” Report no. DOE/2010/1397, National Energy Technology Laboratory, Pittsburgh, PA.
- [11] DiPietro P, Gerdes K and Nichols C, 2009, “Water Requirements for Existing and Emerging Thermoelectric Plant Technologies,” Report no. DOE/NETL-402/080108 (April 2009 Revision), National Energy Technology Laboratory, Pittsburgh, PA.
- [12] Turchi CS, Wagner MJ and Kutscher CF, 2010, “Water Use in Parabolic Trough Power Plants: Summary Results from WorleyParsons’ Analyses,” Report no. NREL/TP-5500-49468, National Renewable Energy Laboratory, Boulder, CO.
- [13] Carnegie Mellon University, *Integrated Environmental Control Model*, <http://www.cmu.edu/epp/iecm>
- [14] Zhai H and Rubin ES, 2010, “Performance and Cost of Wet and Dry Cooling Systems for Pulverized Coal Power Plants With and Without Carbon Capture and Storage,” *Energy Policy*, **38**(10), pp. 5653-5660.
- [15] Zhai H, Rubin ES and Versteeg PL, 2011, “Water Use at Pulverized Coal Power Plants with Postcombustion Carbon Capture and Storage,” *Environ. Sci. Technol.*, **45**(6), pp. 2479-2485.
- [16] Rutberg MJ, Delgado A, Herzog HJ and Ghoniem AF, 2011, “A System-Level Generic Model of Water Use at Power Plants and its Application to Regional Water Use Estimation,” ASME International Mechanical Engineering Congress & Exposition, Denver, CO, November 11-17, 2011, ASME, New York, NY.

- [17] Maulbetsch J, 2004, "Comparison of Alternate Cooling Technologies for U.S. Power Plants: Economic, Environmental, and Other Tradeoffs," Report no. 1005358, Electric Power Research Institute, Palo Alto, CA.
- [18] Berkenpas MB, Kietzke K, Mantripragada H, McCoy S, Rubin ES, Versteeg PL and Zhai H, 2009, "IECM Technical Documentation Updates Final Report," Contract no. DE-AC26-04NT41917, National Energy Technology Laboratory, Pittsburgh, PA.
- [19] Myhre R, 2002, "Water & Sustainability (Volume 3): U.S. Water Consumption for Power Production – The Next Half Century", Report no. 1006786, Electric Power Research Institute, Palo Alto, CA.
- [20] U.S. Energy Information Administration, 2010, *EIA-923 January – December Final, Nonutility Energy Balance and Annual Environmental Information Data*, U.S. Energy Information Administration, Washington, DC.
- [21] U.S. Energy Information Administration, 2010, *EIA-860 Annual Electric Generator Report*, U.S. Energy Information Administration, Washington, DC.
- [22] Vine G, 2010, "Cooling Water Issues and Opportunities at U.S. Nuclear Power Plants," Report no. INL/EXT-10-20208, Idaho National Laboratory, Idaho Falls, ID.
- [23] National Renewable Energy Laboratory, 2009, SolarPACES Concentrating Solar Power Projects, <http://www.nrel.gov/csp/solarpaces>. National Renewable Energy Laboratory, Boulder, CO.
- [24] DiPippo R, 2008, *Geothermal Power Plants: Principles, Applications, Case Studies and Environmental Impact, Second Edition*, Chap. 17, Butterworth-Heinemann, Amsterdam.
- [25] Kloppers JC and Kroger DG, 2005, "A Critical Investigation into the Heat and Mass Transfer Analysis of Counterflow Wet-cooling Towers," *Int. J. Heat Mass Transf.*, **48**(3-4), pp. 765-777.
- [26] ZIP Code Download, 2011, *USA 5-Digit ZIP Code Database, Premium Edition*, <http://www.zipcodedownload.com>
- [27] National Climatic Data Center, 2002, *U.S. Daily Climate Normals 1971-2000*, National Climatic Data Center, Asheville, NC.
- [28] Hendriks P, Personal communications, August 2011.
- [29] Google Earth, <http://earth.google.com>
- [30] Weather Underground, <http://www.wunderground.com>
- [31] ASHRAE, 2009, *ASHRAE Handbook – Fundamentals (SI)*, Chap. 1, ASHRAE, Atlanta, GA.
- [32] U.S. Environmental Protection Agency, 2001, "Economic Analysis of the Final Regulations Addressing Cooling Water Intake Structures for New Facilities," Chap. 11, Report no. EPA-821-R-01-035, U.S. Environmental Protection Agency, Washington, DC.
- [33] California Energy Commission, 2005, "Issues and Environmental Impacts Associated with Once-Through Cooling at California's Coastal Power Plants," Report no. CEC-700-2005-013, California Energy Commission, Sacramento, CA.
- [34] Diehl TH, 2011, "Estimating Forced Evaporation from Surface Water," EPRI Conference on X.
- [35] Stolzenbach KD, 1971, "Environmental Heat Transfer," MIT Summer Session: Engineering Aspects of Heat Disposal from Power Generation, June 28 - July 2, 1971, Cambridge, MA.
- [36] Kroger DG, 2004, *Air-cooled heat exchangers and cooling towers*, Penwell Corp, Tulsa, OK.

- [37] Cheremisinoff NP and Cheremisinoff PN, 1981, *Cooling Towers: Selection, Design and Practice*, Ann Arbor Science Publishers, Ann Arbor, MI.
- [38] Kennedy JF, 1971, "Wet Cooling Towers," MIT Summer Session: Engineering Aspects of Heat Disposal from Power Generation, June 28 - July 2, 1971, Cambridge, MA.
- [39] Lefevre MR, 1984, "Reducing Water Consumption in Cooling Towers," *Chem. Eng. Prog.*, **80**(7), pp. 55-62.
- [40] Baker D, 1984, *Cooling Tower Performance*, Chemical Publishing Co., New York, NY.
- [41] Leung P and Moore RE, 1970, "Water Consumption Determination for Steam Power Plant Cooling Towers: A Heat-and-Mass Balance Method," *Combustion*, **42**(5), pp. 14-23.
- [42] ASHRAE, 2008, "Cooling Towers," *ASHRAE Handbook – HVAC Systems and Equipment*, Chap. 39, ASHRAE, Atlanta, GA.
- [43] Poppe M and Rogener H, 1991, Berechnung von Ruckkuhlwerck, *VDI Warmeatlas*, Mi1–Mi15.
- [44] Al-Waked R and Behnia M, 2006, "CFD simulation of wet cooling towers," *Appl. Therm. Eng.*, **26**, 382-395.
- [45] Klimanek A, Bialecki RA and Ostrowski Z, 2010, "CFD Two-Scale Model of a Wet Natural Draft Cooling Tower," *Numer. Heat Tranf. A-Appl.*, **57**, pp. 119-137.
- [46] Ashwood A and Bharathan D, 2011, "Hybrid Cooling Systems for Low-Temperature Geothermal Power Production," Report no. NREL/TP-5500-48765, National Renewable Energy Laboratory, Boulder, CO.
- [47] Maulbetsch J and DiFilippo M, 2003, "Spray Cooling Enhancement of Air-Cooled Condensers," Report no. 1005360, Electric Power Research Institute, Palo Alto, CA.
- [48] Lindahl PA and Jameson RW, 1993, "Plume Abatement and Water Conservation with the Wet/Dry Cooling Tower," Paper no. TP93-01, Cooling Tower Institute Annual Meeting, February 17-19, 1993, New Orleans, LA.
- [49] Mortensen K, 2009, "Use of Air2Air Technology to Recover Fresh-Water from the Normal Evaporative Cooling Loss at Coal-Based Thermoelectric Power Plants," Contract no. DEFC2605NT42725, National Energy Technology Laboratory, Pittsburgh, PA.
- [50] Balogh A and Szabo Z, 2005, "The Advanced Heller System, Technical Features and Characteristics," Electric Power Research Institute Conference on Advanced Cooling Strategies/Technologies, June 2005, Sacramento, CA.
- [51] Lennon S, 2011, "Advances in Dry Cooling Deployed at South African Power Stations," Electric Power Research Institute Summer Seminar, August 2011.
- [52] McGowin C, DiFilippo M and Weintraub L, 2006, "Program on Technology Innovation: Water Resources for Thermoelectric Power Generation: Produced Water Resources, Wet-Surface Air Cooling, and WARMF Decision Support Framework," Report no. 1014487, Electric Power Research Institute, Palo Alto, CA.
- [53] Electric Power Research Institute, 2008, Workshop abstracts and presentations, Advanced Cooling Technologies Workshop, July 8-9, 2008, Charlotte, NC.
- [54] National Energy Technology Laboratory, 2010, "Department of Energy/National Energy Technology Laboratory's Water-Energy Interface Research Program: December 2010 Update," National Energy Technology Laboratory, Pittsburgh, PA.

- [55] Elcock D, 2011, “Reducing Freshwater Consumption at Coal-Fired Power Plants: Approaches Used Outside the United States,” Report no. DOE/NETL-2011/1493, National Energy Technology Laboratory, Pittsburgh, PA.
- [56] National Renewable Energy Laboratory, *Total Meteorological Year 3*, http://rredc.nrel.gov/solar/old_data/nsrdb/1991-2005/tmy3/
- [57] Dincer I and Rosen MA, 2011, *Thermal Energy Storage: Systems and Applications*, 2nd Ed., Wiley, West Sussex, UK.
- [58] Guyer EC and Golay MW, 1976, “An engineering and economic evaluation of some mixed-mode waste heat rejection systems,” Report no. MITNE-191, MIT, Cambridge, MA.
- [59] Drost MK and Allemann RT, 1978, “An Engineering and Cost Analysis of a Dry Cooling System Augmented With a Thermal Storage Pond,” Report no. PNL-2745, Pacific Northwest Laboratory, Richland, WA.
- [60] Guyer EC and Golay MW, 1983, “Fluid Mechanical Design of a Dry-Cooling System Thermal Storage Reservoir, or Stratification Minimization in Horizontal Channel Flow,” *J. Sol. Energy Eng. Trans.-ASME*, **105**(5), pp. 174-180.
- [61] Pistocchini L and Motta M, 2011, “Feasibility Study of an Innovative Dry-Cooling System With Phase-Change Material Storage for Concentrated Solar Power Multi-MW Size Power Plant,” *J. Sol. Energy Eng. Trans.-ASME*, **133**, pp. 031010-1 – 031010-8.
- [62] Munoz J, Martinez-Val JM, Abbas R and Abanades A, 2012, “Dry cooling with night cool storage to enhance solar power plants performance in extreme conditions areas,” *Appl. Energy*, **92**, pp. 429-436.
- [63] Hewitt GF, Ed., 1998, *Heat Exchanger Design Handbook, Part 3: Thermal and hydraulic design of heat exchangers*, Begell House, New York, NY.
- [64] Mills AF, 1999, *Heat Transfer*, 2nd Ed., Prentice Hall, Upper Saddle River, NJ.
- [65] Pacific Gas & Electric Company, 2011, *Electric Schedule E-20*, Pacific Gas & Electric Company, San Francisco, CA.
- [66] Abengoa Solar, 2011, Press release: “Abengoa awarded two CSP projects by South Africa’s Department of Energy,” available at: http://www.abengoasolar.com/corp/web/en/acerca_de_nosotros/sala_de_prensa/noticias/2011/solar_20111207.html.